AD_____

Award Number: DAMD17-98-1-8219

TITLE: Characterization of the Structure and Immunogenicity of HN654-662 and Variant Peptides Bound to HLA-A2.1

PRINCIPAL INVESTIGATOR: Ashwami Kumar Sharma, Ph.D.
Edward Collins, Ph.D.

CONTRACTING ORGANIZATION: University of North Carolina
Chapel Hill, North Carolina 27599

REPORT DATE: April 2001

TYPE OF REPORT: Final

PREPARED FOR: U.S. Army Medical Research and Materiel Command
Fort Detrick, Maryland 21702-5012

REPORT DOCUMENTATION PAGE

Form Approved
OMB No. 074-0188

1. AGENCY USE ONLY (Leave blank)	2. REPORT DATE	3. REPORT TYPE AND DATES COVERED
	April 2001	Final (1 Jul 98 - 31 Mar 01)

4. TITLE AND SUBTITLE
Characterization of the Structure and Immunogenicity of HN654-662 and Variant Peptides Bound to HLA-A2.1

5. FUNDING NUMBERS
DAMD17-98-1-8219

6. AUTHOR(S)
Ashwami Kumar Sharma, Ph.D.
Edward Collins, Ph.D.

7. PERFORMING ORGANIZATION NAME(S) AND ADDRESS(ES)
University of North Carolina
Chapel Hill, North Carolina 27599
Email - collins1@med.unc.edu

8. PERFORMING ORGANIZATION REPORT NUMBER

9. SPONSORING / MONITORING AGENCY NAME(S) AND ADDRESS(ES)
U.S. Army Medical Research and Materiel Command
Fort Detrick, Maryland 21702-5012

10. SPONSORING / MONITORING AGENCY REPORT NUMBER

11. SUPPLEMENTARY NOTES
Report contains color graphics

12a. DISTRIBUTION / AVAILABILITY STATEMENT
Approved for Public Release; Distribution Unlimited

12b. DISTRIBUTION CODE

13. ABSTRACT *(Max...)*

We propose to establish an approach by which tumor cells are eradicated through selective induction of $CD8^+$ cells specific for a cellular protein, HER-2/neu, that is expressed in many breast and ovarian cancers. Our model system is the class I MHC molecule HLA-A2.1 and the HER-2/neu protein. HLA-A2.1 is present in approximately 50% of Caucasian and African-American women, and HER-2/neu is over-expressed in approximately 30% of breast tumors. A peptide derived from HER-2/neu (HN654-662) has been shown to bind HLA-A2.1 and stimulate cytotoxic T lymphocytes (CTL) that lyse primary tumors from breast or ovarian cancer. The peptide has poor immunogenicity due to poor binding to HLA-A2.1 with low melting temperature (Tm=36.6 °C). We are trying to improve the binding affinity by making substitution in the peptide sequence to make it effective therapeutic agent. The crystallographic structure of HN654-662 co-crystallized with HLA-A2.1 shows that the center of the peptide does not assume one specific conformation and does not make stabilizing contacts with the peptide binding cleft. Altering the primary anchor residues did not improve the binding significantly. Surprisingly, the double variants I2L/V5L are less stable than single substitutions. Also the substitutions at three positions, I2L/V5L/L9V did not improved the stability. The crystallographic studies of HLA-A2.1 plus HN654-662 variant (I2L/V5L/L9V) (Tm=39.5 °C) shows that substituted Leu at fifth position point away from the MHC molecule. It seems that substitution of either of the anchor residues makes the position 5 Leu point away from class I MHC. The crystallographic studies of another variant HLA-A2.1 HN654-662 (I2L/V5L) (Tm=39.0 °C) shows that the orientation of substituted Leu at fifth position is same as that of Val 5 in wild type.

14. SUBJECT TERMS
Breast Cancer

15. NUMBER OF PAGES 75

16. PRICE CODE

17. SECURITY CLASSIFICATION OF REPORT	18. SECURITY CLASSIFICATION OF THIS PAGE	19. SECURITY CLASSIFICATION OF ABSTRACT	20. LIMITATION OF ABSTRACT
Unclassified	Unclassified	Unclassified	Unlimited

TABLE OF CONTENTS

INTRODUCTION

Class I major histocompatibility molecules (MHC) bind short peptides derived from proteins synthesized within the cell. Cytotoxic T Lymphocytes (CTL) are activated when their T cell receptors (TCR) recognizes a complex of peptide and class I MHC molecule and lyse the cell expressing the complex. This process eliminates some tumor cells expressing new or altered proteins. However, not all tumors are recognized efficiently. One reason hypothesized is poor binding of those peptides to class I MHC molecules. Studies have shown that increasing the binding affinity of a peptide can improve its immunogenicity. Many peptides derived from the proto-oncogene HER-2/neu have been shown to be recognized by cytotoxic T cells derived from HLA-A2+ patients with breast cancer and other adenocarcinomas. One of the peptides, GP2 (HN654-662) binds very poorly even though it is predicted to bind well based upon the presence of the correct HLA-A2.1 peptide-binding motif. Creating peptides with greater affinity for HLA-A2.1 that are still recognized by HN654-662 specific CTL will increase CTL efficiency against wild type HER-2/neu HLA-A2.1 complexes and will result in complete eradication of the cancer from the patient. We propose to identify variant peptides that increase the affinity of class I MHC/peptide complex for HER-2/neu specific TCR.

ANNUAL SUMMARY

Specific Aim: Develop HN-654-662 variant peptides with improved affinity for HLA-A2.1

1.1 Determine the co-crystal structure of HLA-A2.1 complexed with wild type HN654-662 peptide.

Rationale: The structures of a number of single peptide/MHC class I co-crystal structures are now known. These structures unfortunately have not allowed us to predict how any single peptide will bind. Much more structural information is required to begin to explain the multitude of mutational and kinetic data already present. The experiments described here seek to address part of this issue. What property of the HN654-662 peptide makes it a poor ligand for HLA-A2.1? These data will guide us in designing second generation epitopes.

Approach: Using synthetic peptides and in vitro folding of HLA-A2.1, sufficient quantities of complex are easily obtained for crystallization. The data will be collected on an R-AXIS II area detector system and the data processed with the program DENZO. The structures will be determined by molecular replacement using the program suite AMoRe and refined by iterative cycles of manual rebuilding using the graphical program O, computational refinement with X-PLOR and if the molecule crystallizes with more than one molecule per asymmetric unit, averaging using the RAVE suite. The resulting structure will be directly compared with crystal structure of HLA-A2.1/peptide complex for which the peptide has high affinity (for example: calreticulin signal sequence, HIV matrix peptide)

Work done: In order to understand why HN654-662 binds poorly to A2.1, we determined the crystallographic structure of A2.1/HN654-62. The molecular replacement solution was unambiguous with a correlation coefficient of ~73% after rigid body fitting. The model was refined in X-PLOR. During refinement, the peptide was omitted to reduce the potential for model bias. Density modification was performed with DM using the X-PLOR output coordinates to generate unbiased averaged electron density maps of the peptide and to fit the structure of A2.1. Unlike all of the pMHC structures that we have determined to date, the entire length of the main chain of the peptide was not visible in the electron density maps at this stage. After 10 cycles of model building and computational refinement with X-PLOR and Refmac and finally with CNS, the refinement converged. In general, the maps are clear and unambiguous. The entire A2.1 molecule is well resolved and fits the density well as evidenced by an average real space correlation coefficient of 83.8%. The positions of the termini of the HN654-662 peptide are also unambiguous and never altered through the course of refinement. However, unlike all reported pMHC structures, the center of the peptide never became clear in the density. In addition, standard 2Fo-Fc maps, simulated annealing omit maps, unaveraged omit maps and composite omit maps failed to show density for the center of the peptide. In particular, the orientation of residue 6 (Val) is completely uninterpretable and the orientation of residues 5 and 7 (Val and Gly respectively) are not well defined. This suggests that the center of the peptide is highly flexible and it does not assume one unique conformation in the center. Crystallographic data and refinement statistics are shown in Table 2a. This work was completed by members of the Collins lab before I arrived.

Training Accomplishments: The training acquired during the course of work helped in learning all the skills related to solving three-dimensional crystal structure. The techniques learned are in-vitro protein folding, protein purification, protein crystallization, data collection, structure solution, refinement, model building. The final interpretation of the solved structure

helped in understanding the forces involved in ligand binding. The training helped in reinforcing the biochemical and crystallographic skills.

1.2 Using the crystallographic structure and peptide libraries, create improved HER-2/neu epitopes

Rationale: The main chain of HN654-662 when bound to HLA-A2.1 will have a different path in the peptide binding cleft and the side chains will be pointing in unique orientations. This has been seen for all peptide/class I MHC molecule co-crystal structures to date. Therefore, the crystallographic structure will provide a starting point from which to improve peptide binding. The choice of which amino acid to change will depend on the orientations of the HN654-662 amino acids in the peptide binding cleft. The goal is to increase affinity without losing immunogenicity. Thus, we chose to change a residue that points down into the peptide cleft rather than up towards the TCR.

Methods: The crystallographic structure will tell us only which amino acid to target for changes, the best residue with which to replace the wild type sequence requires experimentation. To determine this, we will chemically synthesize small libraries of peptides that have as the root the wild type HN654-662 sequence. One amino acid in the sequence will be randomized at a time during the chemical synthesis of the peptide by substituting the wild type FMOC derivatized amino acid with a mixture of all 20 FMOC derivatized amino acids. Thus the synthesis will contain 20 different peptides (the wild type sequence serves as an internal control). This mixture will be used in our standard in vitro folding assays and folded complexes isolated. Complexes that form will be acid treated to denature the complexes and the peptide removed by filtration. The eluted peptides will be separated on a reversed-phase HPLC column and fractions analyzed by time of flight mass spectrometry to identify the peptides in collaboration with Dr. David Klapper in the department of Microbiology and Immunology. To increase the stringency, the complexes will be incubated at 37 °C to remove poorly binding peptides and separated by HPLC gel filtration before acid elution. This type of experiment will allow us to determine both the types of amino acids that may bind, and those that preferentially stabilize the complex. We expect a small number of residues to stabilize the complex based on previous work and perhaps fewer to stabilize better than the wild type sequence. Peptides that contain residues that are shown to increase stabilization will be synthesized and assayed.

Work done: The first library was constructed with 19 amino acids at position 3 of GP2. Cysteine was not included because of its interactions with the redox partners of glutatione in the folding buffer. Additionally, the first residue was altered to lysine to improve the solubility of the peptide library because the serine that is at position 3 in the wild-type peptide is the only polar residue in GP2 (IISAVVGIL). The initial folding experiments showed that the folded complexes were very unstable. When the purified protein was left at room temperature for a short time, all of the protein precipitated. The next preparation of recombinant protein was treated as described above (except kept at 4 °C) and analyzed by mass spectrometry by Dr. Roman Chicz, Zycos Inc. His instrument is reported to be sensitive to fmol levels of peptide. Unexpectedly, all 19 peptides were found in the spectrum of masses present from the purified protein. As the technique is extremely sensitive to the presence of the peptide, but insensitive to the amounts, it is probably not suitable for our use. We intend to repeat the experiment and perform Edman degradation on the resulting material to determine the relative amounts of each peptide present. Until we can resolve these issues, further libraries will not be made.

Training accomplishments: The results from crystallographic structure helped in designing future experiments for improving peptide binding. The particular side chain to be replaced depended on the orientation of side chain in peptide binding cleft. The aim was to improve peptide binding without affecting its immunogenicity. This particular aim helped in designing experiments utilizing previous crystallographic and biochemical data.

1.3 Determine on-rates, off-rates and thermostability of improved epitopes

Rationale: Altered sequences will demonstrate differences in physical characteristics of peptide binding. It has been shown that some peptides with decreased off-rates show greater immunogenicity. Some HN654-662 variants that show increased binding to HLA-A2.1 will likely show greater immunogenicity.

Methods: These substituted peptides will be tested with the peptide transport deficient cell line T2 to determine which peptides form class I/peptide complexes with enhanced cell surface stability. We will use the cell surface stabilization assay using endogenous HLA-A2.1 in T2 cells and the conformationally specific antibody BB7.2 to asses cell surface peptide binding. Briefly cells will be incubated with peptide, washed and stained, and the mean channel fluorescence (MCF) determined by flow cytometry. To estimate off rates from stability assays, cells will be preincubated with peptides at 37 °C and Brefeldin A added to block the egress of new molecules. Aliquots of cells will be removed overtime, stained and the MCF determined as described above.

We will also measure the on and off rates of class I peptide complexes with better precision using surface plasmon resonance (Biacore). We will confirm our initial results based on the cell surface stability with soluble HLA-A2.1 and peptide using standard Biacore protocols. In brief, we will synthesize peptides with cysteine replacements at residues that are pointing towards the TCR as suggested by the crystal structure and through these cysteines the peptides will be coupled to the plasmon resonance chip. Each variant peptide will first be tested for binding to soluble HLA-A2. When the best coupling residue is identified, we will directly measure the binding compared to both the wild type epitope and non-binding controls. To determine the magnitude of the difference in peptide affinity as a result of changing an amino acid to cysteine, we will perform competition binding experiments using an unrelated HLA-A2.1 binding peptide on the chip to compete for binding with both the wild type and altered peptides. Alternatively we can perform the entire assay as a competitive binding assay, using the Biacore signal read out. We do wish to note that the measurement of stability on cells at 37 °C may better reflect *in vivo* stability than the Biacore measurement, while the Biocore will allow much greater precision and accuracy of the measurements

Measurement of the overall thermostability of the peptide/class I complex by circular dichroism (CD) spectroscopy provides a measure of the overall stability of the complex. The thermodynamic stability will be measured using the extracellular portion of HLA-A2.1 produced in E. coli and folded *in vitro* in the presence of the appropriate synthetic peptide. The melting temperature, an indication of the stability of the complex, will be measured by following the loss of circular dichroic signal as a function of temperature. The thermodynamic data will be correlated with the observed half-lives of these peptides bound to the MHC class I molecule for a full description of the binding of each peptide. While a melting temperature in excess of 37 °C may not seem physiologically important, they do reflect the thermodynamic stability of the complexes and will likely yield data important for creating the best binding peptide if a third generation is required.

Work done: We have chemically synthesized the peptides shown in Table 1 and determined their on-rates, off-rates and melting temperatures as described previously. The melting temperature for HN654-662 is 36.4 °C. This complex has the lowest T_m of any complex measured to date. This peptide is perfect example for poor-binding peptide and offers the first opportunity to understand poor binding. Substitutions at peptide anchor positions (I2L, L9V and I2L/L9V) and at both anchor and middle of the peptide (I2L/V5L, I2L/V5L/L9V, V5L/L9V) shown in Table I did not improve the thermal stability significantly (~2-6 °C). Similar substitutions increased the stability drastically in the influenza matrix peptide (~7-9 °C) and for a variant of melanoma peptide (MelA and MelA-A2L (~9 °C). A cell surface binding assay using T2 cells with exogenously added peptide confirms the results found by the circular dichroism studies. Two peptides, one hydrophobic and one hydrophilic, were chosen as representative "high affinity" binders. ML is derived from the signal sequence of calreticulin and RT is derived from HIV-1 reverse transcriptase. The thermal stability (T_m) and relative binding constant (K_r) determined by T2 assay correlate well (91.3% correlation coefficient).

Adding brefeldin A (BFA) to the cell surface stability assay allows us to measure the amount of time a peptide/MHC complex stays on the surface of the cells. The HN654-662 peptide has an extremely short half life ~21 minutes at 37 °C. The half lives of altered peptides/MHC complexes on the cell surface are increased with respect to HN654-662 peptide. However, they are not close to the time constants seen for the positive control, high affinity binders ML or RT.

We planned to measure the on and off rates of class I peptide complexes with better precision using surface plasmon resonance (Biacore). We did not perform above experiments as our recent data describing different interactions in the peptide and interactions between peptide and binding cleft is potentially more informative. Also, our present data of on-rates and off-rates yielded consistent results.

Training Accomplishments: The training acquired during the course of work helped in learning both immunological and biophysical techniques. Cell surface stabilization assays using flow-cytometry technique helped in determining on- and off-rates of class I/peptide complexes. The circular dichroism (CD) spectroscopy, a biophysical technique, helped in determining the melting temperatures of class I/peptide complexes.

1.4 Determine on rates, off rates and thermostability of improved epitopes in the presence of physiological osmolytes

Rationale: MHC complexes *in vivo* exist in a concentrated environment. Osmolytes have been shown to stabilize protein structures and are present in the cellular environment. Physiological concentrations of osmolytes have been shown to preferentially stabilize the poor affinity peptide HN654-662 bound to HLA-A2.1. The affinity and stability of substituted peptides and complexes should be analyzed in the presence of physiological concentrations of osmolytes for a better estimate of overall stability. Osmolytes have not been in previous stability studies of HLA complexes, so we will conduct both sets of experiments to get a better understanding of the degree of stabilization achieved. In addition this information might lead to better crystallization conditions for the parent and substituted peptides; this would facilitate the final structures.

Methods: We will repeat the procedures described in the methods of section 1.3. Briefly, substituted peptides will be tested in the cell surface stabilization assay using endogenous HLA-A2. 1 in T2 cell and the conformationally specific antibody BB7.2 to assess cell surface

peptide binding as described before. Cells will be incubated with peptide in serum-free media with different osmolytes concentrations, washed and stained, and the mean channel fluorescence (MCF) determined by flow cytometry. Biacore measurements and CD measurements will also be performed in the presence of different concentrations of osmolytes centered around the physiological value. In addition to sodium chloride, glucose and sucrose will be examined. Other physiological osmolytes will be tested as time permits.

Work done: We have focused on the mechanism of NaCl thermal stabilization. As described, the thermal stability of these complexes are maximal in the presence of 150 mM NaCl. The potential mechanisms for stabilization are changes in water interactions with the protein by inclusion of NaCl or by direct binding of the salt. Since HLA-A2.1 is actually a ternary complex, the effect could be due to physical stabilization any one of the pieces: peptide, heavy chain or β2m or by changing the interactions of any of the pieces. We have shown that β2m is not stabilized in the presence of increasing concentrations of salt (heavy chain is not soluble in the absence of peptide or β2m). However, we have seen increases in thermal stability when β2m is covalently linked to the MHC complex. This leads us to believe that the mechanism of thermal stabilization is the increased affinity of β2m for heavy chain. This protein acts as a wedge keeping the peptide-binding superdomain closed so that peptide cannot escape.

Training Accomplishments: The training acquired here helped in reinforcing the skills learned in section 1.3. This aim helped in understanding the role of physiological osmolytes in stabilizing the class I/peptide complexes.

1.5 Determine the mechanism for the loss of thermal stability of I2L/V5L compared to I2L and V5L alone.

Rational: The thermal stability of HN654-662 variants is higher when there is only single substitution i.e. either in middle or at anchor position. There was a loss of thermal stability in the variants where substitutions were at both middle and anchor positions. Understanding the reasons for loss of thermal stability in variants having both substitutions as compared to the variants with single substitutions would help to understand the mechanism of binding and allow us to probe how residues influence each other in the peptide

Method: The crystallographic structures of complexes of HLA-A2.1 and variants with single substitution and with two or more substitutions at both anchor position and in the middle of the peptide will help in understanding the mechanism of binding. The resulting structures will be compared with the crystal structure of HLA-A2.1 plus wild type and among themselves.

Work done: In order to understand why substitutions at anchor positions together with substitutions at the middle of the peptide results in loss of thermal stability as compared to single substitutions either at anchor position or in the middle, the crystal structures of HLA-A2.1/HN654 variants (I2L/V5L/L9V) and (I2L/V5L). The molecular replacement solution gave a correlation coefficient of ~ 79% for I2L/V5L/L9V and ~75% for I2L/V5L. The models were refined in CNS and peptide was omitted during refinement to reduce the bias. Density modification was performed with DM to generate unbiased averaged electron density maps of the peptide. The model building was performed using O. The electron density at the center of the peptide is not well defined in both structures. This is quite similar to the structure of wild type. This shows that the center of the peptide is highly flexible. Surprisingly the double or triple variants are less stable than single substitutions. The crystal structures of I2L/V5L/L9V (T_m = 39.5 °C) shows that substituted Leu at fifth position point away from the MHC molecule while that of I2L/V5L (T_m = 39.0 °C) shows that the orientation of substituted Leu at fifth

position is same as that of Val 5 in wild type. It seems that substitutin of either of the anchor residues makes the position 5 Leu point away from class I MHC. Crystallographic data and refinement statistics are shown in Table 2B and 2C. We are trying to crystallize and solve the crystal structure of V5L and I2L variants.

Training Accomplishments: The training here helped in reinforcing all the crystallographic and biochemical skills learned in section 1.1. The interpretation of these two crystal structures helped in understanding how different residues affect each other in peptide binding.

Key Research Accomplishments

- The X-ray crystal structure of the complex of human HLA-A2 plus HN654-662 peptide (IISAVVGIL) was determined to 2.4 Å resolution. The structure suggests that the center of the peptide is highly flexible which may account for its poor binding.

- Thermal denaturation studies of various complexes of HLA-A2 with HN654-662 or an altered peptide ligand provided a measure of overall complex stability. HLA-A2/HN654-662 complex is very unstable (Tm=36.6°C). Substitutions at peptide anchor positions (I2L, L9V and I2L/L9V) and at both anchor and middle of the peptide (I2L/V5L, V5L/L9V and I2L/V5L/L9V) did not improve the thermal stability significantly (~2-6 °C)

- The X-ray crystal structure of HLA-A2 plus HN654-662 variants $A2^{I2L/V5L/L9V}$ and $A2^{I2L/V5L}$ was determined to 2.25Å and 2.3Å resolution respectively. These MHC-I/peptide complexes are slightly more stable (Tm=39.5°C & 39.0°C for I2L/V5L/L9V and I2L/V5L respectively) than its wild type. We expected the substituted Leu to point downwards and interact strongly with the MHC molecule but it seems that the substitution of the anchor residues in I2L/V5L/L9V makes the Leu at the fifth position point away from the MHC molecule. In I2L/V5L structure, though the Leu at position 5 points in the same direction as the wild type Val at position 5, but side chain of Leu5 point away from the hydrophobic pocket.

Reportable Outcomes

Manuscripts

1. Jennifer J. Kuhns, Michael A. Batalia, Shuquin Yan and Edward J. Collins (1999) Poor binding of a HER-2/neu Epitope (GP2) to HLA-A2.1 is due to a lack of interactions with the center of the peptide. *J. Biol. Chem.* 274, 36422-36427.
2. Batalia M.A., Kirksey T.J., Sharma A., Jiang L., Jean-Pierre Abstando, Yan S., Zhao, R., and Collins E. J. (2000) Class I MHC is stabilized against thermal denaturation by physiological concentrations of NaCl. *Biochemistry*, **39** (30), 9030-9038.
3. Sharma, A.K., Kuhns, J.J., Yan S., Freidline R., Long B., Tisch R. and Collins E.J. (2000). Class I MHC anchor substitutions alter the conformation of T cell receptor contacts. *J. Biol. Chem.* (in press).
4. Kuhns J.J. and Collins E.J. (2001) Solvent accessible residue affects peptide binding affinity to class I MHC. (in preparation)

Abstaracts

1. Ashwani K. Sharma, Jennifer J. Kuhns, Michael A. Batalia and Edward J. Collins (2000) Structure-based design of class I MHC/peptide cancer immunotherapeutics. Era of Hope, Department of Defense, Breast Cancer Research Program Meeting, June 8-11, 2000, Hilton Atlanta Towers, Atlanta, Georgia.
2. Edward J. Collins, Ashwani K. Sharma, Jennifer J. Kuhns and Michael A. Batalia (2000) Stimulating CTL towards *Her-2/neu* overexpressing breast cancer. Era of Hope, Department of Defense, Breast Cancer Research Program Meeting, June 8-11, 2000, Hilton Atlanta Towers, Atlanta, Georgia.

Conclusions

GP2 (HN654-662) peptide bind poorly to A2: We have examined the binding of one of the poor binding peptide GP2 (IISAVVGIL), derived from the tyrosine kinase family member HER-2/neu, to HLA-A2. HER-2/neu is overexpressed in approximately 30% of patients with breast cancer and in all other adenocarcinomas examined. Despite the presence of CTL that recognize these peptides bound to A2, the tumors are not eliminated. One proposed explanation for inefficient tumor killing is that the peptide antigens bind poorly to A2 and these complexes are not stable enough to be recognized well by GP2-specifc CTL. Creating peptides with greater affinity for HLA-A2 that are still recognized by GP2 specific CTL will increase CTL efficiency against A2/GP2 complexes and help in complete eradication of cancer. Our long term goal is to design high affinity altered peptide ligand for cancer immunotherapy. The circular dichroism (CD) studies show that A2/GP2 complex has poor thermal stability (T_m = 36.4 °C). The cell surface binding assay using T2 cells confirms the results obtained from CD studies. The crystallographic structure of GP2 co-crystallized with A2 shows that the center of the peptide is highly disordered and does not make stabilizing contacts with the peptide binding clefts.

Substitution of anchor residues do not significantly improve binding of GP2: The anchor substitutions (at position 2 and 9) in GP2 with amino acids most preferred by A2 increased the binding affinity, but not significantly (~2-6 °C). The cell surface binding assay support the finding made by CD data.

A substitution at the center of the peptide coupled with anchor substitutions reduces binding affinity: Based on crystallographic structure of GP2 bound to A2, we synthesized a series of peptides that included the V5L substitution in combination with anchor substitution. Our hypothesis was that larger leucine at position 5 would fit into a hydrophobic pocket in the peptide binding cleft under the α2 α helix where smaller valine could not reach and would enhance the binding affinity. Measurements of binding affinity and peptide off-rates showed that the enhancement in binding of doubly-substituted peptide was not the sum of the increases from the singly-substituted peptides. This means that there are interactions between residues in the peptide which affects the confirmation of the peptide A2/GP2 structure.

The crystallographic structures of $A2^{I2L/V5L/L9V}$ and $A2^{I2L/V5L}$ confirm that the individual residues in peptide interact: In order to understand these interactions, the crystallographic structures of A2 bound to GP2 variants I2L/V5L and I2L/V5L/L9V were determined. In both structures, the electron density at the ends of the peptide is well defined. However, the center of the peptide is disordered. The leucine at position 5, in I2L/V5L/L9V, points towards solvents as compared to A2/GP2 structure where valine at position 5 points towards α1 helix. This shows that anchor substitutions makes Leucine at position 5 to point upwards. In I2L/V5L structure also leucine is more solvent exposed, though it points towards α1 helix. Also, in one of the symmetry related molecule of I2L/V5L, the substitution at position 5 alters the position of all the residues form position 6 to 9. These structures show that the residues in the peptide interact and that these changes can significantly alter the TCR recognition.

The class I MHC/peptide complexes are stabilized against thermal denaturation by physiological osmolytes: Our results shows that various osmolytes stabilizes class I MHC against thermal denaturation. Our studies show that 150 mM NaCl, in particular, demonstrated maximum stabilization. The degree of stabilization by 150 mM NaCl is largest for low affinity class I MHC/peptide complexes. The mechanism of stabilization is independent of peptide sequence. The effect is hypothesized to occur by increasing the affinity of β_2m for the complex and by discrete ion binding.

Peptide	Sequence	T_m	K_r	$T_{1/2}$
HN654-662	IISAVVGIL	36.4	>50	0.35
I2L	**L**LSAVVGIL	42.2	22.9	1.76
L9V	IISAVVGI**V**	38.8	>50	0.69
I2L/L9V	**L**LSAVVGI**V**	42.5	10	2.48
V5L	IISA**L**VGIL	45.8		
I2L/V5L	**L**LSA**L**VGIL	39	49.3	1.059
V5L/L9V	IISA**L**VGI**V**	38.8	>50	1.1769
I2L/V5L/L9V	**L**LSA**L**VGI**V**	39.5	17.5	1.075
I1K	**K**ISAVVGIL		31.2	1.76
I1K/I8F	**K**ISAVVG**F**L		54.1	0.75
I1K/S3F/V5S	**K**I**F**A**S**VGIL		22.2	1.62
I1K/S3FV5S/I8F	**K**I**F**A**S**VG**F**L		33.1	0.26
ML	MLLSVPLLL	52.5	1.8	19.53
RT	ILKEPVHGV	50.0	7.7	9.69
MelA	EAAGIGILTV	40.9	47.2	0.44
MelA-A2L	E**L**AGIGILTV	50.0	1.6	9.98

Table 1. Summary of Binding data of HER-2/neu derived peptides to A2. Residues substituted with respect to wild type peptide are shown in boldface. T_m is the temperature (°C) at which 50% of protein is denatured as measured by circular dichroism. K_r is the relative binding constant as determined by the T2 cell surface assembly assay. K_r is defined as concentration of peptide in uM that yields 50% mean channel fluorescence (MCF) as compared to the maximum fluorescence of the control peptide (ML) at 50 uM. The K_r value for ML is the concentration that yields MCF. $T_{1/2}$ is the half life of peptide/A2 complexes (in hours) as determined by the T2 cell surface stability assay. The error in the T_m is the sum of machine and curve fit errors. It is typically about 1 °C. >50 means that the concentration to yield 50% of ML fluorescence is greater than 50 uM.

A2/IISAVVGIL (GP2)

Parameters		Refinement	
Space group P1	**Resolution**		**30 - 2.4 Å**
Cell Dimensions	a = 50.34 Å	R_{work}[3] (31,969)	24.2%
	b = 63.61 Å	R_{free} (1714)	28.4%
	c = 75.14 Å	Error[5]	0.26Å
	α = 81.98°	Non-hydrogen atoms	6292
	β = 76.25°	<RS fit>[4]	83.8%
	γ = 77.83°	Average B factor	16.8Å^2
		No. Of waters	103
Molecules/ AU	2	RMSD	
Resolution	2.4 Å	bonds	0.009Å
Number of Crystals	1	angles	1.468°
R_{merge}(%)[1]	9.3 (23.3)		
<I/σ>	7.8 (3.46)	Ramachandran	
Unique reflections	34,962	Most favorable	91.6%
Total observations	66,839	Additionally allowed	8.1%%
Completeness (%)	98.2 (97.6)	Generously allowed	0.3%
		Disallowed	0.0%

Table 2A. Summary of crystallographic and refinement statistics.

1. $R_{merge} = \sum_{hkl} \sum_i |I_i - \langle I \rangle| / \sum_{hkl} \sum_i I_i$, where I_i is the observed intensity and <I> is the average intensity of multiple observations of symmetry related reflections.

2. Number in parenthesis refers to the highest resolution shell (2.44 – 2.40Å).

3. $R = \sum_{hkl} | |F_{obs}| - k|F_{cal}| | / \sum_{hkl} |F_{obs}|$, where R_{free} is calculated for a randomly chosen 5% of reflections, R_{work} is calculated for the remaining 95% of reflections used for structure refinement. Numbers in parenthesis refer to the number of structure factors used in the measurements.

4. Rs fit is the average real space fit of all atoms on an electron density map from DM with two fold non crystallographic averaging, histogram matching and solvent flattening

5. Error is the mean coordinate error estimate based on maximum likelihood measurements (27).

A2/ILSALVGIV

Parameters		Refinement	
Space group P1	**Resolution**	**50 - 2.25 Å**	
Cell Dimensions	a = 49.95 Å	R_{work}[3] (36,189)	24.8%
	b = 62.93 Å	R_{free} (1907)	28.6%
	c = 74.65 Å	Error[5]	0.26Å
	α = 82.07°	Non-hydrogen atoms	6292
	β = 76.50°	<RS fit>[4]	80.7%
	γ = 78.04°	Average B factor	19.1Å^2
		No. Of waters	144
Molecules/ AU	2	RMSD	
Resolution	2.25 Å	bonds	0.007Å
Number of Crystals	1	angles	1.3°
R_{merge}(%)[1]	5.5 (18.0)	dihedrals	24.9°
<I/σ>	14.0 (5.7)	Ramachandran	
Unique reflections	38,096	Most favorable	91.6%
Total observations	214687	Additionally allowed	8.1%%
Completeness (%)	93.8(72.0)	Generously allowed	0.3%
		Disallowed	0.0%

Table 2B. Summary of crystallographic and refinement statistics.

1. $R_{merge} = \sum_{hkl} \sum_i |I_i - \langle I \rangle| / \sum_{hkl} \sum_i I_i$, where I_i is the observed intensity and <I> is the average intensity of multiple observations of symmetry related reflections.

2. Number in parenthesis refers to the highest resolution shell (2.44 – 2.40Å).

3. $R = \sum_{hkl} | |F_{obs}| - k|F_{cal}| | / \sum_{hkl} |F_{obs}|$, where R_{free} is calculated for a randomly chosen 5% of reflections, R_{work} is calculated for the remaining 95% of reflections used for structure refinement. Numbers in parenthesis refer to the number of structure factors used in the measurements.

4. Rs fit is the average real space fit of all atoms on an electron density map from DM with two fold non crystallographic averaging, histogram matching and solvent flattening

5. Error is the mean coordinate error estimate based on maximum likelihood measurements (27).

A2/ILSALVGIL

Parameters		Refinement	
Space group P1	**Resolution**	**50 - 2.3 Å**	
Cell Dimensions	a = 50.21 Å	R_{work}[3] (31,833)	26.3%
	b = 62.32 Å	R_{free} (1670)	29.0%
	c = 74.66 Å	Error[5]	0.31Å
	α = 82.15°	Non-hydrogen atoms	6294
	β = 76.38°	<RS fit>[4]	78.4%
	γ = 78.33°	Average B factor	21.3Å^2
		No. Of waters	35
Molecules/ AU	2	RMSD	
Resolution	2.3 Å	bonds	0.008Å
Number of Crystals	1	angles	1.3°
R_{merge}(%)[1]	9.5 (29.3)	dihedrals	24.9°
<I/σ>	4.73 (2.4)	Ramachandran	
Unique reflections	33,403	Most favorable	90.3%
Total observations	114345	Additionally allowed	9.0%
Completeness (%)	87.7(84.8)	Generously allowed	0.7%
		Disallowed	0.0%

Table 2C. Summary of crystallographic and refinement statistics.

1. $R_{merge} = \sum_{hkl} \sum_i |I_i - \langle I \rangle| / \sum_{hkl} \sum_i I_i$, where I_i is the observed intensity and <I> is the average intensity of multiple observations of symmetry related reflections.

2. Number in parenthesis refers to the highest resolution shell (2.44 – 2.40Å).

3. $R = \sum_{hkl} | |F_{obs}| - k |F_{cal}| | / \sum_{hkl} |F_{obs}|$, where R_{free} is calculated for a randomly chosen 5% of reflections, R_{work} is calculated for the remaining 95% of reflections used for structure refinement. Numbers in parenthesis refer to the number of structure factors used in the measurements.

4. Rs fit is the average real space fit of all atoms on an electron density map from DM with two fold non crystallographic averaging, histogram matching and solvent flattening

5. Error is the mean coordinate error estimate based on maximum likelihood measurements (27).

Class I MHC Is Stabilized Against Thermal Denaturation by Physiological Concentrations of NaCl

Michael A. Batalia, Timothy J. Kirksey, Ashwani Sharma, Lihong Jiang, Jean-Pierre Abastado, Shuqin Yan, Rui Zhao, and Edward J. Collins

Department of Microbiology and Immunology, Department of Biochemistry and Biophysics, and Lineberger Comprehensive Cancer Center, The University of North Carolina at Chapel Hill, Chapel Hill, North Carolina 27599-7290, and Institut Pasteur, Unite de Biologie Moleculaire du Gene, Departement d'Immunologie, 25 rue du Dr Roux, 75724, Paris Cedex 15, France

Biochemistry®

Reprinted from
Volume 39, Number 30, Pages 9030–9038

Class I MHC Is Stabilized Against Thermal Denaturation by Physiological Concentrations of NaCl†

Michael A. Batalia,‡,§ Timothy J. Kirksey,‡ Ashwani Sharma,‡ Lihong Jiang,‖ Jean-Pierre Abastado,⊥,# Shuqin Yan,‡ Rui Zhao,‡ and Edward J. Collins*,‡,§,‖

Department of Microbiology and Immunology, Department of Biochemistry and Biophysics, and Lineberger Comprehensive Cancer Center, The University of North Carolina at Chapel Hill, Chapel Hill, North Carolina 27599-7290, and Institut Pasteur, Unite de Biologie Moleculaire du Gene, Departement d'Immunologie, 25 rue du Dr Roux, 75724, Paris Cedex 15, France

Received February 28, 2000; Revised Manuscript Received May 11, 2000

ABSTRACT: Class I MHC molecules are ternary complexes composed of an allotype specific heavy chain, a noncovalently associated protein β_2-microglobulin (β_2m), and a peptide. The complexes are assembled in the endoplasmic reticulum by a complex series of chaperones and peptide-loading mechanisms. In the absence of β_2m or peptide, very little class I heavy chain is transported to the surface of the cell. Complexes that do not contain all three parts of the protein are not made productively in vivo and not at all in vitro. The ability of the complex to withstand thermal denaturation in vitro has been shown to be related to the binding affinity of the peptide. Paradoxically, some low-affinity peptide complexes denature at or below human basal body temperatures in vitro but are effective biological agents in vivo. Here we show that these complexes are stabilized against thermal denaturation by physiological cosolvents and maximally stabilized by 150 mM NaCl. While the degree of stabilization by 150 mM NaCl is greatest for low-affinity peptide/MHC complexes, the mechanism of stabilization is independent of peptide sequence. This effect is hypothesized to occur by multiple mechanisms including increasing the affinity of β_2m for the complex and charge screening.

Class I molecules are ternary complexes that are expressed on the plasma membrane of nearly all cells in the body (*1*). These molecules are composed of a 44 kDa polymorphic heavy chain, a noncovalently associated light chain (~11 kDa) called β_2-microglobulin (β_2m),[1] and a small peptide (*2*). In vitro studies typically only use the extracellular portion of the heavy chain (*2*−*4*) which contains the peptide-binding superdomain and an immunoglobulin domain (*5*). Both the peptide-binding superdomain and the immunoglobulin domain make extensive contacts with β_2m (*6*).

Class I MHC molecules bind small peptides (8−11 amino acids) and present them to circulating T cells at the plasma membrane. In so doing, the class I MHC molecules serve to signal to T cells the identity of the proteins being expressed within the cell. The peptides that class I MHC bind are endogenously derived from host or intracellular pathogens. They are processed by the proteasome in the cytosol and are transported into the endoplasmic reticulum by specific transporters (*7*). The peptides are actively loaded onto class I MHC molecules within the endoplasmic reticulum before export to the cell surface (*1*). These peptide/MHC (pMHC) complexes are recognized by clonotypic T cells via their T cell receptors (TCR). Upon proper binding of TCR with pMHC, the T cells lyse the cell. A properly functioning cell will present unmutated self-peptides with class I MHC. These cells are typically untouched by the immune system, because either self-reactive T cells are eliminated during T cell development or they are functionally inactivated in the periphery. Cells that are infected by a virus or transformed to a cancerous state by DNA mutation present peptides that have not been seen by the immune system. Thus, this signal of the state of the cell prevents further viral or tumor propagation by selectively destroying aberrant cells [reviewed in (*8*)].

Class I MHC molecules bind many different peptides primarily through the invariant peptidic termini. These termini dock in pockets composed of conserved amino acids found within a large cleft in a superdomain formed by the α1 and α2 domains of the heavy chain (*5*). Altering the chemical nature of the peptidic termini drastically reduces

† This work was funded by NIH Grant AI20288, by a SPORE grant from the Lineberger Comprehensive Cancer Center, by the USAMRMC Breast Cancer Research Program (M.A.B., A.S.), and by the Cancer Research Institute (R.Z.).

* Address correspondence to this author at the Department of Microbiology and Immunology, The University of North Carolina at Chapel Hill. Phone: (919) 966-6869, Fax: (919) 962-8103, E-mail: collins1@med.unc.edu.

‡ Department of Microbiology and Immunology, The University of North Carolina at Chapel Hill.

§ Lineberger Comprehensive Cancer Center, The University of North Carolina at Chapel Hill.

‖ Department of Biochemistry and Biophysics, The University of North Carolina at Chapel Hill.

⊥ Institut Pasteur, Unite de Biologie Moleculaire du Gene.

Present address: Institut de Recherches, Biomedicales des Cordeliers, LUTI: laboratoire IDM, 15 rue de l'Ecole de Medecine, 75006 Paris, France.

[1] Abbreviations: CTL, cytotoxic T cell; TCR, T cell receptor; MHC, major histocompatibility complex; pMHC, peptide/MHC complex; A2, human class I MHC HLA-A2.1; D^b, murine class I MHC molecule H-2D^b; K^b, murine class I MHC molecule H-2K^b; β_2m, β_2-microglobulin (h or m prefix refers to human or murine protein); HEL, hen egg white lysozyme; CD, circular dichroism spectropolarimetry; T_m, temperature at which 50% protein is denatured.

10.1021/bi000442n CCC: $19.00
Published on Web 07/01/2000

the stability of the class I MHC complex as measured by thermostability experiments (*9*). Sequencing of pooled peptides eluted from class I (*10*) and determination of individual sequences (*11, 12*) showed that class I MHC restricts the use of amino acids at specific positions within the antigenic peptide. These positions within the peptides are termed anchors; a combination of anchors constitutes a peptide-binding motif (*5, 13*−*15*). The anchors are bound by the polymorphic residues within the peptide-binding superdomain of class I MHC. Because the polymorphic nature of the cleft forms the basis for the amino acids selected within the peptide, the motifs are specific for each class I allotype. These anchor residues may (*9, 16*) or may not (*17*) be used to generate significant binding free energy. It is unclear how many peptides may really be able to bind to each class I MHC. Estimates of the numbers of peptides bound to a class I MHC allotype on the cell surface have been in excess of 10^4 based on mass spectrometry (*18*), but are surely underestimated because of sampling error due to MHC preparation and vaporization for mass spectrometry.

Immunotherapies for cancer or viral infection that utilize class I molecules and peptides have been proposed (*19*). For this therapy to be successful, some critical quantity of class I molecules have to present antigenic peptide for a significant duration to signal the immune system (*20*). Understanding what makes a particular peptide bind well and another bind poorly is of critical importance to this work. Unfortunately, little is known about the mechanism of peptide binding beyond qualitative descriptions.

Poor peptide binding to class I has been postulated to be the cause for inefficient immunogenicity against tumor antigens in vivo (*21, 22*). Clearly, if a peptide does not bind well, the pMHC complex cannot be detected by circulating T cells. We examined binding of a group of peptides that are known to be recognized by cytotoxic T cells (CTL) derived from the tyrosine kinase HER-2/neu using circular dichroism (CD) spectropolarimetry and flow cytometry. Previous experiments have shown that the T_m calculated from CD thermal denaturation profiles is proportional to the peptide equilibrium binding constant (*23*). Our CD thermal denaturation experiments of class I MHC complexes with HER-2/neu-derived peptides displayed a range of T_ms. Interestingly, some of the complexes had T_ms that are at or below human basal body temperature (*24*). This result generated an interesting question. How can class I complexes fall apart at human physiological temperatures in vitro and stimulate an immune response in vivo? A hypothesis developed which states that physiological osmolytes stabilize class I MHC/peptide complexes against thermal denaturation in vitro and in vivo.

Many osmolytes are found in vivo as cosolvents (*25*). Salts, monosaccharides, and amino acids are typically found in micromolar to millimolar concentrations in the cellular environment. Most of these molecules have multiple functions inside the cell, but one function, which has been frequently neglected, is protein stabilization. Protein chemists have shown that specific osmolytes such as glycerol and sucrose can stabilize protein exposed to denaturing conditions at high concentrations (>1.0 M). Physiological concentrations of these agents do not typically have significant effects by themselves. We have performed numerous stability experiments with class I complexes using different cosolvents. The results were generally as expected; osmolytes stabilized class I MHC to thermal denaturation. The surprising result was that physiological concentrations of NaCl demonstrated the largest stabilization. We hypothesize that the stabilization is partly due to the increase of β_2m binding to heavy chain and partly due to stabilization by Debye−Hückel charge screening.

Table 1: Effect of 150 mM NaCl on the T_m of Class I MHC/Peptide Complexes[a]

MHC allotype	peptide	T_m (°C) (0.0 mM NaCl)	T_m (°C) (150 mM NaCl)	ΔT_m (°C)
A2	IISAVVGIL	36.2	60.0	23.8
A2	IISAVVGIV	38.8	59.8	21.0
A2	KISAVVGIL	41.6	55.9	14.3
A2	ILKEPVHGV	50.0	58.6	8.6
A2	YLKEPVHGV	56.0	61.7	5.7
A2	FLKEPVHGV	55.0	60.0	5.0
A2	KTWGQYWQV	52.7	57.7	5.0
A2	IMDQVPFSV	49.5	56.5	7.0
A2	ITDQVPFSV	45.1	53.9	8.8
A2	MLLSVPLLL	53.1	55.9	2.8
A2	ALGIVCPIC	45.3	63.4	18.1
D^b	KAVYNFATM	43.7	53.7[b]	10.0
D^b	FAPGVFPYM	41.0	65.0[b]	24.0

[a] Thermal melts were performed on multiple pMHC complexes as described in the text. [b] These values are for 100 mM NaCl.

EXPERIMENTAL PROCEDURES

Synthetic Peptides. All peptides were synthesized by the Peptide Synthesis Facility at the University of North Carolina, Chapel Hill. The sequences of the peptides are given in Table 1. All peptides were purified by reverse-phase HPLC to greater than 95% purity, and the sequences were confirmed by matrix-assisted laser desorption ionization−time-of-flight spectrometry.

Production of Class I MHC/Peptide Complexes. pMHC complexes were prepared as previously described (*26*). Briefly, the extracellular portions of class I MHC heavy chain were produced in *E. coli* as inclusion bodies. Purified inclusion bodies were rapidly diluted in the presence of β_2m, individual peptides, and a chaotropic buffer consisting of 100 mM Tris-HCl, pH 8.0, 400 mM L-arginine, pH 8.0, 6 mM glutathione (10:1 mixture of reduced/oxidized), and a cocktail of protease inhibitors. Folded pMHC complexes were concentrated by ultrafiltration (Amicon, Inc., Beverly, MA) with a YM10 membrane. The concentrated protein was purified to homogeneity by gel filtration on a BIOSEP SEC-S2000 column (Phenomenex, Torrance, CA) in a running buffer of 50 mM Tris-HCl, pH 7.5, 150 mM NaCl and exchanged into 10 mM KH_2PO_4/K_2HPO_4, pH 7.5, using Centricon filtration devices (Amicon, Inc.). Buffer was exchanged at least 3 times (8000-fold dilution) to ensure the removal of any residual buffers or salts. For those experiments requiring β_2m alone, the β_2m inclusion body material was folded in vitro as described above for pMHC except that a 3000 MW cutoff membrane was used for concentration before purification on the gel filtration column.

K^d covalently bound to β_2m (SC-K^d) and single-chain K^d complexes (sBDH) were produced in CHO cells and purified as described previously (*27, 28*). The purified protein was concentrated and exchanged into 10 mM KH_2PO_4/K_2HPO_4, pH 7.5, using Centricon filtration devices (Amicon, Inc.).

Circular Dichroism (CD) Spectroscopy and Thermal Denaturation Measurements. Purified complexes were diluted to 4−12 μM protein with 10 mM KH_2PO_4/K_2HPO_4 with or without additional cosolvents. The pH of the resulting solution was monitored carefully due to the known shift in T_m of class I complexes at low and high pH (*29*). The thermal denaturation profile (melting curve) of class I complexes was collected by monitoring the change in the circular dichroic signal as a function of temperature as described previously (*9, 30*). Thermal scans were performed on an AVIV 62DS spectrophotometer (Aviv Associates, Lakewood, NJ) equipped with a Peltier-effect temperature controller using 0.1 cm path length cuvettes. Thermal denaturation data were typically collected at 218 nm with 1 °C intervals from 4 to 95 °C. All measurements were made at least 3 times from different preparations and averaged. Thermal denaturation curves were scaled between 0 and 1 to provide plots of the fraction unfolded versus temperature for analysis. The T_m of a class I complex is the temperature at which 50% of the molecules are unfolded. CD spectra were collected between 350 and 200 nm at 1 nm increments and 10 s averaging times. Five or more spectra were averaged for the final spectrum of each sample.

Cell Surface Class I Measurements. Measurements of cell surface class I molecules loaded with endogenous peptides were performed as previously described (*31*). Briefly, T2 cells (ATCC no. CRL-1992), that are defective in antigen presentation (*32*), were loaded with the peptide of interest by incubating the cells in the presence of 50 μM each of peptide and β_2m. Peptide-pulsed T2 cells were cultured in serum-free AIM V media in a 5% CO_2 environment with and without additional salts. Flow cytometry was performed on a Becton Dickinson FACScan (Lincoln Park, NJ). Propidium iodide insensitive cells were used for all experiments to be sure only live cells were analyzed. The conformationally specific antibodies BB7.2 (HLA-A2 specific) (*33*), W6/32 (class I α3 chain/β2m specific) (*34*), and HbV (HLA-A2/HIV peptide specific; Dr. Ralph Kubo, personal communication) were used as the markers of folded class I structure.

RESULTS

During our examination of the thermal stability of peptides recognized by CTL from the tyrosine kinase HER-2/neu, we found some of the peptide/MHC (pMHC) complexes have denaturation midpoints that are at, or below, human basal body temperature (*24*). Knowing that these complexes bind to their cognate TCR and elicit an immune response in vivo, we sought to determine what factors might stabilize the class I MHC complexes in vitro to extrapolate to in vivo conditions. Physiological osmolytes are well-known as stabilizers (or destabilizers) of protein structure (*35*) as such were reasonable candidates as stabilizers of class I MHC against thermal denaturation. Therefore, the effect of cosolvents on the thermal stability of class I MHC molecules was examined.

Various osmolytes including polyalcohols such as glucose and PEG, amino acids, and amino acid derivatives such as glycine and betaine, and salts such as NaCl were each added to purified recombinant proteins, and the thermal stability was measured by circular dichroism. Since the yield of

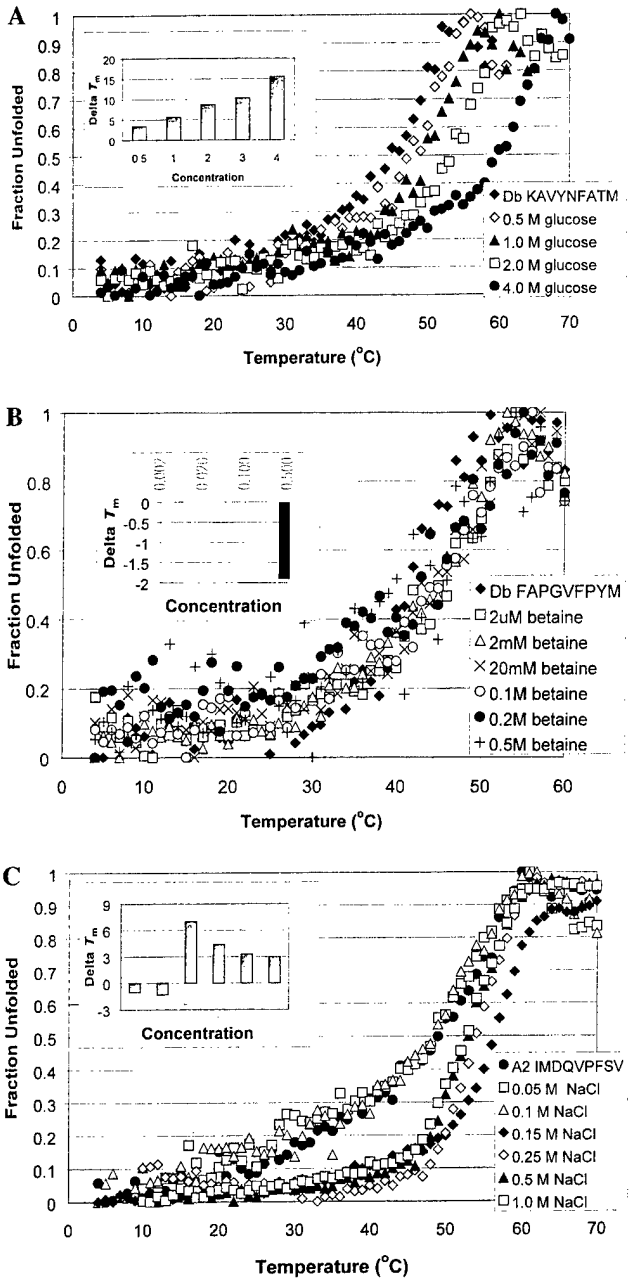

FIGURE 1: Class I MHC is stabilized against thermal denaturation by cosolvents. Thermal denaturation profiles of class I MHC in the presence of the indicated concentration of cosolvent. (A) Effect of added glucose. D^b KAVYNFATM folded in vitro was denatured in the presence of the indicated concentrations of glucose. (B) Effect of the amino acid analogue betaine. D^b FAPGVFPYM was thermally denatured in the absence of the indicated concentrations of betaine. (C) Effect of NaCl. A2 IMDQVPFSV was thermally denatured in the presence of the indicated concentrations of NaCl. The inset panels describe the difference in the calculated T_m from the T_m observed in the absence of added cosolvent. Each curve is the average of three independent experiments using 4−12 μM protein.

protein folded in vitro depends on the affinity of the peptide [(*36*) and unpublished observations], we used complexes that contained moderate- to high-affinity peptides for most analytical tests. Figure 1 shows representative results for glucose, betaine, and NaCl. Glucose shows a typical stabilization to thermal denaturation at increasing concentration (Figure 1A). Sucrose shows a similar stabilization at half the concentration. That observation is consistent with its

2-fold increase in volume relative to glucose (data not shown). Betaine showed very little effect at low concentration and a destabilizing effect at higher concentrations (Figure 1B). Glycine shows a similar destabilizing phenotype (data not shown). Interestingly, NaCl did not appear to give an easily interpretable result (Figure 1C).

Unlike the results seen with polyols and amino acids, titrations with NaCl from 5 μM to 1 M show that there is an optimal concentration of NaCl (150 mM for human class I MHC, 100 mM for murine class I MHC) for thermal stabilization. The titration shows an initial spike of stabilization at low concentration, followed by a relative destabilization, finishing with stabilization again at very high concentrations. The stabilization at high concentrations of NaCl (>0.5 M) is what has been seen many times previously for other proteins (*35*). The large increase in thermal stability at low salt concentration has not been observed previously. These effects were consistently seen for A2 and HLA-Aw68. The results seen for polyols, amino acids, and salts are not constrained to a specific MHC with a specific peptide; they are found with different peptides and different MHC molecules (data not shown). The degree of stabilization changes, but the concentration trends are the same for any class I MHC with one exception. The murine class I MHC molecule D^b showed maximum stabilization at 100 mM NaCl, not 150 mM as was seen for the human pMHC (data not shown).

We typically examine denaturation of these complexes at 218 nm. An uninteresting explanation for this effect would be if the shift in denaturation of all these pMHC complexes were due to artifactual wavelength-specific stabilization. Therefore, wavelength scans of class I MHC/peptide complexes with and without 150 mM NaCl were performed at different critical temperatures. There were no significant differences between the CD spectra of pMHC complexes at 4, 37, and 50 °C with or without 150 mM NaCl present (data not shown). There were small differences between the two conditions at 4 or 95 °C, and this observation was attributed to the solubility differences of these denatured complexes at the elevated temperatures. Denatured class I MHC complexes in the absence of NaCl are slightly soluble, while those with NaCl are not soluble as evidenced by a white precipitate at the bottom of the cuvette. These data suggest that there are no gross rearrangements of the secondary structure as a function of the NaCl concentration, and the effect is due to protein denaturation at different temperatures (data not shown). Additionally, the thermal denaturation of pMHC is reversible by the following criteria. Protein that has been heated to 90 °C for 5 min and cooled retains the same spectra as the native protein. Furthermore, the resulting protein gives the same T_m if denatured again. The denaturation is locally reversible as the T_m does not shift if a scan rate twice as long is used. Three-fold differences in pMHC concentration had no effect on T_m. However, it is not fully reversible. Much of the protein is not recovered from the first denaturation curve, and the solution must be filtered to remove the insoluble material before the second experiment is performed.

We also sought to confirm that this thermal stabilization is not artifactual by using an entirely different assay. We examined the condition of class I MHC on the surface of cells in the presence of different concentrations of NaCl by flow cytometry. T2 cells were chosen because they do not have functional peptide transporters, and thus a large fraction of the class I complexes bind exogenous peptide on the cell surface (*32*). NaCl could not be removed from the medium because the cells would die, but it could be added to the media in small amounts. Based on the data described above (Figure 1C, inset panel), NaCl concentrations above 150 mM reduce the T_ms relative to 150 mM NaCl. The hypothesis was that additional NaCl would lower the T_ms of class I on the surface of cells, resulting in fewer available complexes. First, we tested how much salt the cells could tolerate. Additional NaCl was added in 25 mM increments to AIM V serum-free medium and T2 cell viability assessed. The cells tolerated up to an additional 75 mM NaCl added to the medium over the course of the experiment (~24 h). Next, cell surface complexes of A2 were measured as a function of added NaCl. As can be seen from Figure 2, the additional NaCl reduced the number of A2 complexes on the surface of T2 cells. Different peptides bound in the pMHC showed different degrees of destabilization on the T2 cells depending on the concentration of added NaCl (Figure 2). The most affected were cells incubated with IISAVVGIV, and the least affected were cells incubated with MLLSVPLLL. Therefore, the magnitude of the effect on the surface of T2 cells correlated directly with the magnitude of the effect on T_m as measured by CD (Table 1). The effect was also not due to the hydrophobicity of the peptide, because these two peptides are very similar hydrophobicities. The shifts in fluorescence were also not due to a reduction in affinity of the BB7.2 antibody for HLA-A2, because similar effects were seen with two different antibodies that bind in distinctly different locations on the class I molecule (antibodies W6/32 and HbV, data not shown).

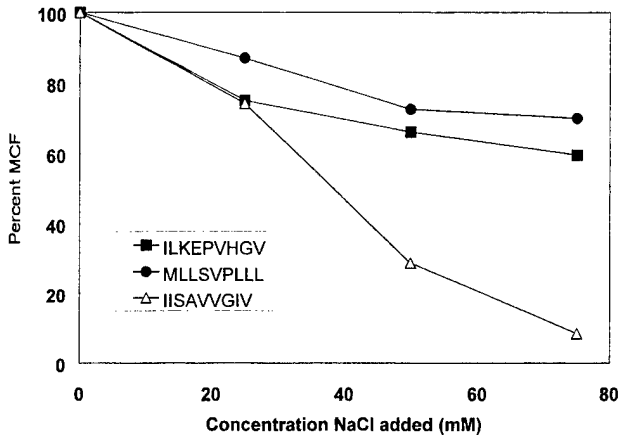

FIGURE 2: Destabilizing effect of NaCl above 150 mM is also seen on the surface of cells. Cell surface assembly assays of A2 were performed on T2 cells with the indicated peptides in the presence of 25, 50, and 75 mM NaCl added to the cell culture medium. As additional NaCl was not perfectly tolerated by the cells, live cells were analyzed by gating on propidium iodide negative cells.

Having concluded that the NaCl effect on pMHC is not an artifact of the CD experiment, we reexamined the effect of NaCl on a well-studied protein, hen egg white lysozyme (HEL), and also β_2m. Figure 3 shows the change in T_m for HEL and β_2m in the presence of increasing concentrations of NaCl. There are relatively small, nearly monotonic positive changes in T_m up to 500 mM NaCl for HEL and larger, positive changes at 1.0 and 2.0 M NaCl. There was no peak of stabilization, and the observed stabilization of HEL at 150

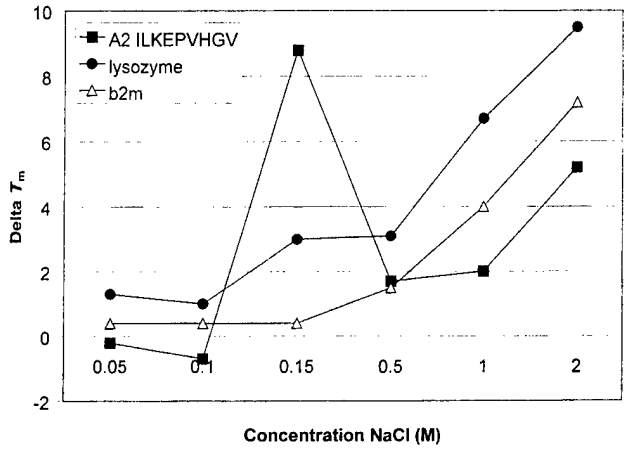

FIGURE 3: Effect of NaCl on class I MHC is not generalizable to other proteins. The indicated amounts of NaCl were added to samples of A2 ILKEPVHGV, lysozyme, or β_2m and the thermal denaturation profiles determined. Delta T_m is the calculated T_m in the absence of NaCl subtracted from calculated T_m at the indicated concentration.

mM NaCl (~2 °C) was not nearly as large as most of the effects on class I MHC (Table 1). There was no observed change in the T_m of β_2m until 0.5 M NaCl was added.

The effects of other salts on class I MHC were also examined. Figure 4A demonstrates that KCl shifts the T_m of complexes to greater temperatures than NaCl. However, the maximum was observed to be 150 mM, suggesting that ionic strength may be part of the reason the protein is stabilized. Figure 4B shows the effects of Na_2SO_4 on class I complexes. At an equivalent point of ionic strength, the effects of NaCl, KCl, and Na_2SO_4 are very similar, but different in intensity. Additionally, some salts shifted the T_ms of complexes to lower values. For example, at 150 mM NaSCN, the A2 ILKEPVHGV complex was so disrupted an accurate T_m could not be assessed. Also, LiBr at 150 mM shifted the T_m of the A2 ILKEPVHGV complex by approximately −20 °C (data not shown). In a survey of other biologically important ions, we tested the effect of 5 mM Ca^{2+} ($CaCl_2$, estimated to be the physiological concentration of Ca^{2+} in the ER) on the thermal denaturation of pMHC [in MES buffer due to the precipitation of $Ca_2(PO_4)_3$]. There was no effect on the T_m of pMHC with 5 mM Ca^{2+} (data not shown). NaCl does not change the size, shape, or oligomeric state of pMHC as determined by dynamic light scattering and sedimentation velocity experiments (data not shown).

Determining how NaCl could exert its effects on class I MHC is made difficult because of the nature of the complex. Most experiments looking at cosolvent effects were performed on small single-domain proteins. If we consider the pMHC ternary complex as a single unit, the effect would be due to changes in protein solvation, discrete ion binding to the protein, or charge screening on the protein. However, we may consider class I MHC to be a heavy chain with two ligands (peptide and β_2m). If we examine the molecule that way, the stabilization effect could be due to stabilization of either peptide binding or β_2m binding to the heavy chain as each ligand has been shown to be required for complex formation [(*37, 38*) and unpublished data].

Does the nature of the peptide affect the degree of thermal stabilization by NaCl? A summary of different peptides and different complexes tested for thermal stability by CD is

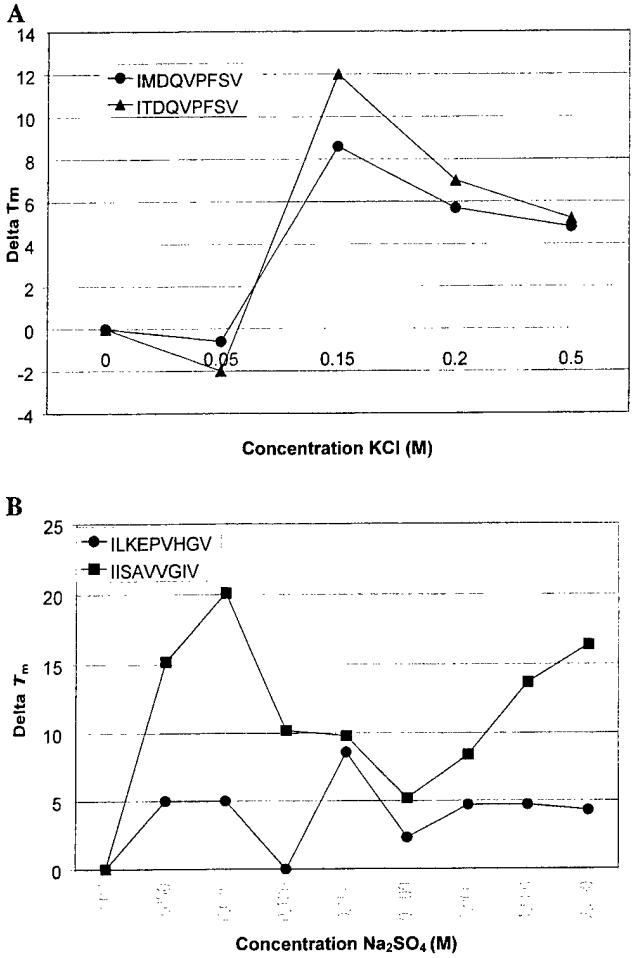

FIGURE 4: Effect generally correlates with the Hofmeister series for anions. Change in melting temperature of the class I complexes versus concentration of KCl and Na_2SO_4. (A) KCl stabilization of class I complexes of A2 bound to IMDQVPFSV or ITDQVPFSF. (B) Effect on thermal stabilization of pMHC (A2 and ILKEPVHGV or IISAVVGIV) in the presence of the indicated amounts of Na_2SO_4.

shown in Table 1. All of the peptides conform to the known peptide-binding motif for its allotype. Therefore, differences are not due to specific interactions with the peptide-binding cleft. However, peptide hydrophobicity could play a role. One can imagine that the addition of salt to the solvent would drive the association of peptide with the heavy chain. If peptide release is an important early step in thermal denaturation, then the stabilization would be greatest for nonpolar peptides and least for more polar peptides. Figure 5A shows a plot of the calculated hydrophobicity of a series of peptides versus the observed increase in T_m. There is clearly not a simple relationship suggesting that the hydrophobicity of the peptide does not affect the stability of the complex and that peptide release is not affected by the polarity of the solvent. This has been seen before for HLA-Aw68 (*39*). Additionally, if peptide dissociation were to affect the thermal stability of the protein, the pMHC in the cuvette should show a higher T_m in the presence of excess additional peptide. Addition of 5 μM IISAVVGIL excess peptide to A2 IISAVVGIL does not change the T_m (data not shown). Therefore, thermal denaturation is not keyed to peptide dissociation. Figure 5B shows a plot of the initial T_m versus the degree of stabilization. It is clear from the 77% correlation coefficient that the degree of stabilization

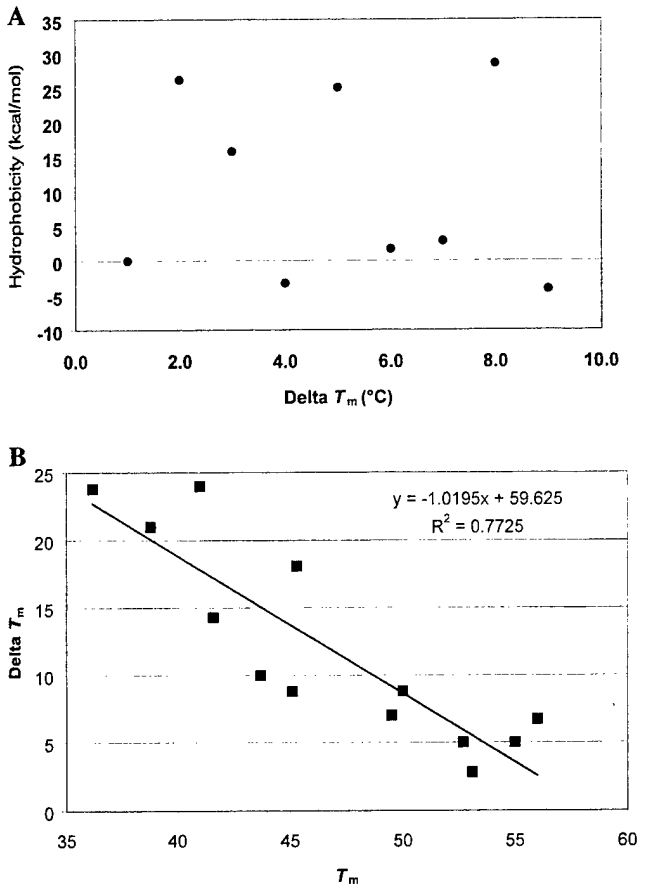

FIGURE 5: NaCl-induced change in T_m depends on the initial T_m and not on the hydrophobicity of the peptide ligand. (A) The plot of peptide hydrophobicity versus the delta T_m demonstrates that the change in T_m of class I MHC complexes is not dependent on the peptide sequence. Hydrophobicities are calculated from the sum of the free energies of transfer of the individual amino acids from cyclohexane to water (*50*). (B) Plot of the change in T_m versus initial T_m shows that the change in T_m is dependent on the initial T_m. The peptides and their respective T_ms are listed in Table 1.

is maximal for the poorest binding peptides. These data suggest that the stabilization by NaCl is not primarily due to any effect of the composition of the peptide, but it is related to how well the complex is held together.

Another ligand-binding scenario is that NaCl stabilizes the interaction of β_2m with the complex and thereby increases the thermal stability. The dissociation of β_2m has been described as a good measure of the dissociation of the peptide (*40*). Thus, it appears that peptide and β_2m dissociate from the heavy chain in a dependent fashion. The affinity of β_2m does not have a great effect on the T_m. Human β_2m has a 3-fold greater affinity for murine heavy chain than does murine β_2m (*41*). A murine class I MHC complex D^b folded with human β_2m and a low-affinity peptide FAPGVFPYM has a slightly higher T_m than the complex folded with murine β_2m (47 versus 42 °C) (Figure 6A). If β_2m dissociation were the first step in pMHC complex denaturation, addition of excess β_2m should shift the equilibrium to higher T_ms. However, if an excess of β_2m is added to the cuvette that contains the pMHC to be denatured, it does not increase the T_m (Figure 6B). Addition of NaCl to a mixture of pMHC and a 2-fold molar excess of β_2m and 100 mM NaCl stabilizes the protein to the degree seen in the absence of excess β_2m. To examine how a very large increase in affinity

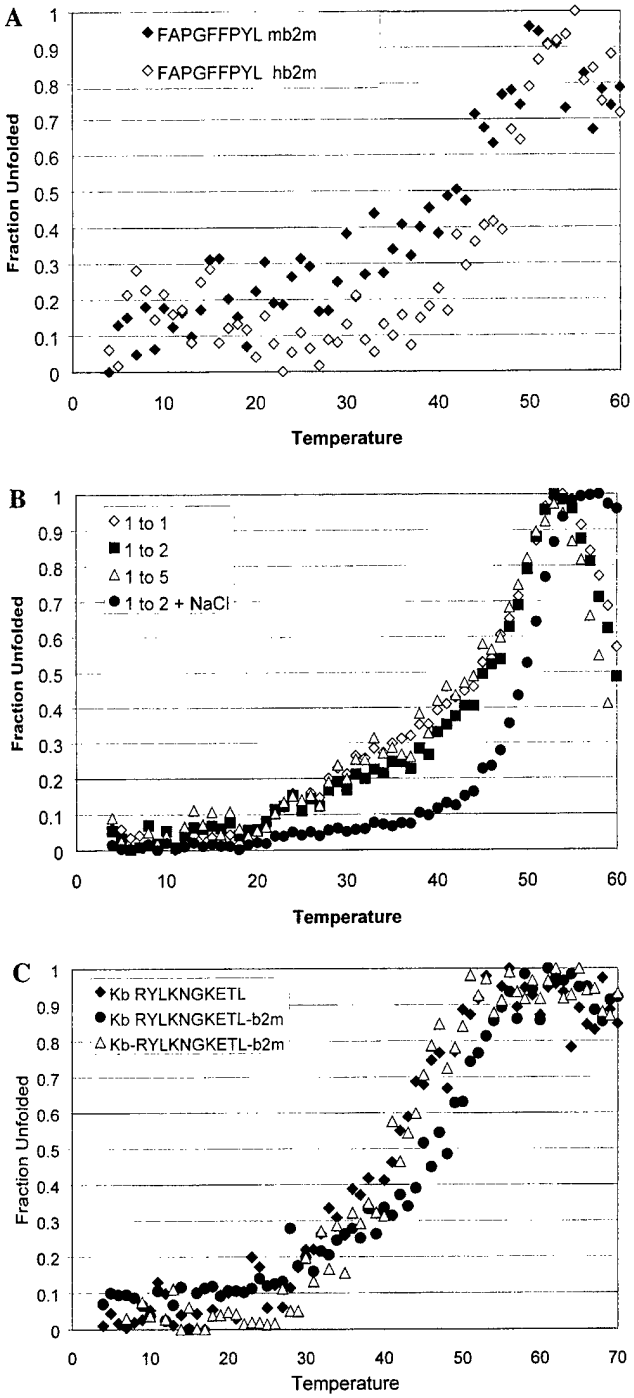

FIGURE 6: Increased association of β_2m increases the thermal stability, but not to the levels seen by the addition of NaCl. (A) D^b FAPGFFPYL has a higher T_m with hβ_2m bound than with mβ_2m. (B) The addition of molar excess of β_2m does not increase the T_m of pMHC. D^b KAVYNFATM was thermally denatured in the in the absence or presence of 1:1, 2:1, or 5:1 molar excess of mβ_2m added or in the presence of 2-fold molar excess β_2m plus 100mM NaCl. (C) Covalent addition of β_2m to the protein (Kb RYLKNGKETL-β_2m) increases the thermal stability of pMHC. However, covalent addition of peptide to make a fully covalent complex (Kb-RYLKNGKETL-β_2m) is not as thermally stable as the β_2m-attached and peptide-"free" complex.

would affect the thermal stability, we looked at protein that has β_2m covalently attached to the heavy chain (*42*). As can be seen in Figure 6C, the protein has a higher T_m compared to the noncovalently associated material (shift of ~5 °C). As the covalently linked protein has been produced in

mammalian cells and is glycosylated, we cannot exclude that the protein may be stabilized by the glycosylation. However, a complex that has covalently linked peptide and covalently linked β_2m (*43*) has a nearly identical T_m to that of the noncovalently associated ternary complex folded from material made in *E. coli* (Figure 6C). The fully covalent complex is most likely destabilized with respect to the covalent β_2m because the antigenic peptide extends from the peptide-binding groove. This has already been shown to be destabilizing due to the disruption of a conserved hydrogen bond with the peptide carboxyl terminus (*3*).

DISCUSSION

Class I MHC proteins have a simple role: to bind peptides in the endoplasmic reticulum and transport them to the cell surface. Differentiation of immunogenic versus ignored peptides is performed by TCR on the surface of circulating $CD8^+$ T cells. Most previously identified immunogenic viral epitopes bind to class I MHC well. However, peptides that bind poorly to class I MHC in vitro are also recognized by $CD8^+$ T cells in vivo (*24*). To resolve the paradox of the in vivo biological activity (i.e., T cell activation) with these in vitro physical measurements, we looked for other molecules that could stabilize proteins in vivo. This led to the examination of osmolytes as stabilizing agents and to the surprise observation that class I MHC stabilization was keyed to 150 mM NaCl.

When we began these studies, we expected to see modest increases in stability at high concentrations that we would extrapolate back to physiological conditions. As was anticipated, class I MHC molecules are stabilized by polyols such as glucose (Figure 1A) and sucrose (data not shown) at high concentrations. Other polyols, such as glycerol and poly(ethylene glycol), are destabilizing (data not shown). Amino acids (glycine data are not shown) and amino acid derivatives (Figure 1B) are destabilizing. NaCl (Figure 1C) and KCl (Figure 4A) are stabilizing at molar amounts compared to the absence of NaCl as is seen for other proteins. However, in a manner not seen before, class I MHC is maximally stabilized to thermal denaturation at physiological concentrations of added NaCl.

The mechanism of class I MHC stabilization to thermal denaturation by NaCl is not clear. There are two different levels of potential stabilization to consider. The first treats the trimolecular complex as the sum of its parts. In that scheme, peptide and β_2m may be considered as ligands binding to the heavy chain. Enzyme stability has been shown to be increased by increases in ionic strength. This phenomenon has been attributed to an increase in the affinity of the ligand for the protein due to the hydrophobic effect. The observation that the increased thermal stability in the more polar environment does not correlate with peptide hydrophobicity suggests that the release of peptide is not the critical event in thermal denaturation of this complex. Similarly, changes in β_2m affinity can increase thermal stability, but the effect is very small and does not account for the large change in thermal stability in the presence of salt. Last, in both of these instances, if the effect were due to a change in partitioning of the parts of the protein due to polarity of the environment, we would expect the effect to saturate, but not peak and decline as we observe here.

The second potential mechanism of stabilization treats the trimolecular complex as a single unit. This is not necessarily a poor assumption because the thermal denaturation is two-state. If the protein is a single unit, there are three potential explanations for this stabilization by salts: changes in protein solvation, discrete ion binding, and Debye–Hückel charge screening. 150 mM NaCl is considered to be a dilute aqueous salt solution and is not considered to contribute significantly to the protein solvation (hydrophobic) effect (*44, 45*). However, if protein solvation is a factor here, anions should dominate, and the effect should follow the Hofmeister series (*46*). If discrete ion binding plays a role, the effect should follow the electroselectivity series of anions binding to ion-exchange resins (*47*). In the absence of clear evidence of either of the other two possibilities, we would propose that Debye–Hückel screening is important, but it is normally seen in solutions below 0.1 M (*48*).

All of these factors probably contribute to the observed phenotype of class I MHC. While it is difficult to dissect the contributions from each of these factors from these experiments, we can make the following statements. The effect of the various ions does not appear to follow the electroselectivity series. It does follow the Hofmeister series, but as stated above, this effect is not typically described for dilute solutions. The most reasonable explanation is Debye–Hückel screening because stabilization (a) roughly follows ionic strength (compare NaCl versus Na_2SO_4 effects), (b) is observed at low concentrations of salts, and (c) is primarily associated with the cation (KCl stabilizes more than an equimolar amount of NaCl). Therefore, at concentrations up to 150 mM NaCl, a relatively long-range destabilizing charge within the protein is shielded (Debye length ~8 Å). At concentrations above 150 mM (shorter Debye length), the situation is reversed, and a stabilizing charge is shielded. This would make the protein less stable.

Thermal denaturation studies have been shown to be an accurate way to evaluate peptide binding to class I MHC molecules (*9, 30*), and the derived T_ms have been shown to be proportional to the peptide equilibrium dissociation constant (*23*). We have performed many experiments comparing T_ms and relative binding constants on the surface of T2 cells. The relative binding constant that we derive has shown an excellent correlation with T_m as long as there are no cosolvents present in the CD buffer (unpublished data). However, this correlation must be qualified. As demonstrated here, it clearly does not hold true under all conditions. In the absence of salts, measurement of the T_m of the class I ternary complex by CD spectroscopy is indicative of the inherent affinity of the peptide for class I receptors (*23*). In the presence of salts, the T_m no longer reflects the peptide affinity for the class I receptor but represents the overall thermal stability of the class I ternary complex. Therefore, it seems likely that the different experiments are measuring two different processes. In the absence of salt, the denaturation of the complex is tied to the affinity of the peptide. In the presence of salts, the T_m is not related to peptide binding affinity. As can be seen in Table 1, the T_m is basically the same (60 °C) for each complex independent of the peptide bound (the error in T_m is roughly 1 °C). Thus, the process measured by CD in the presence of NaCl is different from the process measured during equilibrium peptide binding measures. The CD experiment in the presence of NaCl

apparently evaluates the inherent protein stability independent of the peptide bound.

Class I molecules have a difficult role in the adaptive immune response. They must bind a diverse set of peptides with different affinities and low specificity. Anchor residues reduce the number of peptides that may bind and limit the repertoire of presentable peptides. An examination of the structure of class I MHC shows that the peptidic termini are buried deep in pockets in the peptide-binding groove. It appears likely that a large conformational change would be required to release peptide. Some evidence of this phenomenon has been seen with specific antibodies (*49*). Here we show that class I MHC is less soluble in the presence of 150 mM NaCl than it is in the absence of NaCl. This may be an important aspect of the role of class I MHC in the immune system. Class I MHC must hold potentially antigenic peptides for long half-lives in order to allow the clonotypic T cells time to engage the ligands. $CD8^+$ T cells that recognize these complexes lyse the cells presenting the peptide ligand on class I MHC. Thus, it is critical that the viral or cancer indicating peptide be only presented on the infected or cancerous cells; therefore, peptide exchange from one class I molecule to another at the cell surface is undesirable. Here we show that class I molecules denature in the absence of peptide, which makes them incapable of binding another peptide. Additionally, this is another mechanism to fully exploit the available repertoire of peptides; the class I MHC molecules take advantage of the cellular environment. In particular, we have shown salts can stabilize the class I MHC ternary complex against thermal denaturation. Therefore, researchers measuring peptide-binding affinity by CD for development of immunotherapeutics should be careful to observe that the link between affinity and T_m does not hold true in the presence of NaCl. However, these insights allow the selection of peptides once classified as unusable because of their low T_m. These results resolve the dilemma of how class I MHC molecules loaded with extremely low-affinity peptides can have subphysiological T_ms yet are able to stimulate T cells in the immune system.

ACKNOWLEDGMENT

We thank Drs. Richard Wolfenden, Gary Pielak, Dorothy Erie, John Sondek, and Jeffrey Frelinger for critical reading of the manuscript and many stimulating discussions, Dr. Jan Hermans for discussions about charge screening effects, and the laboratories of Dr. Frelinger and Dr. Erie for many helpful discussions.

REFERENCES

1. Heemels, M. T., and Ploegh, H. (1995) *Annu. Rev. Biochem. 64*, 463−491.
2. Collins, E. J. (1996) in *MHC Molecules: Expression, Assembly and Function* (Urban, R. G., and Chicz, R. M., Eds.) pp 113−134, Chapman & Hall, Austin.
3. Collins, E. J., Garboczi, D. N., and Wiley, D. C. (1994) *Nature 371*, 626−629.
4. Zhao, R., Loftus, D., Appella, E., and Collins, E. J. (1999) *J. Exp. Med. 189*, 359−370.
5. Batalia, M. A., and Collins, E. J. (1997) *Biopolym., Pept. Sci. 43*, 281−302.
6. Saper, M. A., Bjorkman, P. J., and Wiley, D. C. (1991) *J. Mol. Biol. 219*, 277−319.
7. Rock, K. L., and Goldberg, A. L. (1999) *Annu. Rev. Immunol. 17*, 739−779.
8. Ploegh, H. L. (1998) *Science 280*, 248−253.
9. Bouvier, M., and Wiley, D. C. (1994) *Science 265*, 398−402.
10. Falk, K., Rotzchke, O., and Rammensee, H.-G. (1990) *Nature 351*, 290−296.
11. Guo, H. C., Jardetzky, T. S., Garrett, T. P., Lane, W. S., Strominger, J. L., and Wiley, D. C. (1992) *Nature 360*, 364−366.
12. Hunt, D. F., Henderson, R. A., Shabanowitz, J., Sakaguchi, K., Michel, H., Sevilir, N., Cox, A. L., Appella, E., and Engelhard, V. H. (1992) *Science 255*, 1261−1263.
13. Ruppert, J., Kubo, R. T., Sidney, J., Grey, H. M., and Sette, A. (1994) *Behring Inst. Mitt. 94*, 48−60.
14. Madden, D. R., Gorga, J. C., Strominger, J. L., and Wiley, D. C. (1992) *Cell 70*, 1035−1048.
15. Sigal, L. J., and Wylie, D. E. (1996) *Mol. Immunol. 33*, 1323−1333.
16. Ruppert, J., Sidney, J., Celis, E., Kubo, R. T., Grey, H. M., and Sette, A. (1993) *Cell 74*, 929−937.
17. Collins, E. J., Booth, B. J. J., and Cerundolo, V. (1999) *J. Immunol. 162*, 331−337.
18. Engelhard, V. H. (1994) *Annu. Rev. Immunol. 12*, 181−207.
19. Germain, R. N. (1994) *Int. J. Technol. Assessment Health Care 10*, 81−92.
20. Alam, S. M., Travers, P. J., Wung, J. L., Nasholds, W., Redpath, S., Jameson, S. C., and Gascoigne, N.-R. J. (1996) *Nature 381*, 616−620.
21. Peoples, G. E., Goedegebuure, P. S., Smith, R., Linehan, D. C., Yoshino, I., and Eberlein, T. J. (1995) *Proc. Natl. Acad. Sci. U.S.A. 92*, 432−436.
22. Yoshino, I., Goedegebuure, P. S., Peoples, G. E., Parikh, A. S., DiMaio, J. M., Lyerly, H. K., Gazdar, A. F., and Eberlein, T. J. (1994) *Cancer Res. 54*, 3387−3390.
23. Morgan, C. S., Holton, J. M., Olafson, B. D., Bjorkman, P. J., and Mayo, S. L. (1997) *Protein Sci. 6*, 1771−1773.
24. Kuhns, J. J., Batalia, M. A., Yan, S., and Collins, E. J. (1999) *J. Biol. Chem. 274*, 36422−36427.
25. Yancey, P. H., Clark, M. E., Hand, S. C., Bowlus, R. D., and Somero, G. N. (1982) *Science 217*, 1214−1222.
26. Garboczi, D. N., Hung, D. T., and Wiley, D. C. (1992) *Proc. Natl. Acad. Sci. U.S.A. 89*, 3429−3433.
27. Mottez, E., Langlade-Demoyen, P., Gournier, H., Martinon, F., Maryanski, J., Kourilsky, P., and Abastado, J. P. (1995) *J. Exp. Med. 181*, 493−502.
28. Abastado, J. P., Lone, Y. C., Casrouge, A., Boulot, G., and Kourilsky, P. (1995) *J. Exp. Med. 182*, 439−447.
29. Reich, Z., Altman, J. D., Boniface, J. J., Lyons, D. S., Kozono, H., Ogg, G., Morgan, C., and Davis, M. M. (1997) *Proc. Natl. Acad. Sci. U.S.A. 94*, 2495−2500.
30. Fahnestock, M. L., Johnson, J. L., Feldman, R. M., Tsomides, T. J., Mayer, J., Narhi, L. O., and Bjorkman, P. J. (1994) *Biochemistry 33*, 8149−8158.
31. Pogue, R., Eron, J., Frelinger, J., and Matsui, M. (1995) *Proc. Natl. Acad. Sci. U.S.A. 92*, 8166−8170.
32. Salter, R. D., Howell, D. N., and Cresswell, P. (1985) *Immunogenetics 21*, 235−246.
33. Parham, P., and Brodsky, F. (1981) *Hum. Immunol. 3*, 277−299.
34. Barnstable, C., Bodmer, W., Brown, G., Galfre, G., Milstein, C., Williams, A., and Ziegler, A. (1978) *Cell 14*, 9−20.
35. Timasheff, S. N. (1995) in *Protein Stability and Folding: Theory and Practice* (Shirley, B. A., Ed.) pp 253−270, Humana Press, Totawa, NJ.
36. Robbins, P. A., Garboczi, D. N., and Strominger, J. L. (1995) *J. Immunol. 154*, 703−709.
37. Ljunggren, H. G., Stam, N. J., Ohlen, C., Neefjes, J. J., Hoglund, P., Heemels, M. T., Bastin, J., Schumacher, T. N., Townsend, A., Karre, K., and et, a. (1990) *Nature 346*, 476−480.
38. Townsend, A., Ohlen, C., Bastin, J., Ljunggren, H. G., Foster, L., and Karre, K. (1989) *Nature 340*, 443−448.

39. Collins, E. J., Booth, B., and Cerundolo, V. (1999) *J. Immunol 162*, 331−337.
40. Parker, K. C., DiBrino, M., Hull, L., and Coligan, J. E. (1992) *J. Immunol. 149*, 1896−1904.
41. Pedersen, L. O., Stryhn, A., Holter, T. L., Etzerodt, M., Gerwien, J., Nissen, M. H., Thogersen, H. C., and Buus, S. (1995) *Eur. J. Immunol. 25*, 1609−1616.
42. Abastado, J. P., Ojcius, D. M., Casrouge, A., Yeh, P., Schumacher, T. N., Ploegh, H. L., and Kourilsky, P. (1993) *Eur. J. Immunol. 23*, 1776−1783.
43. Delon, J., Gregoire, C., Malissen, B., Darche, S., Lemaitre, F., Kourilsky, P., Abastado, J. P., and Trautmann, A. (1998) *Immunity 9*, 467−473.
44. Timasheff, S. N., and Arakawa, T. (1990) in *Practical Approach Series* (Rickwood, D., and Hames, B. D., Eds.) pp 331−345, IRL Press, Oxford.
45. Tanford, C. (1991) *The Hydrophobic Effect: Formation of Micelles and Biological Membranes*, 2nd ed., Kreiger Publishing Company, Malabar, FL.
46. Collins, K. D., and Washabaugh, M. W. (1985) *Q. Rev. Biophys. 18*, 323−422.
47. Gjerde, D. T., Schmuckler, G., and Fritz, J. S. (1980) *J. Chromatogr. 187*, 35−45.
48. Eisenberg, D., and Crothers, D. (1979) *Physical Chemistry with Applications to the Life Sciences*, The Benjamin/ Cummings Publishing Company, Inc., Menlo Park, CA.
49. Yu, Y. Y. L., Myers, N. B., Hilbert, C. M., Harris, M. R., Balendiran, G. K., and Hansen, T. H. (1999) *Int. Immunol. 11*, 1897−1905.
50. Radzicka, A., and Wolfenden, R. (1988) *Biochemistry 27*, 1664−1670.

BI000442N

JBC Papers in Press. Published on April 3, 2001 as Manuscript M010791200

Class I MHC Anchor Substitutions Alter the Conformation of T Cell Receptor Contacts

Ashwani K. Sharma[1], Jennifer J. Kuhns[1], Shuqin Yan[1], Randy Freidline[1], Brian Long[1], Roland Tisch[1,3] and Edward J. Collins[1,2,3]

Department of Microbiology and Immunology[1], Department of Biochemistry and Biophysics[2], Lineberger Comprehensive Cancer Center[3], University of North Carolina, Chapel Hill, North Carolina 27599

Running title: Anchor substitutions alter TcR contacts in GP2.

Correspondence should be addressed to EJC, Department of Microbiology and Immunology, University of North Carolina, CB#7290, 804 M.E. Jones Building, Chapel Hill, NC 27599, phone: (919) 966-6869, fax: (919) 962-8103; e-mail: edward_collins@med.unc.edu

Abstract

An immunogenic peptide (GP2) derived from HER-2/*neu* binds to HLA-A2.1 (A2) very poorly. Some altered-peptide ligands (APL) of GP2 have increased binding affinity and generate improved CTL recognition of GP2 presenting tumor cells, but most do not. Increases in binding affinity of singly-substituted APL are not additive in doubly-substituted APL. A common first assumption about peptide binding to class I MHC is that each residue binds independently. In addition, immunologists interested in immunotherapy frequently assume that anchor substitutions do not affect T cell receptor (TCR) contact residues. However, the crystal structures of two GP2 APL show that the central residues change position depending on the identity of the anchor residue(s). Thus, it is clear that subtle changes in the identity of anchor residues may have significant effects on the positions of the TCR contact residues.

Introduction

Class I major histocompatibility complex (MHC) proteins bind short peptides (8-11 amino acids) endogenously derived either from host or pathogen. These peptides bind to newly formed class I molecules in the endoplasmic reticulum (ER). Peptide binding appears to be the final step in assembly of the complex (1). The complexes are presented to circulating T cells at the plasma membrane where clonotypic T cell receptors (TCR) on the surface of circulating cytotoxic T lymphocytes (CTL) may recognize the peptide/MHC complex (pMHC) and kill the presenting cell. An unaltered cell presents a population of self-peptides bound to class I MHC and is, for the most part, ignored by circulating T cells. However, cells infected by a virus or altered by neoplastic transformation present different peptides bound to class I MHC at the cell surface. These altered cells are recognized by clonotypic T cell receptors on CD8+ T cells and the T cells lyse the presenting cell. This action removes either the source of virus replication or the potential tumor (2).

The class I MHC molecule is a ternary complex consisting of a polymorphic heavy chain, a noncovalently associated light chain β_2-microglobulin (β_2m) and a small peptide (8-10 residues) (3-8). The peptide-binding cleft is formed by the α1 and α2 domains of the heavy chain. For effective CD8+ T cell responses, class I MHC molecules must bind many peptides of diverse sequence in sufficient abundance for long periods of time. Typical half-lives of immunodominant peptides are greater than 20 h at 37 °C (9,10). Peptides bind to class I MHC primarily through the invariant peptidic termini (11-13). In addition, the polymorphic residues within the peptide-binding groove create specificity pockets that select specific amino acids in the peptide (14,15). The specificity pockets for HLA-A2.1 (A2) are found close to the peptidic termini and are complementary in shape and charge to residues 2 (P2) and the last residue of the

peptide (PΩ). The specificity pockets play a large role in binding affinity to A2 (16,17), but not to all class I MHC (18). The result of this set of interactions in A2 is the binding of the ends of the peptide leaving the center relatively free of interactions. The center of the peptide bulges out of the peptide-binding cleft and the main chain rarely traverses the same path in two different peptides (19). The co-crystal structures of class I MHC and TCR show that the means of engagement between pMHC and TCR is conserved (20-24). The TCR binds in a diagonal manner with the TCR α chain interacting with the carboxyl end of the MHC α2 helix and the TCR β chain interacting with the carboxyl end of the MHC α1 helix. The CDR3 regions of the TCR α and β chains interact with the center of the peptide (P5 to P7 depending on the peptide) (25,26).

Two aspects about peptide binding to class I MHC are explored by the experiments presented here. The first aspect is an assumption that each amino acid in the peptide binds independently of one another to enhance or detract from the overall binding affinity. Using this assumption, a popular algorithm was designed to predict peptide epitopes that bind well (http://bimas.dcrt.nih.gov/molbio/hla_bind). This algorithm is predicated on the assumption that each residue binds independently (27). While this algorithm predicts many good binding peptides from proteins of interest (28-32), it fails to accurately predict the results of single amino acid substitutions for unknown reasons. The second aspect of peptide binding explored here is that residues at the anchor positions do not affect the conformation of residues elsewhere in the peptide. If one assumes that each residue binds independently, homologous substitutions would be the best choice to amplify and activate T cells specific for the parental antigen (33-35). The clear choice for modification is the anchor residues because they point into the binding cleft and are restricted in space by the specificity pockets. Thus, the conformation flexibility of the

peptide backbone should be limited and any alterations in the structure due to the anchor substitution would be expected to be local and small. This idea has been used to design peptides with increased affinity for class I MHC in order to enhance CTL stimulation. This approach has been successful in some cases (36-38), and varied in others (39). T cell stimulated using altered-peptide ligands (APL) are not necessarily the same population of T cells (40). This change in reactivity may be a result of interactions between the single amino acid changes and the MHC or between the substitutions and the other amino acids within the peptide. Our studies provide an explanation for the instances where alteration reduces or eliminates reactivity. These data show that substitutions at the anchor positions can directly alter the conformation of the residues at the center of the peptide and conversely that substitutions in the center can cause large changes at the termini.

We examined binding of a selection of known immunologically recognized peptide ligands from the tyrosine kinase family member HER-2/*neu* to the class I MHC molecule A2. HER-2/*neu* is overexpressed in approximately 30% of patients with breast cancer and similarly in all adenocarcinomas examined. Despite the presence of CTL that recognize these peptides bound to A2, the tumors are not eliminated. These HER-2/*neu*-derived peptides contain appropriate anchor residues, but still bind poorly to A2 molecules (41). One proposed explanation for inefficient tumor killing is that the peptide antigens bind poorly to A2 and these complexes are not stable enough to be recognized well by HER-2/*neu* peptide-specific CTL. Our long-term goal is to design high affinity APL for cancer immunotherapy. We have examined binding of one of these poor binding peptides, GP2 (IISAVVGIL), in order to design a ligand for immunotherapy. The crystallographic structure of GP2 co-crystallized with A2 ($A2^{GP2}$) shows that the center of the peptide is disordered and apparently does not make

stabilizing contacts with the peptide-binding cleft (41). GP2 has anchor residues that are present in high affinity peptides (isoleucine at position 2 and leucine at position 9) (42). Substitution of these anchor residues with amino acids most preferred by A2 increased the binding affinity, but not significantly (41).

Based on the crystallographic structure of GP2 (IISAVVGIL) bound to A2, we designed a new APL in which we substituted the position 5 (P5) valine with leucine (V5L). We hypothesized that the larger leucine would fit into a hydrophobic pocket in the peptide binding cleft under the $\alpha 2$ α helix where the smaller valine could not reach. We synthesized a series of peptides that included the V5L substitution in combination with our anchor substitutions in order to maximize binding affinity. Measurements of binding affinity and peptide off-rates showed that the enhancement in binding of doubly-substituted peptides was not the sum of the increases from the singly-substituted peptides. We interpreted this to mean that there are interactions between residues in the peptide or changes in the peptide structure. In order to understand these interactions, the crystallographic structures of A2 bound to the GP2 variants I2L/V5L ($A2^{I2L/V5L}$) and I2L/V5L/L9V ($A2^{I2L/V5L/L9V}$) were determined. These structures show that the peptide residues interact and that the TCR contact residues alter their positions depending on the identity of the anchor residue. Therefore, homologous substitutions anywhere in the peptide may have large unintended consequences in T cell recognition.

Methods

Peptides: The peptides used in this study are listed in Table I. All peptides were synthesized by the Peptide Synthesis Facility at the University of North Carolina, Chapel Hill. The peptides were purified to greater than 95% purity as confirmed by reversed-phased chromatography and

matrix-assisted laser desorption ionization time-of-flight mass spectrometry. Peptides were dissolved in 100% DMSO 10 mg/ml by weight. Final concentrations were determined by amino acid analysis by the Protein Chemistry Laboratory in the Department of Chemistry, University of North Carolina, Chapel Hill.

Preparation of HLA-A2.1/peptide complexes: HLA-A2.1/peptide complexes were prepared as described previously (43). Briefly, residues 1-275 of HLA-A2.1 (A2) and residues 1-99 of β_2-microglobulin (β_2-m) were produced in *E. coli* as inclusion bodies. Peptide, solubilized β_2-m and A2 heavy chain, solubilized in 8M urea, were rapidly diluted into folding buffer (100 mM Tris, pH 8.0, 400 mM L-Arg, 10mM GSH, 1 mM GSSG and protease inhibitors) at molar ratios of 10:2:1 respectively. The solution was incubated at 10 °C for 36 to 48 h, concentrated by ultrafiltration (Amicon), and purified by HPLC gel filtration (Phenomenex, BioSep-SEC-S2000)

Thermal Denaturation Studies: The thermal denaturation properties of peptide/A2 complexes were determined as described previously (12). Purified A2/peptide complexes were exchanged into a 10 mM KH_2/K_2HPO_4 buffer, pH 7.5 and adjusted to final concentration of 4-12 μM. Thermal denaturation curves (melting curve) of peptide/MHC complexes were recorded by monitoring the change in circular dichroic (CD) signal at 218 nm as a function of temperature from 4 °C to 95 °C on an AVIV 62-DS spectropolarimeter (Aviv Associates, Lakewood, NJ). The final melting curves were the average of at least three measurements for each complex. T_m values were calculated as the temperature at which 50% of the complexes are unfolded.

Cell surface stabilization assays: The ability of peptide to stabilize HLA-A2.1 (A2) on the surface of T2 (ATCC # CRL-1992) cells was determined as previously described (10). Briefly, T2 cells (2.5 x 10^5 cell/well) were incubated overnight in AIM V media (Gibco) with varying concentrations of peptide. The following morning, cells were stained with the A2 specific monoclonal antibody BB7.2. After 2 washes with wash buffer (1X PBS/ 2% FBS/0.1% sodium azide), the cells were incubated for 30 minutes at 4 °C with a 1:50 dilution of FITC-conjugated goat anti-mouse IgG antibody (Southern Biotechnologies). Fluorescence was detected on a FACScan (Becton-Dickinson, Lincoln Park, NJ). The data were then normalized to the mean channel fluorescence for the index peptide MLL at 50 μM. The MLL peptide (MLLSVPLLL) is derived from the signal sequence of calreticulin and has a similar hydrophobicity as the peptides used in this study.

Cell surface half-life assay: The half-life of peptide/A2 complexes on the surface of T2 cells was determined as previously described (10). Briefly, T2 cells (8 X 10^5 cell/well) were incubated overnight in AIM V media (Gibco) with 50 μM peptide. Cells were incubated in RPMI-1650, 10% FCS, 10 μg/ml brefeldin A (BFA) for 1 h. Because this concentration of BFA is toxic to the cells if they are exposed for long periods of time, the cells were transferred and maintained at 0.5 μg/ml through FACScan analysis. Cells were then stained with BB7.2 at various time points and analyzed by flow cytometry as described above. The mean fluorescence for the peptide at each time point minus the mean fluorescence of T2 cells incubated without exogenous peptide was calculated and normalized to the maximum level of fluorescence of for each APL (at t=0).

Crystallization, Data Collection and Data Processing: Crystals were grown by the hanging drop vapor diffusion method. Crystals were grown from 14-20% PEG 8000, 25 mM MES, pH 6.5 for both $A2^{I2L/V5L/L9V}$ and $A2^{I2L/V5L}$ over the course of two days by microseeding. Crystallographic data for both structures were collected at 100K in house (UNC Macromolecular Crystallography Facility) on a RIGAKU RU200 equipped with RAXIS IIC imaging plate detector and Oxford Cryostream. Data were collected from a single crystal of $A2^{I2L/V5L/L9V}$ and from two crystals of $A2^{I2L/V5L}$. Data for both structures were integrated with DENZO and intensities scaled with SCALEPACK (44). The statistics for each data set for both structures are given in Table II.

Structure Determination and Refinement: Both structures were determined by molecular replacement using AMoRe (45) within the CCP4 program suite (46). The A2/hepatitis peptide complex (PDB accession code 1HHH) was used as the search model (47). The crystal is triclinic, space group P1 with two molecules per asymmetric unit. The search model was divided into three pieces: the peptide binding superdomain ($\alpha1\alpha2$), the $\alpha3$ domain and β_2m light chain. Rigid body refinement was performed in CNS (48-50) leaving the $\alpha1\alpha2$, $\alpha3$ and β_2m as three separate rigid bodies. Nine rounds of torsional dynamics refinement with CNS and manual intervention with O (51) were performed. NCS restraints for regions not involved in crystal contacts were maintained and model was built for one copy in the asymmetric unit and the second generated using the NCS operators. To reduce model bias, peptide was not included in the initial three rounds of refinement. The electron density maps were generated using DM (46) using the functions for two-fold non-crystallographic averaging, histogram matching and solvent flattening. 144 water molecules for $A2^{I2L/V5L/L9V}$ and 35 waters for $A2^{I2L/V5L}$ were added to the

structure using the program ARP (52) combined with Refmac and confirmed by visual inspection of the electron density maps. Refinement statistics for each model are given in Table II.

Results

Stabilization derived from individual anchor substitutions is not additive in doubly-substituted peptides.

Previous studies had shown that substitutions at anchor positions increased thermal stability of $A2^{GP2}$ (41). The thermal stability of the peptides given in Table I show that the individual anchor substitutions generate increases in T_m from 2.4 °C ($A2^{L9V}$) to 5.8 °C ($A2^{I2L}$). If stabilization of binding were the sum of the increases, the double substitution should generate 8.4 °C increased thermal stability, but the observed difference is 6.1 °C ($A2^{I2L/L9V}$) suggesting that the mechanism of stabilization is not entirely peptide position independent. The T2 assays of binding and kinetics of dissociation confirm that there is an improvement in the double anchor substitution peptide. The binding is better (smaller K_r) and dissociation is slower (longer $T_{1/2}$) for the double anchor variant, but the expected changes in the values cannot be examined for the K_r because we cannot measure the value for $A2^{L9V}$.

A substitution at the center of the peptide designed to improved binding affinity actually reduces binding affinity by itself and interacts with anchor substitutions unexpectedly.

Based on the crystallographic structure of GP2 bound to A2 (41), we designed a new peptide in hopes that it would bind with higher affinity and reduce the disorder in the center of the peptide. In the structure, a large hydrophobic pocket was found near the P5 valine under the

α2 α helix. We hypothesized that a leucine in place of the valine at position five in the center of peptide would be more complementary to the size and shape of the pocket. The V5L peptide was synthesized and tested for binding affinity using T2 and circular dichroism (CD) assays. As can be seen in Table I, the V5L peptide actually binds worse than does GP2. In fact, it binds so poorly that $A2^{V5L}$ cannot be isolated in sufficient quantity to use in CD or structural studies. Combinations of anchor substitutions and the V5L substitutions were synthesized in order to determine whether better anchors would facilitate use of this hydrophobic pocket by the leucine at P5. It quickly became clear that these substituted residues were interacting in unexpected ways. For example, the T_m of $A2^{L9V}$ is 38.8 °C and the T_m of $A2^{V5L/L9V}$ is also 38.8 °C suggesting that the V5L substitution makes no difference to the stability of the complex. However, as described above, V5L alone binds with lower affinity compared to GP2 suggesting that it detracts from binding affinity. Confirming this, the T_m for the $A2^{I2L/V5L}$ double substitution is 39.0 °C, which is 3.2 °C lower than the single substitution I2L. Similarly, the T_m for the triple substitution $A2^{I2L/V5L/L9V}$ is 39.5 °C, which is 3.0 °C lower than the double substitution $A2^{I2L/L9V}$. These unexpected interactions as measured by CD are substantiated by the binding assays using T2 cells (Figure 1 and Table I). In order to understand these interactions, we decided to determine the crystal structures of some of these complexes.

The crystallographic structures of $A2^{I2L/V5L/L9V}$ and $A2^{I2L/V5L}$ confirm that the individual residues interact.

The molecular replacement solutions for the two complexes were unambiguous and gave correlation coefficients of 79% for $A2^{I2L/V5L/L9V}$ and 75% for $A2^{I2L/V5L}$ using 1HHH as a search model (47). These initial models were refined in CNS (48-50) and peptide was omitted during

the first three stages of refinement (until the R_{work} was below 30%) in both structures to reduce model bias. Density modification was performed with DM (46) to generate unbiased averaged electron density maps. The final structures are well defined in the electron density maps with average real-space-correlation coefficients of 78.4 and 80.7% with all fragments of $A2^{I2L/V5L}$ and $A2^{I2L/V5L/L9V}$. The final models have an overall R_{free} of 29.0% from 50-2.3 Å for $A2^{I2L/V5L}$ and 28.6% from 50 to 2.25 Å for $A2^{I2L/V5L/L9V}$ with good stereochemistry and no residues in the disallowed regions of a Ramachandran plot (Table II).

In both structures, the positions of the peptidic termini are unambiguous. However, the electron density at the center of the peptide is not well defined in both I2L/V5L and I2L/V5L/L9V peptides as was seen in the GP2 peptide (41). The peptides in the two molecules in the asymmetric unit are not equivalent in these structures demonstrating some of the dynamics that are known to be in the system. These differences in the peptides are not due to crystal contacts.

$A2^{I2L/V5L}$ structure

The electron density for the I2L/V5L peptide in molecule 2 (MOL2) in the asymmetric unit is broken at valine at P6 and glycine at P7 (Figure 2B). This is similar to what was observed in the GP2 peptide in the $A2^{GP2}$ crystal structure (41). However, in molecule 1 (MOL1) the peptide density is continuous over the main chain of the peptide (Figure 2A). However, the side chain for residue 6 is undefined and the temperature factors are higher for the central residues in the peptide demonstrating that the central residues in molecule 1 have greater disorder than the termini. The orientation of side chain of leucine at P5 is different between the two NCS symmetry-related molecules of $A2^{I2LV5L}$ (a rotation of ~83 ° of the Cα-Cβ bond) and they refine

to these different positions regardless of the starting position before CNS refinement. Although, there is not density to have absolute confidence in the position of the valine at position 6, there is sufficient electron density to strongly suggest that they orient in opposite directions. It appears that the P6 valine in molecule 2 points diagonally towards the α2 α helix and down into the cleft and the P6 valine in molecule 1 points towards the α1 α helix.

$A2^{I2L/V5L/L9V}$ structure

Although there are differences in the electron density for the peptides in molecule 1 and 2 in the asymmetric unit of the $A2^{I2L/V5L/L9V}$, the differences are much smaller than those observed for the two copies of $A2^{I2LV5L}$ and do not effect the orientations of the peptide in either model. There is a break in the electron density at valine at P6 and glycine at P7 in both symmetry related molecules as in the $A2^{GP2}$ structure and the orientation of valine at P6 can not be interpreted in either molecule (Figure2 C and D). The electron density for the leucine at P5 is not well defined but the direction of the electron density clearly indicates the orientation of the side chain as towards solvent in both copies in the asymmetric unit.

Discussion

For an effective immune response, it is necessary that class I MHC present antigenic peptides for long periods of time on the cell surface in order to allow detection of these complexes by circulating T cells (53). Many tumor cells appear to escape the immune response because antigenic peptides do not bind well to the class I MHC molecule that present them (54,55). If peptide does not bind efficiently to the MHC molecule, circulating T cells will not recognize the pMHC complex and cells presenting them will not be eliminated. To enhance the

binding affinity of antigenic peptides to class I MHC molecules, it is necessary to understand the forces that determine the binding affinity of peptide to class I MHC. We have examined a poor-binding peptide antigen derived from the tyrosine kinase family member HER-2/*neu*.

Our initial studies were focused on improving the binding affinity of GP2 to A2 by producing variants of GP2 at the anchors. The long-term goal is to use the variant peptide of GP2 to stimulate a vigorous GP2-specific CTL response in the cancer patient or as a vaccine in a healthy person. Because the prevalent belief is that each amino acid acts independently to generate positive or negative effects to binding energy (27), we expected to be able to generate the best binder in a stepwise fashion. That is, we saw an increase in thermal stability with I2L and L9V peptides bound to A2, and we expected to be able to add them together to get the best binding peptide (I2L/L9V). The data showed that increased affinity generated by this approach was not as great as we expected.

We determined the crystal structure of $A2^{GP2}$ and during our analysis of the structure, we hypothesized that if the valine at P5 was a leucine, it could take advantage of a hydrophobic pocket under the $\alpha 2$ α helix. However, our data clearly show this substitution also did not improve binding affinity. More surprisingly, we saw that combinations of anchor substitutions with the V5L substitution resulted in unexpected changes to the thermal stability of the complex. In one case, the substitution had no effect (V5L/L9V) and in others, it made a large difference (V5L and I2L/V5L/L9V peptides). In order to understand this phenomenon, we determined the crystal structures of $A2^{I2L/V5L}$ and $A2^{I2L/V5L/L9V}$.

The crystallographic structures show that electron density at the centers of the I2L/V5L and I2L/V5L/L9V peptides is disordered in most cases (3 out of 4 copies), highly mobile and poorly fit into the electron density in the last case ($A2^{I2L/V5L}$ molecule 1, Figure 2A, Table 3).

These data show that the substitutions at the anchors and at P5 have not decreased the flexibility at the center of the peptide and hence the binding affinity did not improve substantially.

Based on the crystal structure of $A2^{GP2}$, we expected the substituted leucine at the P5 position to point down into the peptide-binding cleft under the $\alpha 2$ α helix and to fit into a hydrophobic pocket there. The closest we came to predicting the orientation was in the structure of $A2^{I2L/V5L}$. A comparison of the structure of GP2 bound to A2 with the structure of $A2^{I2L/V5L}$ shows that the leucine points in the same direction as valine in molecule 1, but the side chain points away from the hydrophobic pocket (Figure 3A). In molecule 2 of $A2^{I2L/V5L}$, the leucine is more solvent exposed and is nowhere close to the pocket (Figure 3B). One of the surprises found in this analysis was that there were many changes seen in the positions of the amino acids past the P5 residue. Although there is not a great deal of confidence in the absolute positions of these central residues, it is clear that the density defines very different paths for the peptide molecule 1 (Figure 3A). The effect of this substitution on the carboxyl terminus in molecule 2 is even clearer. The position of the P5 residue alters the position of all the residues from P6 to P9 in molecule 2 such that the carboxylate is displaced by 1.0 Å (Figure 3B). The error associated with this model is 0.31 Å. Interestingly, an examination of the termini of these peptides (except for one copy of I2L/V5L/L9V) shows high temperature factors for the carboxyl termini as compared to the amino terminus (Table 3). This may reflect the more buried nature of the P1 residue as compared to the P9 residue.

The most apparent difference between the structures of GP2 and I2L/V5L/L9V peptides is the position of the leucine side chain at P5. In $A2^{I2L/V5L/L9V}$, the leucine points towards solvent away from A2 and does not interact with any residue of the peptide-binding superdomains regardless of which molecule is examined (Figure 3 C and D).

A comparison of the structures of $A2^{I2L/V5L}$ and $A2^{I2L/V5L/L9V}$ illustrates the types of differences that may occur when changing anchor residues (Figure 3 E and F, comparing both molecules 1 or molecules 2). In these peptides, the only difference is a substitution of the GP2 P9 leucine with valine. The result of the substitution can be a 90 ° rotation of the Cα-Cβ bond at P5 as observed in molecule 1 (Figure 3E). The rotation moves the leucine from pointing towards the α1 α helix ($A2^{I2L/V5L}$) to pointing towards solvent ($A2^{I2L/V5L/L9V}$). The P5 residue is directly in the center of the peptide and based on the co-crystal structures of pMHC and TcR would directly contact the CDR3 regions of the α and β chains of the TcR. Or the result of this substitution can be a reordering of the positions of all the atoms nearby at positions 7 through 9 as observed in molecule 2 (Figure 3F).

These data show large structural changes may occur by small homologous substitutions in the center or in the anchors of the peptide. These structural changes can greatly change TCR recognition. The observed changes in $A2^{I2L/V5L/L9V}$ and $A2^{V5L/L9V}$ are significantly larger than those previously seen to change TCR reactivity (22,56). In particular, changes as small as a substitution of tyrosine for phenylalanine at P1 can cause only localized changes about the P1 residue, but significant changes in T cell recognition (56). These changes are much more drastic. Immunization with I2L/L9V peptide generates small, but reproducible CTL reactivity in $A2K^b$ transgenic mice. Similarly, we are able to generate small responses to I2L/V5L/L9V, but we are unable to generate any responses to the I2L/V5L or V5L/L9V peptides (data not shown). These CTL data are not significant in themselves, but confirm the not unexpected idea that TCR recognition is different with respect to these peptides.

In summary, the data presented here show that substitutions in the center of a peptide bound to class I MHC may affect the positions of all of the residues within the peptide. In

addition, small homologous substitution in the anchor residues can dramatically alter the TCR contacting residues. Clearly, the presence of substituted residues may alter the positions of nearly all of the other residues even when the substitution is a minor homologous substitution as is seen in the case of peptides I2L/V5L and I2L/V5L/L9V. These types of changes were implicated previously in a study of H-2K^b with a panel of antibodies (57) that showed unexpected changes in antibody reactivity with a series of peptide substitutions. Similarly, homologous amino acid changes in TcR contact residues show greatly changed reactivity (58). This may be explained in terms of a change in the affinity between the peptide/MHC complex and the TcR, but could also be due to secondary changes in the peptide conformation as observed here. Examinations of clones induced by immunization of anchor substituted APL in a clinical trial showed large differences in the set of T cells expanded as compared to immunization with tumor-infiltrating lymphocytes (59). These data are surprising because substitutions have been shown to have very limited effects on the path of the peptide ((56) and unpublished data). One difference between those studies and these data are the relative binding affinity of the peptides studied. GP2 is a poor binding peptide and the others bind much better. Perhaps in the case of weak affinity, substitutions have a more dramatic effect. This may have important implications in cancer immunotherapy, because most peptides studied are of low affinity (41).

Figure Legends

Figure 1. Thermal denaturation as measured by circular dichroism shows unpredicted interactions between residues in the peptide. A. Thermal denaturation curves of complexes of A2 bound to GP2 variants. Each curve is the average of three independent experiments using 4 – 12 μM protein. The T_m is the temperature at which 50% of the complexes are unfolded. The error associated with this type of measurement is the sum of the error in the temperature controller and the curve fitting error. This is approximately 0.5 °C for each complex. **B.** Cell surface A2 was stabilized on T2 cells by the addition of the indicated amounts of peptide. The amount of peptide/A2 on the cell surface was measured by flow cytometry using the A2-specific monoclonal antibody, BB7.2. **C.** The rate of loss of cell surface peptide/A2 complexes was measured by treating the peptide-pulsed cells (as in panel B) with BFA to halt vesicular transport. Aliquots of cells were removed at the indicated times and the remaining peptide/A2 on the cells determined by incubating with BB7.2. Error bars are the standard error of the mean.

Figure 2. Averaged omit electron density maps contoured at 1σ show that the central residues of I2L/V5L and I2L/V5L/L9V are disordered as in the structure of $A2^{GP2}$. A. Averaged omit map of peptide $GP2^{I2L/V5L}$ in molecule 1 (MOL1) in the asymmetric unit. **B.** Averaged omit map of peptide molecule 2 (MOL2) in the $GP2^{I2L/V5L}$ asymmetric unit. **C.** Averaged omit map of peptide $GP2^{I2L/V5L/L9V}$ in molecule 1 of asymmetric unit. **D.** Averaged omit map of peptide $GP2^{I2L/V5L/L9V}$ in molecule 2 of asymmetric unit. All molecules displayed have A2 removed for clarity and the maps are contoured at 1σ with a cover radius of 1 Å.

Figure 3. Substitutions of amino acids in the peptide alter the position of other residues in the peptide. A. Superpositioning the α1α2 peptide-binding superdomains of $A2^{GP2}$ and

$A2^{I2L/V5L}$ molecule 1 (MOL1) shows that the central residues are in very different positions as a result of the double substitution. **B.** Superpositioning $A2^{GP2}$ and molecule 2 (MOL2) of $A2^{I2L/V5L}$ demonstrates the changes that occur from positions 6-9 in the peptide as a result of the changes. **C.** Comparisons of GP2 and I2L/V5L/L9V show moderate changes, and most are focused on the V5L substitution. **D.** A similar comparison with molecule 2 in I2L/V5L/L9V shows even fewer changes. **E.** A comparison of the peptides in I2L/V5L and I2L/V5L/L9V (both molecule 1 (MOL1)) shows alterations at the carboxyl end of the peptide as a result of the change L9V. **F.** A similar comparison (with molecules 2) illustrates, as did panel C, that the position 5 is altered drastically as a consequence of the L9V substitution.

Peptide	Sequence	T_m [b]	K_r [c]	$T_{1/2}$
HN654-662[a]	IISAVVGIL	36.4	>50	0.35
I2L[a]	ILSAVVGIL	42.2	22.9	1.76
L9V[a]	IISAVVGIV	38.8	>50	0.69
V5L	IISALVGIL	DNF	>50	<0.20
I2L/L9V[a]	ILSAVVGIV	42.5	10.0	2.48
I2L/V5L	ILSALVGIL	39.0	49.3	1.06
V5L/L9V	IISALVGIV	38.8	>50	1.18
I2L/V5L/L9V	ILSALVGIV	39.5	17.5	1.08
ML[a]	MLLSVPLLL	52.5	1.8	19.53

Table I: Summary of binding data of GP2 variant peptides to A2. Residues substituted with respect to wild type peptide are shown in boldface. T_m is the temperature (°C) at which 50% of protein is denatured as measured by circular dichroism. K_r is the relative binding constant as determined by the T2 cell surface assembly assay. $T_{1/2}$ is the half life of peptide/A2 complexes (in hours) as determined by the T2 cell surface stability assay. The error in the T_m is the sum of machine and curve fit errors and is typically about 0.5 °C. [a] values taken from Kuhns et al (41). [b] >50 means that the concentration to yield 50% of ML fluorescence is greater than 50 μM. [c] K_r is defined as concentration of peptide in μM that yields 50% mean channel fluorescence (MCF) as compared to the maximum fluorescence of the control peptide (ML) at 50 μM. The K_r value given for ML is the concentration that yields 50% MCF. DNF: did not fold in vitro so a T_m could not be derived.

Data	$A2^{I2L/V5L}$	$A2^{I2L/V5L/L9V}$
Space group	P1	P1
Cell Dimensions	a = 50.21 Å	a = 49.95 Å
	b = 62.32 Å	b = 62.93 Å
	c = 74.66 Å	c = 74.65 Å
	$\alpha = 82.15°$	$\alpha = 82.07°$
	$\beta = 76.38°$	$\beta = 76.50°$
	$\gamma = 78.33°$	$\gamma = 78.04°$
Molecules/ AU	2	2
R_{merge} (%)[1]	9.5 (29.3)	5.5 (18.0)
$\langle I/\sigma \rangle$	4.73 (2.4)	14.07 (5.7)
Unique reflections	33403	38,096
Total observations	114345	214687
Completeness (%)	87.7 (84.8)	93.8 (72.0)
Refinement		
Resolution	50-2.3	50-2.25
R_{work}[3]	26.3% (31833)	24.8% (36189)
R_{free}	29.0% (1670)	28.6% (1907)
Error[5]	0.31 Å	0.26 Å
Non-hydrogen atoms	6294	6292
<RS fit>[4]	78.4%	80.7%
Average B factor	21.3 $Å^2$	19.1 $Å^2$
No. of waters	35	144
RMSD		
Bonds	0.008 Å	0.007 Å
Angles	1.3°	1.3°
Ramachandran		
Most favorable	90.3%	91.6%
Additionally allowed	9.0%	8.1%
Generously allowed	0.7	0.3%
Disallowed	0.0%	0.0%

Table II :Summary of crystallographic and refinement statistics.

1. $R_{merge} = \Sigma_{hkl} \Sigma_i |I_i - \langle I \rangle| / \Sigma_{hkl} \Sigma_i I_i$, where I_i is the observed intensity and $\langle I \rangle$ is the average intensity of multiple observations of symmetry related reflections.
2. Number in parenthesis refers to the highest resolution shell. It is 2.44-2.3 Å for $A2^{I2L/V5L}$ and 2.39-2.25 Å for $A2^{I2L/V5L/L9V}$.
3. $R = \Sigma_{hkl} | |F_{obs}| - k |F_{cal}| | / \Sigma_{hkl} |F_{obs}|$, where R_{free} is calculated for a randomly chosen 5% of reflections, R_{work} is calculated for the remaining 95% of reflections used for structure refinement. Numbers in parenthesis refer to the number of structure factors used in the measurements.
4. <RS fit> is the average real space fit of all atoms on an electron density map from DM with two fold non-crystallographic averaging, histogram matching and solvent flattening
5. Error is the mean coordinate error estimate based on maximum likelihood measurements (46).

	Molecule 1						Molecule 2			
Peptide	GP2		I2L/V5L		I2L/V5L/L9V		I2L/V5L		I2L/V5L/L9V	
Position	B	RSCC	B	RSCC	B	RSCC	B	RSCC	B	RSCC
1	13.87	0.88	14.91	0.84	20.54	0.79	9.97	0.85	17.44	0.86
2	15.33	0.85	15.18	0.85	21.10	0.83	11.91	0.83	18.12	0.86
3	19.31	0.90	17.30	0.84	23.12	0.83	17.52	0.81	20.45	0.75
4	24.57	0.86	21.29	0.74	25.46	0.63	24.42	0.79	23.28	0.76
5	30.17	0.68	24.40	0.75	26.30	0.55	29.95	0.63	25.31	0.53
6	33.82	0.39	27.88	0.52	25.60	0.55	32.21	0.58	25.39	0.65
7	31.92	0.67	28.73	0.64	23.23	0.71	32.06	0.64	24.00	0.78
8	27.95	0.75	27.95	0.54	21.20	0.85	30.46	0.72	22.16	0.80
9	23.89	0.87	23.81	0.66	20.22	0.83	31.20	0.69	20.89	0.75

Table III: Comparison main chain temperature factors (B in $Å^2$) and real-space correlation coefficient (RSCC) between peptides GP2, I2L/V5L and I2L/V5L/L9V in the two molecules in the asymmetric unit. The GP2 peptides are identical for both molecules in the asymmetric unit.

References

1. Lehner, P. J., and Trowsdale, J. (1998) *Current Biology* **8**(17), R605-8
2. Ploegh, H. L. (1998) *Science* **280**(5361), 248-53
3. Silver, M. L., Guo, H. C., Strominger, J. L., and Wiley, D. C. (1992) *Nature* **360**(6402), 367-9
4. Young, A. C., Zhang, W., Sacchettini, J. C., and Nathenson, S. G. (1994) *Cell* **76**(1), 39-50.
5. Madden, D. R., Gorga, J. C., Strominger, J. L., and Wiley, D. C. (1992) *Cell* **70**(6), 1035-48
6. Fremont, D. H., Matsumura, M., Stura, E. A., Peterson, P. A., and Wilson, I. A. (1992) *Science* **257**(5072), 919-27.
7. Bjorkman, P. J., Saper, M. A., Samraoui, B., Bennett, W. S., Strominger, J. L., and Wiley, D. C. (1987) *Nature* **329**(6139), 506-12.
8. Bjorkman, P. J., Saper, M. A., Samraoui, B., Bennett, W. S., Strominger, J. L., and Wiley, D. C. (1987) *Nature* **329**(6139), 512-8.
9. Stuber, G., Leder, G. H., Storkus, W. T., Lotze, M. T., Modrow, S., Szekely, L., Wolf, H., Klein, E., Karre, K., and Klein, G. (1994) *Eur J Immunol* **24**(3), 765-768
10. Pogue, R. R., Eron, J., Frelinger, J., and Matsui, M. (1995) *Proc. Natl. Acad. Sci. USA* **92**, 8166-8170
11. Bouvier, M., Guo, H. C., Smith, K. J., and Wiley, D. C. (1998) *Proteins* **33**(1), 97-106.
12. Bouvier, M., and Wiley, D. C. (1994) *Science* **265**, 398-402
13. Khan, A. R., Baker, B. M., Ghosh, P., Biddison, W. E., and Wiley, D. C. (2000) *J Immunol* **164**(12), 6398-405.
14. Guo, H. C., Madden, D. R., Silver, M. L., Jardetzky, T. S., Gorga, J. C., Strominger, J. L., and Wiley, D. C. (1993) *Proc Natl Acad Sci U S A* **90**(17), 8053-7

15. Garrett, T. P., Saper, M. A., Bjorkman, P. J., Strominger, J. L., and Wiley, D. C. (1989) *Nature* **342**(6250), 692-6

16. Ruppert, J., Sidney, J., Celis, E., Kubo, R. T., Grey, H. M., and Sette, A. (1993) *Cell* **74,** 929-937

17. Colbert, R. A., Rowland-Jones, S. L., McMichael, A. J., and Frelinger, J. A. (1994) *Immunity* **1**(2), 121-30

18. Collins, E. J., Booth, B. J. J., and Cerundolo, V. (1999) *J. Immunol.* **162,** 331-337

19. Batalia, M. A., and Collins, E. J. (1997) *Biopoly* **43,** 281-302

20. Garboczi, D. N., Ghosh, P., Utz, U., Fan, Q. R., Biddison, W. E., and Wiley, D. C. (1996) *Nature* **384**(6605), 134-41.

21. Ding, Y. H., Smith, K. J., Garboczi, D. N., Utz, U., Biddison, W. E., and Wiley, D. C. (1998) *Immunity* **8**(4), 403-11

22. Ding, Y. H., Baker, B. M., Garboczi, D. N., Biddison, W. E., and Wiley, D. C. (1999) *Immunity* **11**(1), 45-56

23. Garcia, K. C., Degano, M., Stanfield, R. L., Brunmark, A., Jackson, M. R., Peterson, P. A., Teyton, L., and Wilson, I. A. (1996) *Science* **274**(5285), 209-19

24. Garcia, K. C., Degano, M., Pease, L. R., Huang, M., Peterson, P. A., Teyton, L., and Wilson, I. A. (1998) *Science* **279**(5354), 1166-72

25. Garboczi, D. N., and Biddison, W. E. (1999) *Immunity* **10**(1), 1-7.

26. Garcia, K. C., Teyton, L., and Wilson, I. A. (1999) *Annu Rev Immunol* **17,** 369-97

27. Parker, K. C., Bednarek, M. A., and Coligan, J. E. (1994) *Journal of Immunology* **152**(1), 163-75

28. Harada, M., Li, Y. F., El-Gamil, M., Rosenberg, S. A., and Robbins, P. F. (2001) *Cancer Research* **61**(3), 1089-1094

29. Kessler, J. H., Beekman, N. J., Bres-Vloemans, S. A., Verdijk, P., van Veelen, P. A., Kloosterman-Joosten, A. M., Vissers, D. C. J., ten Bosch, G. J. A., Kester, M. G. D., Sijts, A., Drijfhout, J. W., Ossendorp, F., Offringa, R., and Melief, C. J. M. (2001) *Journal of Experimental Medicine* **193**(1), 73-88

30. Heukamp, L. C., van der Burg, S. H., Drijfhout, J. W., Melief, C. J. M., Taylor-Papadimitriou, J., and Offringa, R. (2001) *International Journal of Cancer* **91**(3), 385-392

31. Dannull, J., Diener, P. A., Prikler, L., Furstenberger, G., Cerny, T., Schmid, U., Ackermann, D. K., and Groettrup, M. (2000) *Cancer Research* **60**(19), 5522-5528

32. Minev, B., Hipp, J., Firat, H., Schmidt, J. D., Langlade-Demoyen, P., and Zanetti, M. (2000) *Proceedings of the National Academy of Sciences of the United States of America* **97**(9), 4796-4801

33. Slansky, J. E., Rattis, F. M., Boyd, L. F., Fahmy, T., Jaffee, E. M., Schneck, J. P., Margulies, D. H., and Pardoll, D. M. (2000) *Immunity* **13**(4), 529-538

34. Micheletti, F., Guerrini, R., Formentin, A., Canella, A., Marastoni, M., Bazzaro, M., Tomatis, R., Traniello, S., and Gavioli, R. (1999) *European Journal of Immunology* **29**(8), 2579-2589

35. Sloan-Lanchester, J., and Allen, P. (1996) *Annu Rev Immunol*,

36. Overwijk, W. W., Tsung, A., Irvine, K. R., Parkhurst, M. R., Goletz, T. J., Tsung, K., Carroll, M. W., Liu, C., Moss, B., Rosenberg, S. A., and Restifo, N. P. (1998) *J Exp Med* **188**(2), 277-86

37. Fong, L., Ruegg, C. L., Brockstedt, D., Engleman, E. G., and Laus, R. (1997) *J Immunol* **159**(7), 3113-7

38. Rosenberg, S. A., Yang, J. C., Schwartzentruber, D. J., Hwu, P., Marincola, F. M., Topalian, S. L., Restifo, N. P., Dudley, M. E., Schwarz, S. L., Spiess, P. J., Wunderlich, J. R., Parkhurst, M. R., Kawakami, Y., Seipp, C. A., Einhorn, J. H., and White, D. E. (1998) *Nat Med* **4**(3), 321-7

39. Parkhurst, M. R., Salgaller, M. L., Southwood, S., Robbins, P. F., Sette, A., Rosenberg, S. A., and Kawakami, Y. (1996) *J Immunol* **157**(6), 2539-48

40. El-Shami, K. M., Tirosh, B., Popovic, D., Carmon, L., Tzehoval, E., Vadai, E., Feldman, M., and Eisenbach, L. (2000) *Int J Cancer* **85**(2), 236-42

41. Kuhns, J. J., Batalia, M. A., Yan, S., and Collins, E. J. (1999) *J. Biol. Chem.* **274**(51), 36422-36427

42. Rammensee, H. G., Friede, T., and Stevanoviic, S. (1995) *Immunogenetics* **41**(4), 178-228

43. Garboczi, D. N., Hung, D. T., and Wiley, D. C. (1992) *Proc. Natl. Acad. Sci. U.S.A.* **89,** 3429-3433

44. Otwinowski, Z., and Minor, W. (1996) in *Methods in Enzymology* (Carter, C. W. J., and Sweet, R. M., eds) Vol. 276, pp. 307-326, A vols., Academic Press, Inc., New York, NY

45. Navaza, J., and Saludjian, P. (1998) *Methods in Enzymology* **276,** 581-594

46. Dodson, E. J., Winn, M., and Ralph, A. (1998) *Methods in Enzymology* **277,** 620-633

47. Madden, D. R., Garboczi, D. N., and Wiley, D. C. (1993) *Cell* **75**(4), 693-708

48. Brunger, A. T. (1992) *Nature* **355,** 472-474

49. Pannu, N. S., and Reed, R. J. (1996) *Acta Cryst* **A52,** 659-668

50. Adams, P. D., Pannu, N. S., Read, R. J., and Brunger, A. T. (1997) *Proc. Natl. Acad. Sci. USA* **94,** 5018-5023

51. Jones, T. A., Zou, J.-Y., Cowan, S. W., and Kjeldgaard, M. (1991) *Acta Crystallogra* **A47,** 110-119

52. Lamzin, V. S., and Wilson, K. S. (1998) *Methods in Enzymology* **277,** 269-305

53. Alam, S. M., Travers, P. J., Wung, J. L., Nasholds, W., Redpath, S., Jameson, S. C., and Gascoigne, N. R. J. (1996) *Nature* **381,** 616-620

54. Peoples, G. E., Goedegebuure, P. S., Smith, R., Linehan, D. C., Yoshino, I., and Eberlein, T. J. (1995) *Proceedings of the National Academy of Sciences of the United States of America* **92**(2), 432-6

55. Yoshino, I., Goedegebuure, P. S., Peoples, G. E., Parikh, A. S., DiMaio, J. M., Lyerly, H. K., Gazdar, A. F., and Eberlein, T. J. (1994) *Cancer Research* **54**(13), 3387-90

56. Kirksey, T. J., Pogue-Caley, R. R., Frelinger, J. A., and Collins, E. J. (1999) *J. Biol. Chem* **274,** 37259-37264

57. Chen, W., Fecondo, J., and McCluskey, J. (1994) *Mol Immunol* **31**(14), 1069-75

58. Ono, T., DiLorenzo, T. P., Wang, F., Kalergis, A. M., and Nathenson, S. G. (1998) *J Immunol* **161**(10), 5454-63

59. Clay, T. M., Custer, M. C., McKee, M. D., Parkhurst, M., Robbins, P. F., Kerstann, K., Wunderlich, J., Rosenberg, S. A., and Nishimura, M. I. (1999) *J Immunol* **162**(3), 1749-55

Acknowledgements

We thank Carrie Barnes for excellent technical assistance; members of the Collins and Frelinger labs for stimulating discussions; and Dr. Jeffrey Frelinger for critical reading of the manuscript. Supported by DOD grant DAMD17-97-1-7052. Coordinates for $A2^{I2L/V5L/L9V}$ (1EEY) and $A2^{I2L/V5L}$ (1EEZ) have been deposited in the Protein Data Bank.

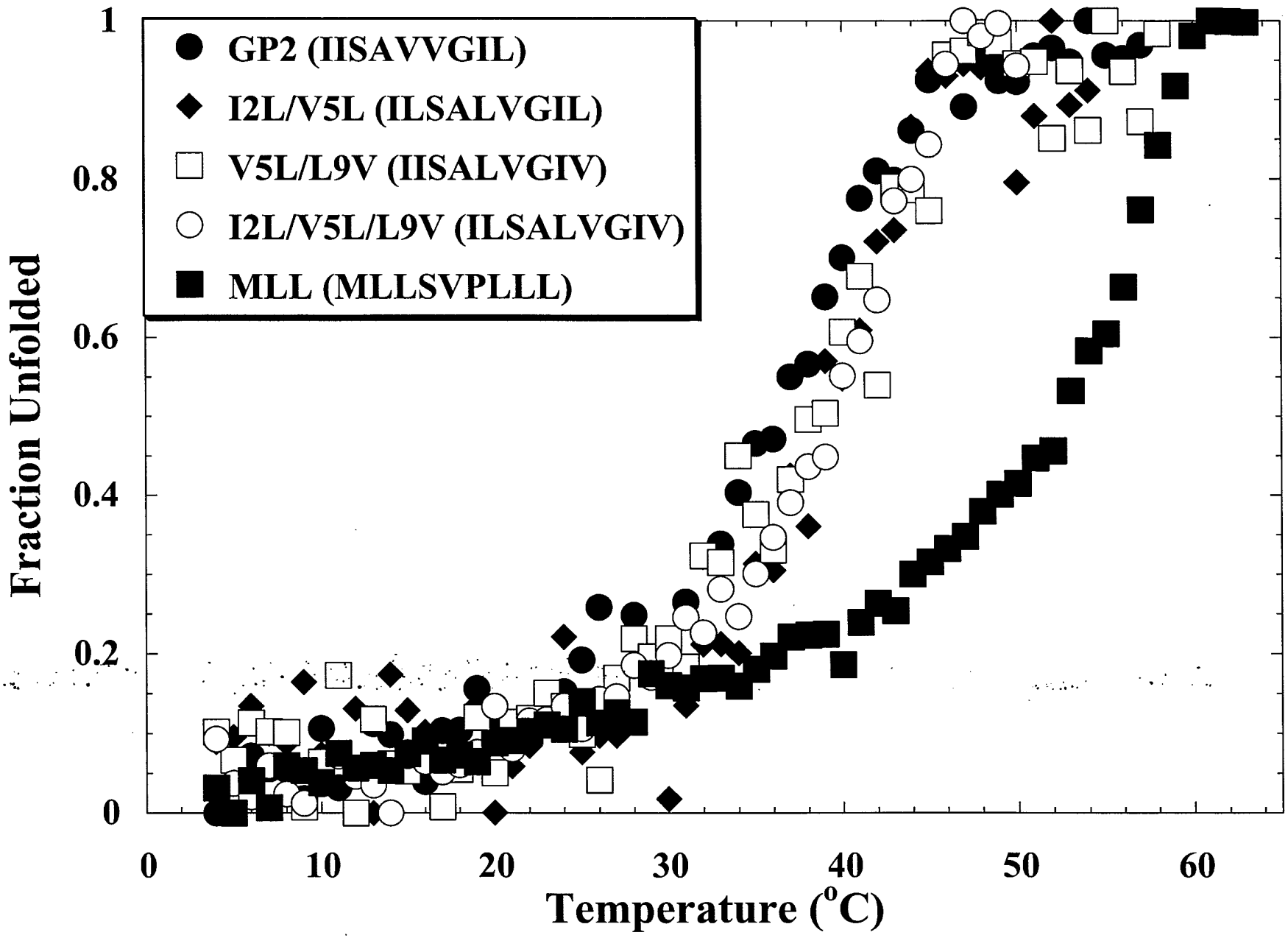
GP2 (IISAVVGIL)
I2L/V5L (ILSALVGIL)
V5L/L9V (IISALVGIV)
I2L/V5L/L9V (ILSALVGIV)
MLL (MLLSVPLLL)
Fraction Unfolded
1
0.8
0.6
0.4
0.2
0
0
10
20
30
40
50
60
Temperature (°C)

Figure 1A

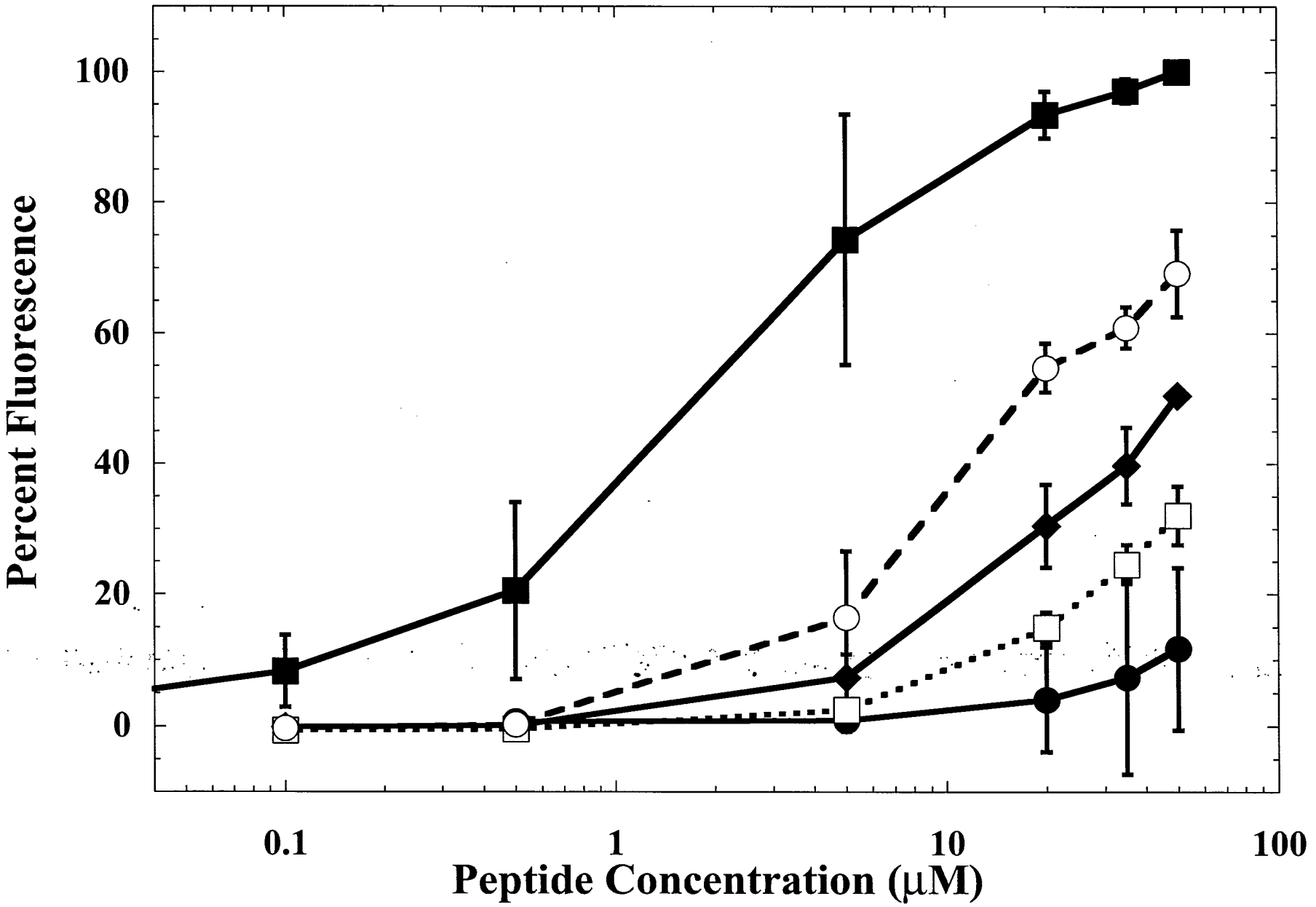
Percent Fluorescence
100
80
60
40
20
0
0.1
1
10
100
Peptide Concentration (μM)

Figure 1B

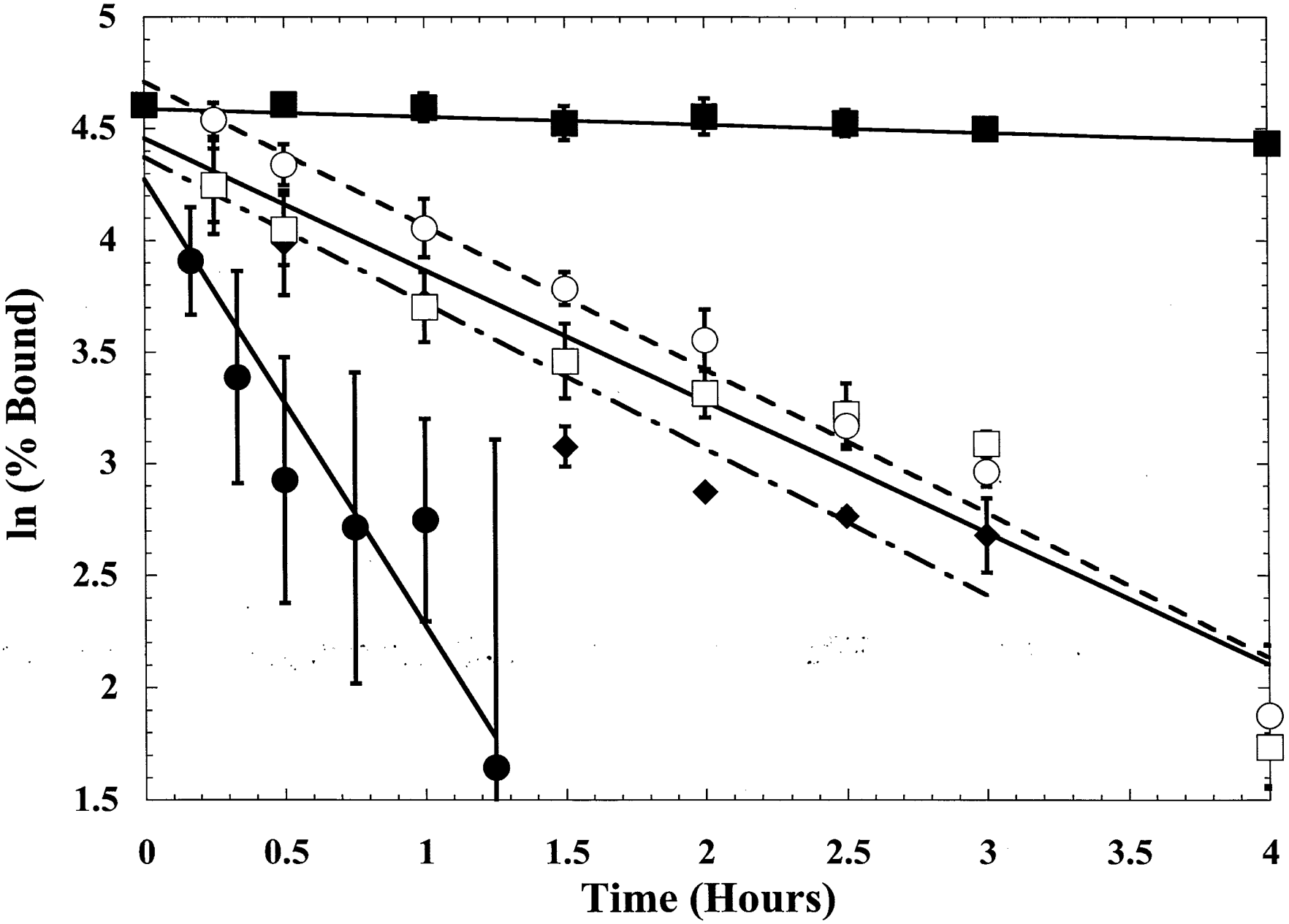

Figure 1C

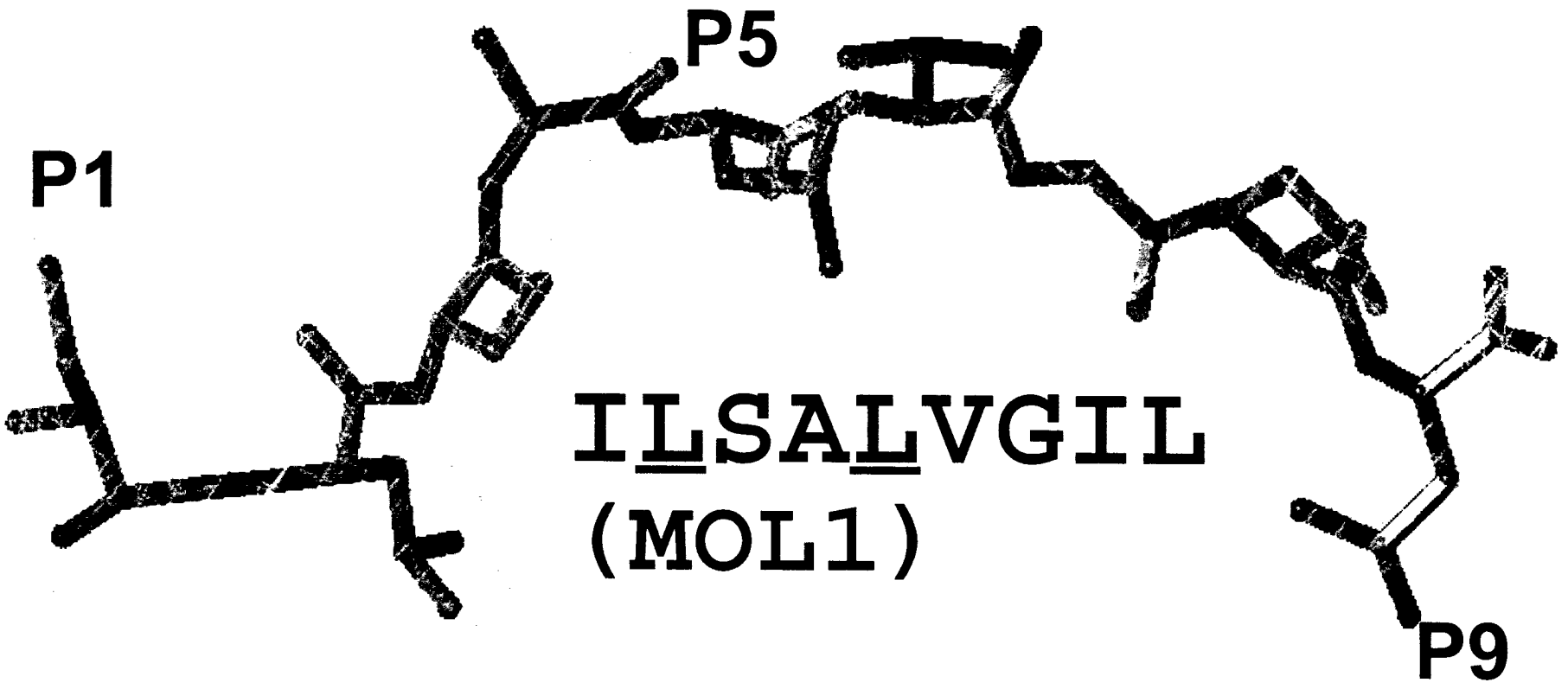

Figure 2A

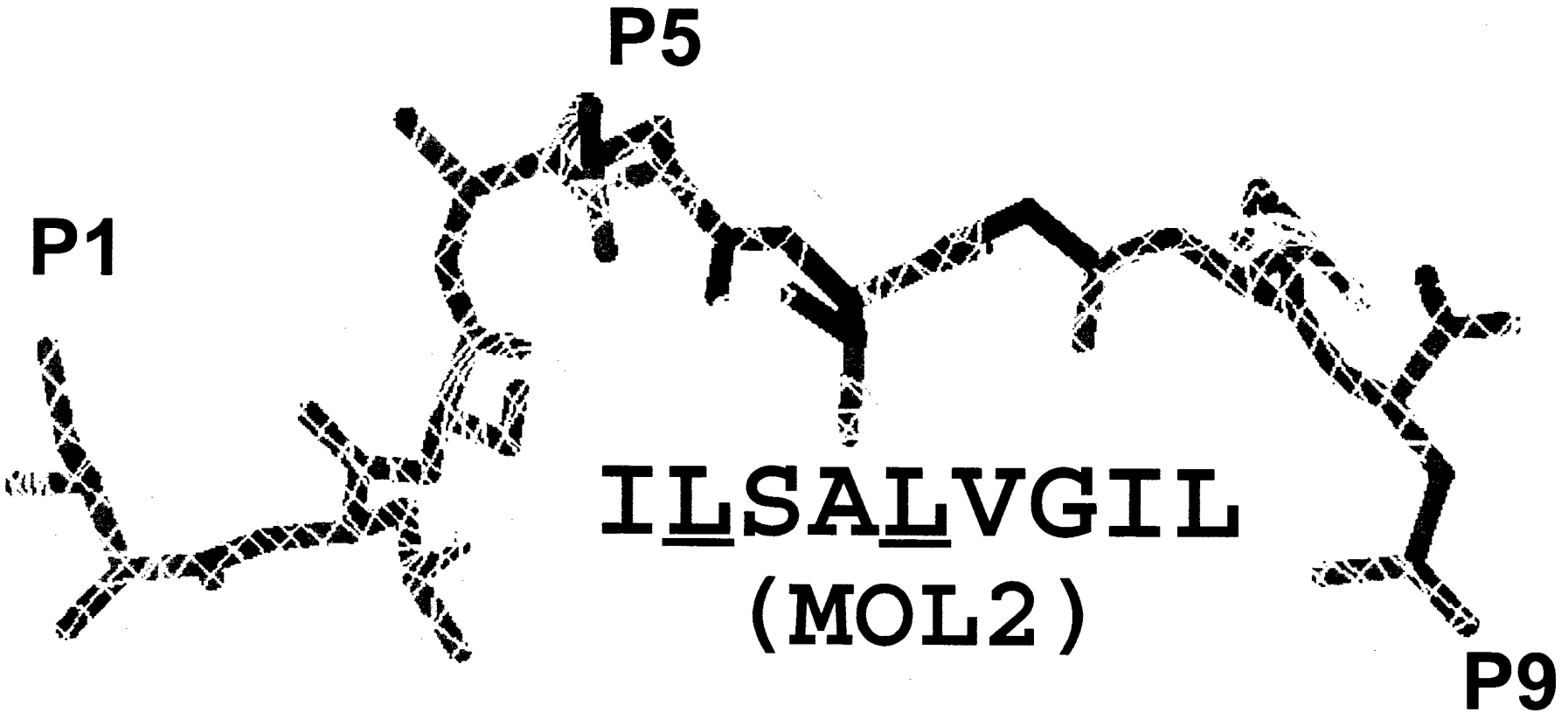

Figure 2B

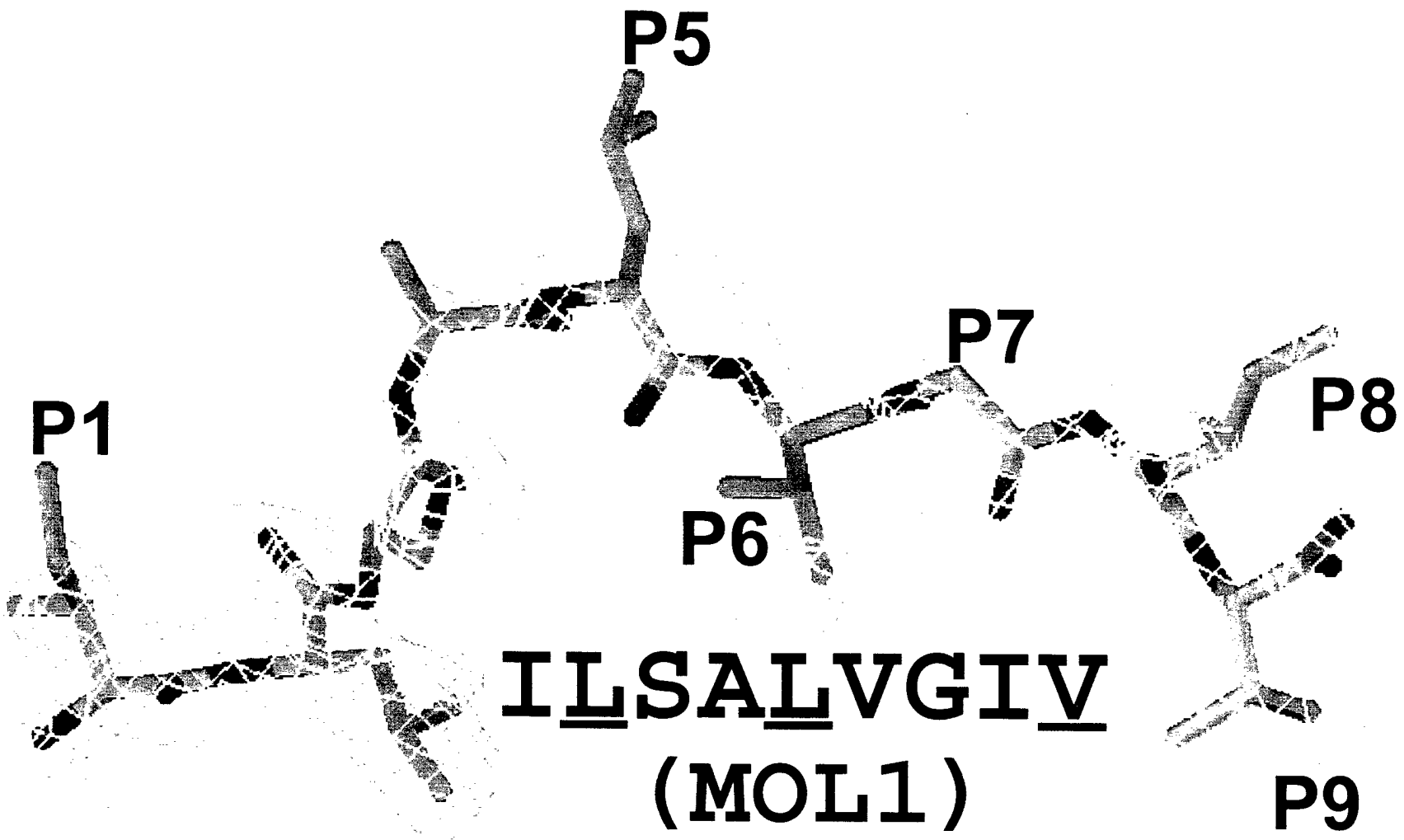

Figure 2C

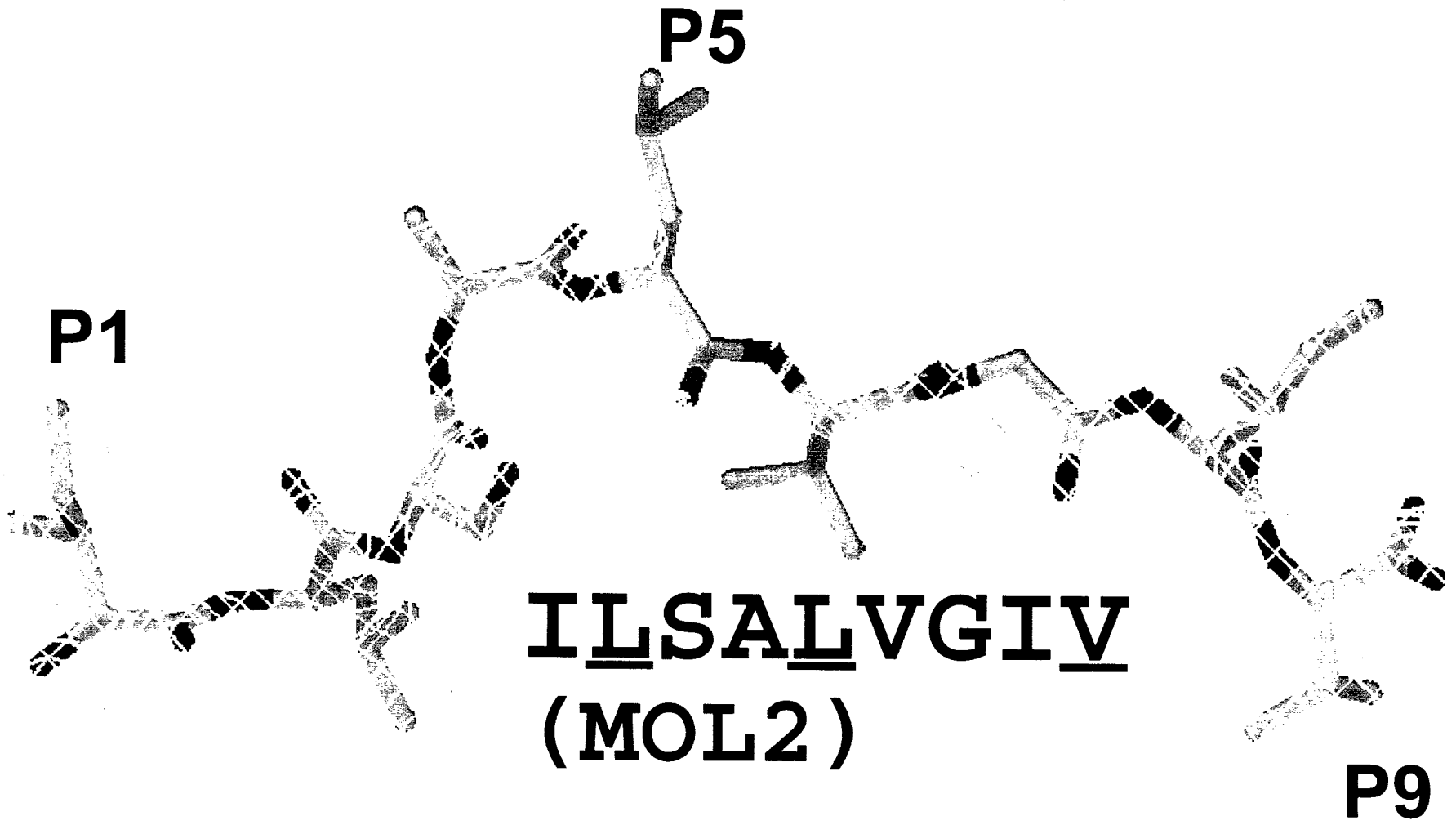

Figure 2D

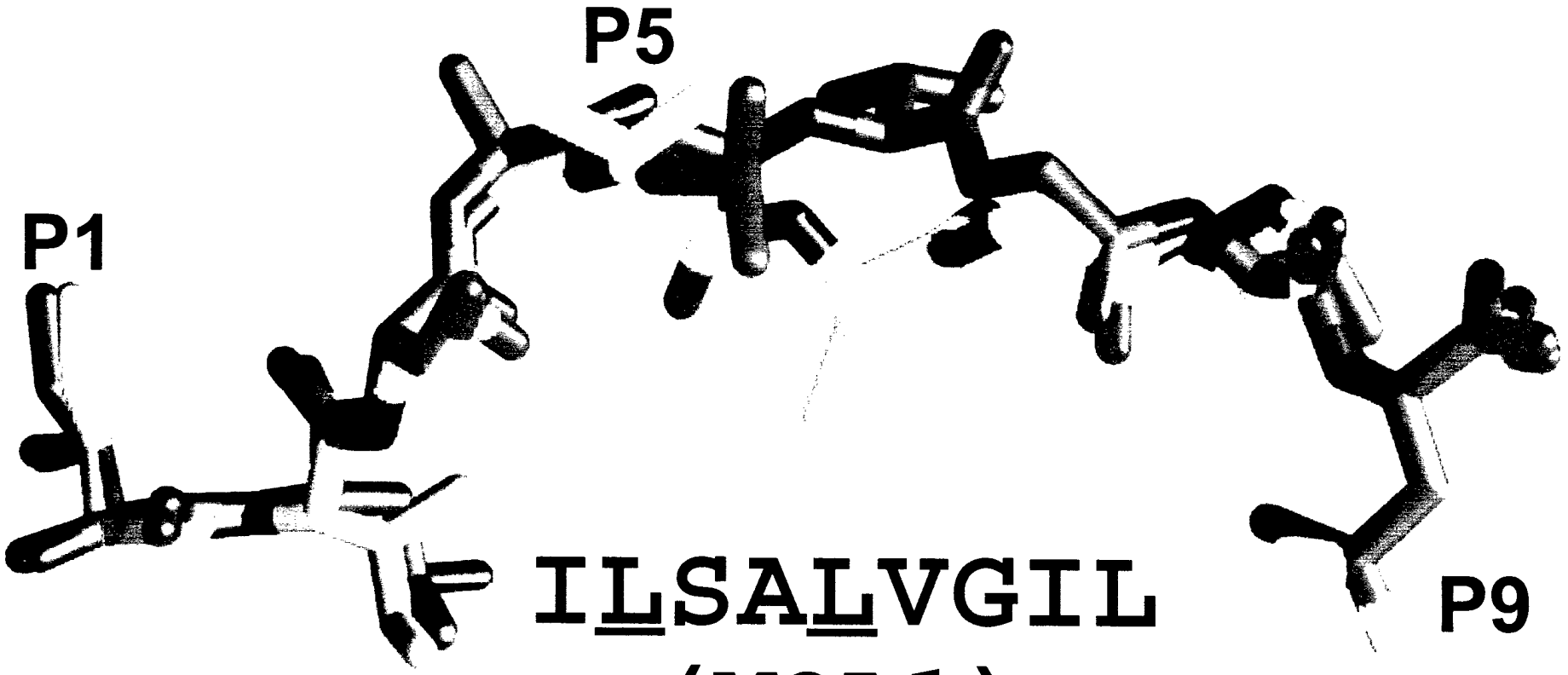

Figure 3A

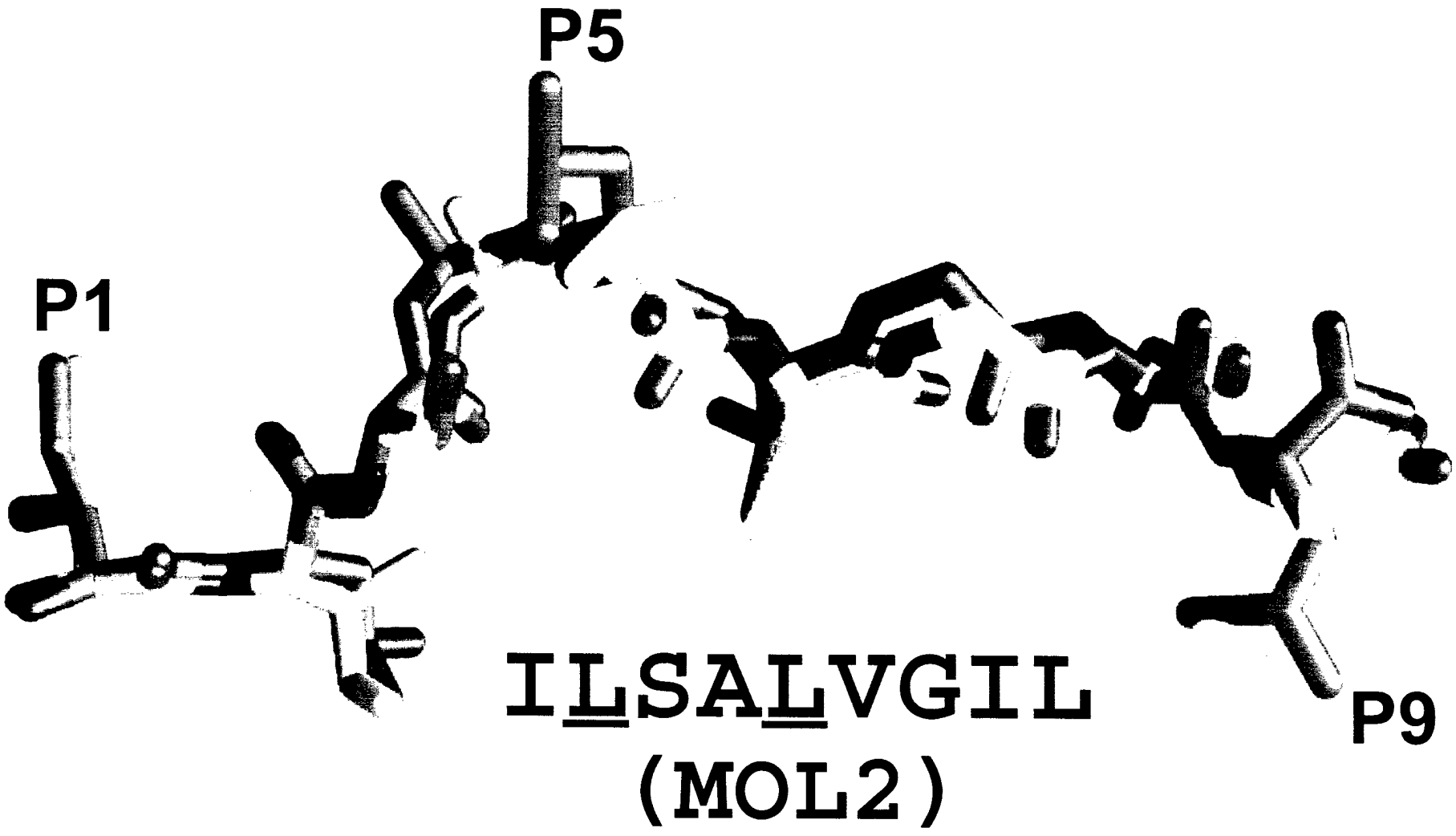

Figure 3B

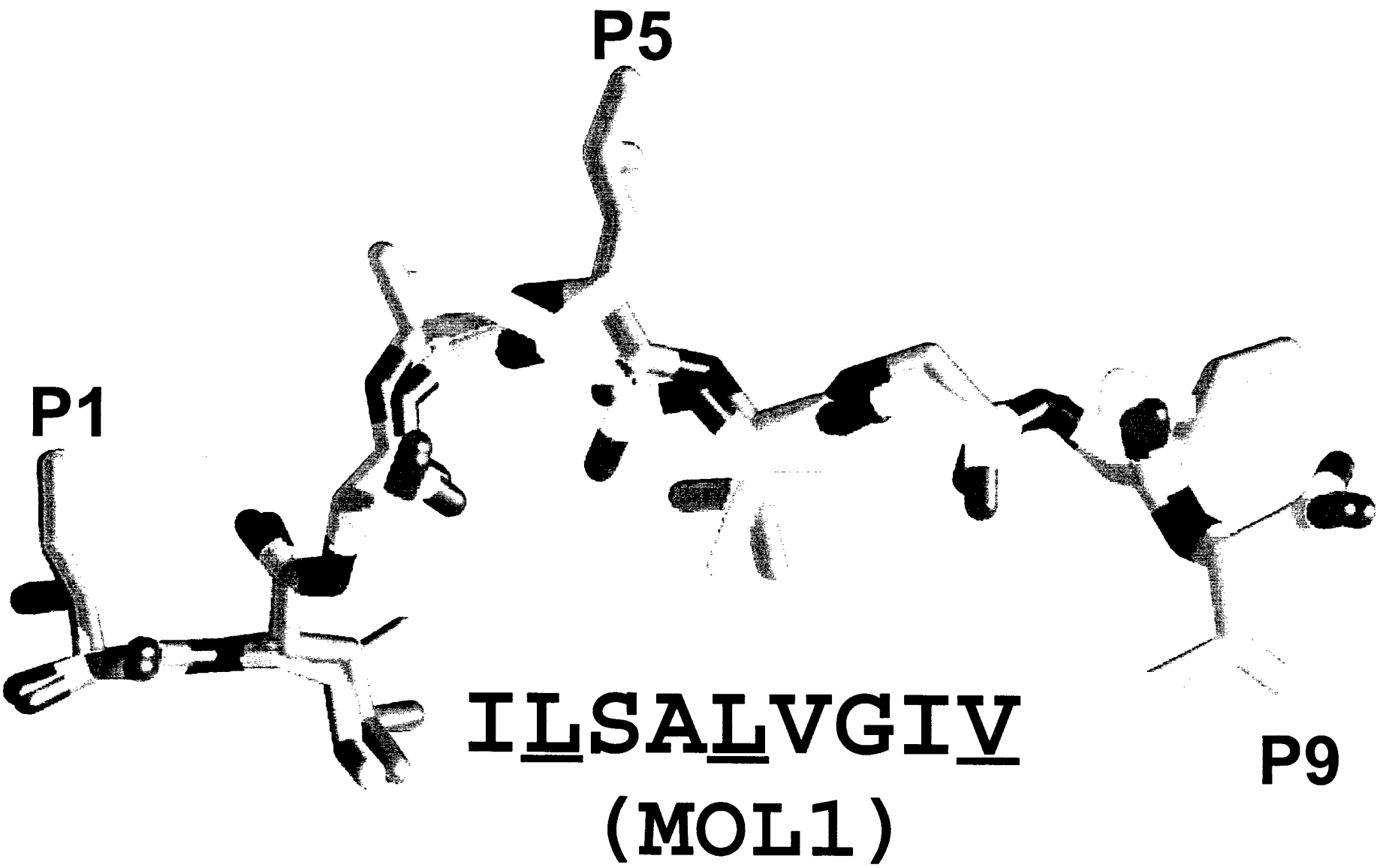

Figure 3C

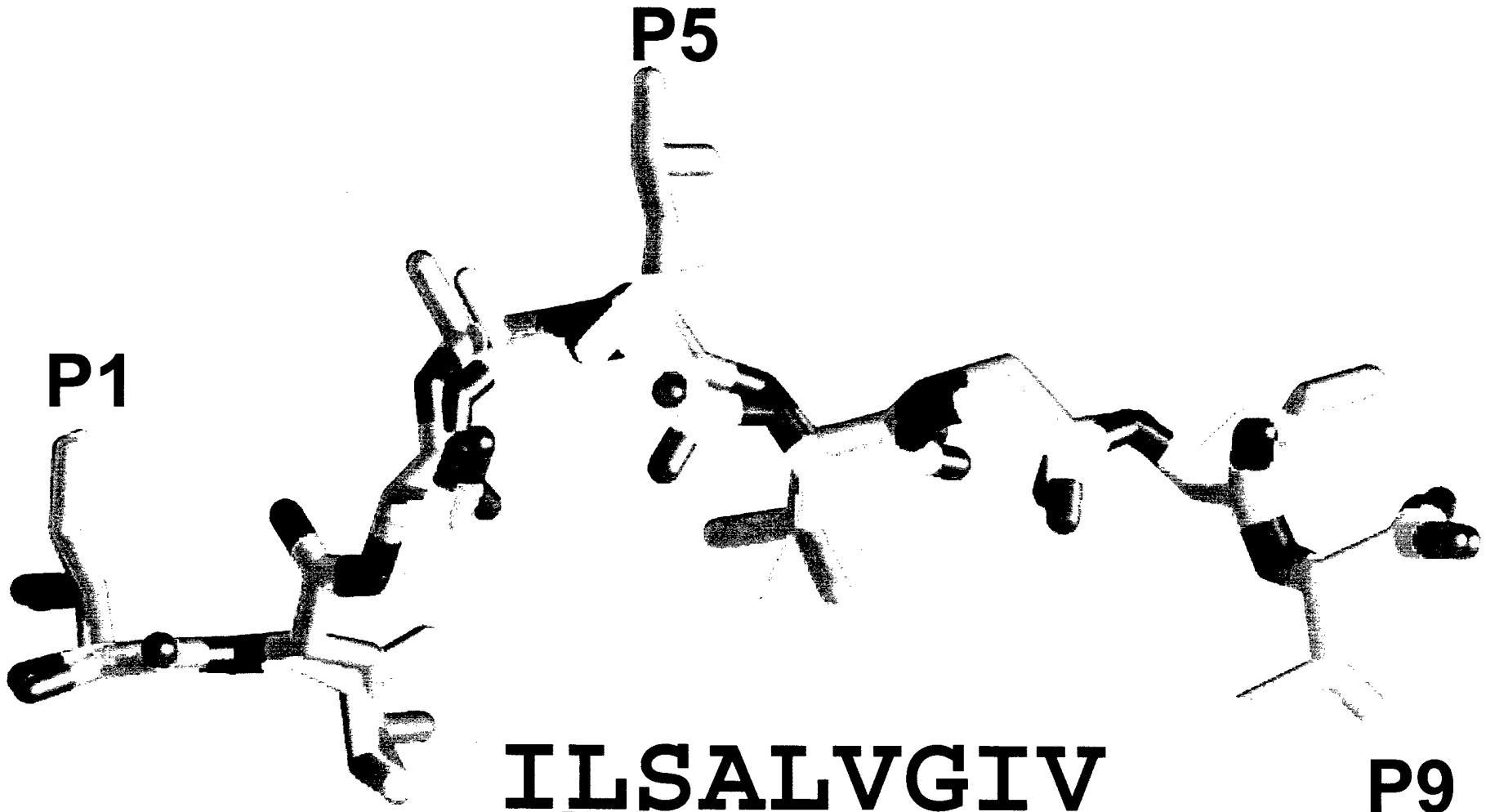

Figure 3D

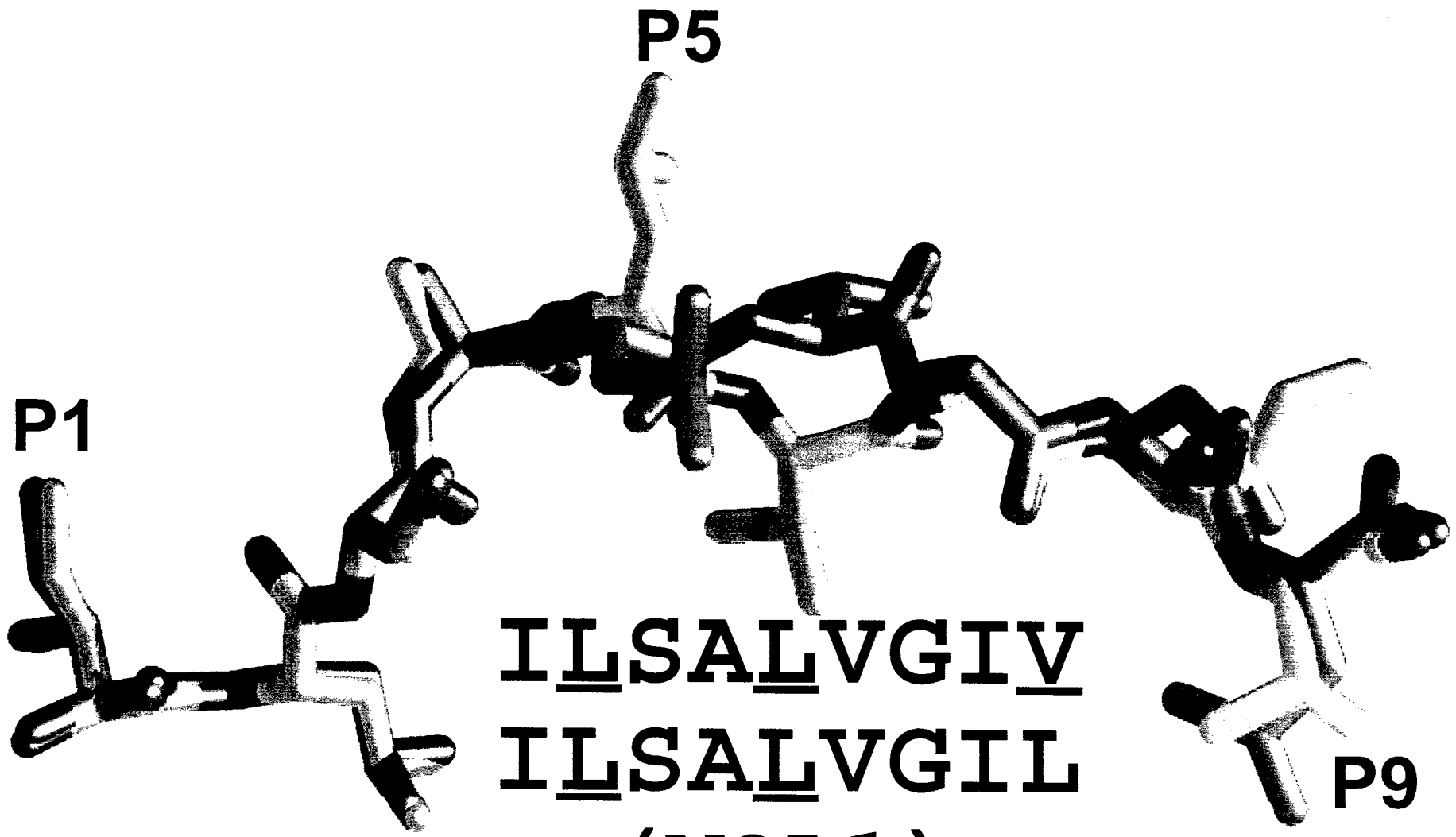

Figure 3E

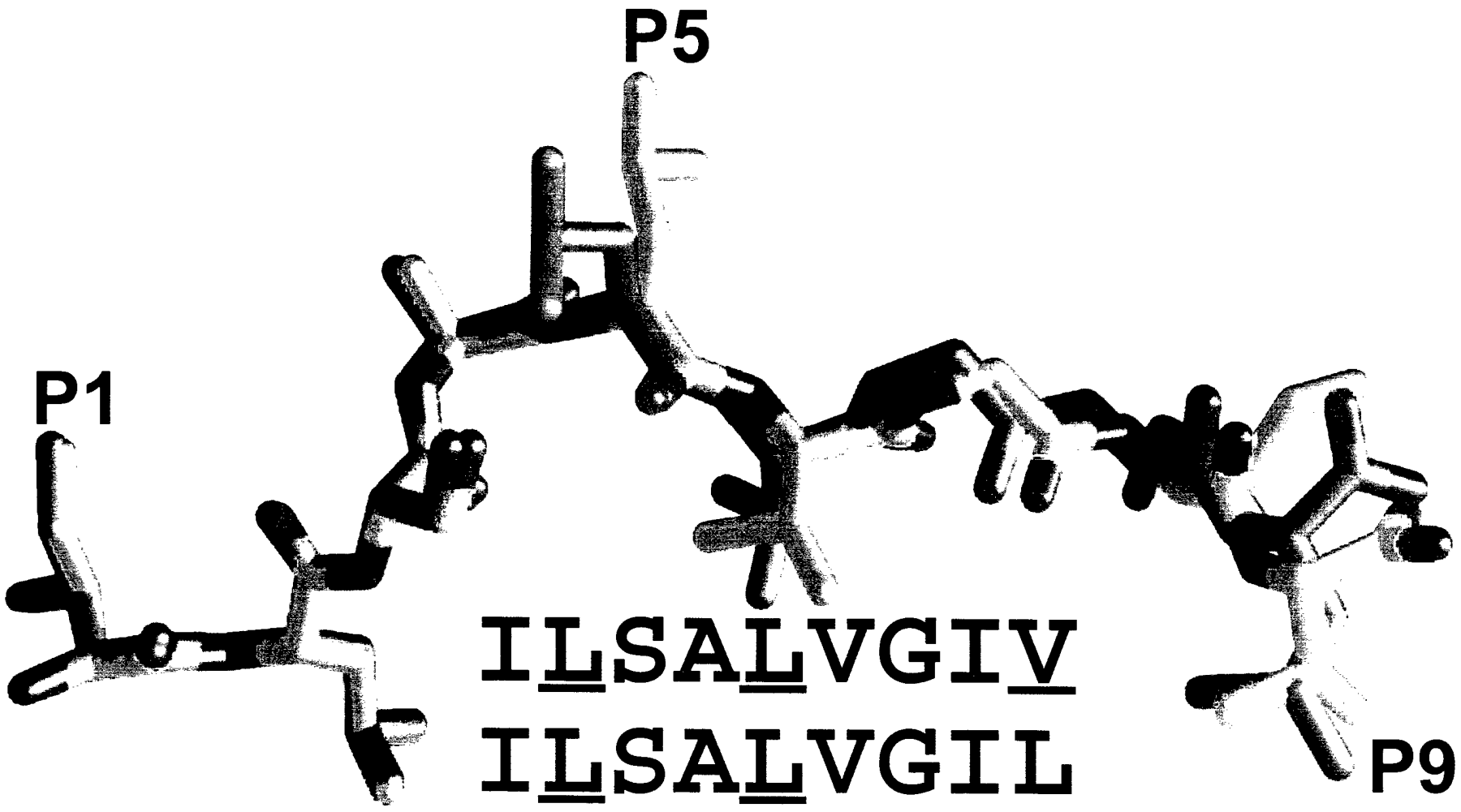

Figure 3F

THE JOURNAL OF BIOLOGICAL CHEMISTRY
Vol. 274, No. 51, Issue of December 17, pp. 36422–36427, 1999
Printed in U.S.A.

Poor Binding of a HER-2/neu Epitope (GP2) to HLA-A2.1 Is due to a Lack of Interactions with the Center of the Peptide*

(Received for publication, August 4, 1999, and in revised form, August 31, 1999)

Jennifer J. Kuhns‡, Michael A. Batalia§, Shuqin Yan‡, and Edward J. Collins‡§¶‖

From the ‡Department of Microbiology and Immunology, §Lineberger Comprehensive Cancer Center, and the ¶Department of Biochemistry and Biophysics, University of North Carolina, Chapel Hill, North Carolina 27599

Class I major histocompatibility complex (MHC) molecules bind short peptides derived from proteins synthesized within the cell. These complexes of peptide and class I MHC (pMHC) are transported from the endoplasmic reticulum to the cell surface. If a clonotypic T cell receptor expressed on a circulating T cell binds to the pMHC complex, the cell presenting the pMHC is killed. In this manner, some tumor cells expressing aberrant proteins are recognized and removed by the immune system. However, not all tumors are recognized efficiently. One reason hypothesized for poor T cell recognition of tumor-associated peptides is poor binding of those peptides to class I MHC molecules. Many peptides, derived from the proto-oncogene HER-2/neu have been shown to be recognized by cytotoxic T cells derived from HLA-A2$^+$ patients with breast cancer and other adenocarcinomas. Seven of these peptides were found to bind with intermediate to poor affinity. In particular, GP2 (HER-2/neu residues 654–662) binds very poorly even though it is predicted to bind well based upon the presence of the correct HLA-A2.1 peptide-binding motif. Altering the anchor residues to those most favored by HLA-A2.1 did not significantly improve binding affinity. The crystallographic structure shows that unlike other class I-peptide structures, the center of the peptide does not assume one specific conformation and does not make stabilizing contacts with the peptide-binding cleft.

Class I major histocompatibility complex (MHC)[1] proteins bind short peptides (9–11 amino acids) derived from cytosolically degraded proteins. These peptides are transported into the endoplasmic reticulum and bind to newly formed class I molecules. Peptide binding appears to be the final step in assembly of the complex (1). Following peptide binding, the complexes are transported to the plasma membrane. At the plasma membrane, clonotypic T cell receptors on the surface of circulating cytotoxic T lymphocytes (CTL) may recognize the peptide-MHC complex (pMHC). If the pMHC is recognized by the T cell receptor, the T cell is activated and the cell presenting the pMHC is killed. A normal cell will have a large assortment of pMHC on the cell surface that are not recognized by CTL. However, viral or mutated self-proteins are degraded by these same mechanisms, and many of the resulting pMHC are recognized by CTL. In this manner, virus-infected or mutated cells are targeted for lysis by cytotoxic T cells (reviewed in Ref. 2). Self-proteins that are expressed in abnormally high amounts or in abnormal cell types may also be targets for CTL (3).

Class I MHC molecules bind many peptides with diverse sequences and high affinity (4). To bind all these peptides, the class I protein primarily interacts with the invariant portions of the peptides, the N and C termini (5). Class I MHC also uses a subset of amino acid side chains within the peptide termed "anchors" to generate significant binding (6). These peptide anchor residues bind within "specificity pockets" that are primarily formed by the polymorphic residues within the peptide-binding cleft of the MHC molecule (7). Peptides that bind with high affinity to a given allotype are typically found to have one of a few preferred amino acids at each anchor position. The corresponding hypothesis is that peptides that do not have those preferred amino acids at the anchor positions will not bind well. The combination of amino acids that may bind at the anchor positions is known as the peptide-binding motif (8). These motifs have proven to be extremely valuable in predicting peptides that will bind to class I MHC. Other residues within the peptide besides the anchors may be used to generate increased binding affinity (9–11).

Interestingly, many peptides that appear to have the correct peptide-binding motif still bind poorly. Substituting the anchor residues of poor binding peptides with those that are most preferred by the allotype can generate high affinity binding. (10, 12). Some of these altered peptide ligands (APL) are even effective therapeutics (13). We show here that there are also peptides for which altering the anchor residues does not significantly increase binding affinity. It is not clear from the previously available data in the literature why these peptides bind poorly.

HER-2/neu (c-erb-2) encodes a receptor tyrosine kinase with homology to the epidermal growth factor receptor. Overexpression of HER-2/neu in many adenocarcinomas, including breast and ovarian tumors, correlates with a poor prognosis for remission and recovery (14). Tumor infiltrating lymphocytes have been found in cancer patients that overexpress HER-2/neu, and these tumor infiltrating lymphocytes are able to recognize and lyse the solid tumor (3, 15, 16), but these CTL do not eliminate the tumor. It has also been shown that several peptide epitopes derived from the gene product of HER-2/neu are presented by class I MHC molecules to circulating CTL. As with many other

* This work was supported by National Institutes of Health Grants AI 29324 and CA 58223 and Department of Defense Grants DAMD17-970-1-7052 (to E. J. C.) and DAMD17-98-1-8219 (to M. A. B.). The costs of publication of this article were defrayed in part by the payment of page charges. This article must therefore be hereby marked "*advertisement*" in accordance with 18 U.S.C. Section 1734 solely to indicate this fact.

The atomic coordinates and structure factors (code 1QR1) have been deposited in the Protein Data Bank, Research Collaboratory for Structural Bioinformatics, Rutgers University, New Brunswick, NJ (http://www.rcsb.org).

‖ To whom correspondence should be addressed: Dept. of Microbiology and Immunology, University of North Carolina, CB#7290, 804 M. E. Jones Bldg, Chapel Hill, NC 27599. Tel.: 919-966-6869; Fax: 919-962-8103; E-mail: collins1@med.unc.edu.

[1] The abbreviations used are: MHC, major histocompatibility complex; CTL, cytotoxic T lymphocyte; pMHC, peptide-MHC complex(es); APL, altered peptide ligand(s); HPLC, high pressure liquid chromatography; BFA, brefeldin A; A2, HLA-A2.1.

tumor-associated antigens, most of these peptides bind poorly to HLA-A2.1 (A2). There are many potential reasons for the lack of immune removal of tumors including the down-regulation of class I MHC or down-regulation of the protein from which the peptide is derived. It has also been proposed that one reason for poor recognition by CTL is weak binding of the immunogenic peptides to class I MHC (3).

Here we show that HER-2/neu-derived peptides, identified in the literature as recognized by CTL, bind with a range of affinities, but all are lower affinity than two index peptides of high affinity. One peptide was chosen for further study. This peptide, GP2 (IISAVVGIL), binds very poorly to A2 but has anchor residues that are present in high affinity peptides (Ile at position 2 and Leu at position 9). Its inherently poor affinity is not significantly increased by substitution of its anchor residues. To understand why this peptide binds poorly, the crystallographic structure of the A2-GP2 complex was determined. Unlike all previously determined peptide-class I MHC (pMHC) structures, there is a large region of unresolved electron density in the center of the peptide. We interpret this to mean that the peptide assumes more than one conformation within the peptide-binding cleft. We hypothesize that the observed poor binding is due to the lack of important secondary interactions within the center of the peptide.

EXPERIMENTAL PROCEDURES

Preparation of HLA-A2.1-Peptide Complexes—Residues 1–275 of HLA-A2.1 (A2) and residues 1–99 of human β_2-microglobulin were expressed in *Escherichia coli*, produced as inclusion bodies, purified, and folded as described previously (17). Briefly, peptide, solubilized β_2-microglobulin and solubilized A2 heavy chain were rapidly diluted into folding buffer (10 mM Tris, pH 8.0, 0.4 M L-Arg, 10 mM reduced glutathione, 1 mM oxidized glutathione, and protease inhibitors) at molar ratios of 10:5:1, respectively. The final protein concentration was kept below 50 μg ml^{-1}. The solution was incubated at 10 °C for 36–48 h and then concentrated (Amicon) and purified by HPLC gel filtration (Phenomenex, BioSep-SEC-S2000).

Synthetic Peptides—All peptides were synthesized by the Peptide Synthesis Facility at the University of North Carolina at Chapel Hill. The peptides were purified to greater than 95% purity by reversed-phase HPLC and identity confirmed by matrix-assisted laser desorption ionization-time-of-flight spectroscopy. Peptides were dissolved in 100% dimethyl sulfoxide at 20 mg ml^{-1} by weight. The final peptide concentration was determined by amino acid analysis (Protein Chemistry Laboratory, Department of Chemistry, University of North Carolina, Chapel Hill). The list of peptides and references for immunogenicity are given in Table I.

Determination of Thermal Stability—Purified A2-peptide complexes were exchanged into a 10 mM KH_2/K_2HPO_4 buffer, pH 7.5, and adjusted to a final protein concentration of 4–12 μM. The change in CD signal at 218 nm was measured as a function of temperature from 4 to 95 °C on an AVIV 62-DS spectropolarimeter (Aviv Associates Inc, Lakewood, NJ). The final melting curve was the average of at least three experiments for each A2-peptide complex. T_m values were calculated as the temperature at which 50% of the complexes are denatured using a two-state denaturation model (12).

Cell Surface Stabilization Assay—Cell surface stabilization of A2 was performed as described previously (11). Briefly, 2.5×10^5 T2 cells (ATCC CRL-1992) were incubated overnight in AIM V serum-free medium (Life Technologies, Inc.) at 37 °C, 5% CO_2 in the presence of GP2 or APL, at concentrations varying from 50 to 0.05 μM. Cells were then stained with the monoclonal antibody BB7.2 (18) specific for A2, followed by fluorescein isothiocyanate-labeled (1:50) goat anti-mouse IgG antibody (Southern Biotechnology Associates). Cells were analyzed by flow cytometry (FACScan, Becton Dickinson), and the mean channel fluorescence was determined using the CYCLOPS software package (Cytomation, Fort Collins, CO). All data are normalized as the percentage of the mean channel fluorescence for the calreticulin-signal-sequence peptide, ML, bound to A2 at 50 μM. Binding by the A2-specific antibody, BB7.2, was not dependent on the peptide bound because W6/32, an antibody that binds to an epitope between the α3 domain and β_2-microglobulin, gave similar results (data not shown).

Cell Surface Half-life Assay—The determination of cell surface half-lives ($T_{1/2}$) of A2-peptide complexes was performed as described previously (11). Briefly, 2.5×10^6 T2 cells were incubated overnight in AIM V serum-free medium at 37 °C, 5% CO_2 in the presence of 50 μM peptide. To block the egress of new A2 molecules to the surface, cells were incubated at 37 °C, 5% CO_2 in RPMI 1640, 15% fetal calf serum and 10 μg ml^{-1} brefeldin A (BFA, Sigma). This concentration of BFA is toxic to the cells. Therefore, after 1 h the cells were then transferred to RPMI 1640, 15% fetal calf serum, and 0.5 μg ml^{-1} BFA. At the indicated time points, 2.5×10^5 cells were removed, incubated with BB7.2, and analyzed by flow cytometry as described above for cell surface stabilization assay. Each time point is evaluated as mean fluorescence with peptide minus mean fluorescence without peptide and normalized to the maximal level of fluorescence (at time zero) for each peptide.

TABLE I

Summary of binding data of HER-2/neu-derived peptides to A2

Residues substituted with respect to wild-type peptide are shown in boldface type. T_m is the temperature (°C) at which 50% of the protein is denatured as measured by circular dichroism. K_r is the relative binding constant as determined by the T2 cell surface assembly assay. K_r is defined as the concentration of peptide in μM that yields 50% mean channel fluorescence as compared to the maximum fluorescence of the control peptide (ML) at 50 μM. The K_r value for ML is the concentration that yields 50% mean channel fluorescence. $T_{1/2}$ is the half-life of peptide-A2 complexes (in hours) as determined by the T2 cell surface stability assay. ND, not determined. DNF, did not fold *in vitro*. The error in the T_m is the sum of the machine and curve fit errors. It is typically about 1 °C. >50 means that the concentration to yield 50% of ML fluorescence is greater than 50 μM.

Peptide	Sequence	T_m	K_r	$T_{1/2}$
GP2 (16)	IISAVVGIL	36.4	>50	0.35
S1 (38)	SIISAVVGI	44.2	13.2	4.05
L10 (38)	IISAVVGILL	41.3	>50	1.58
E74 (15)	DVRLVHRDL	DNF	>50	DNB
E75 (15)	KIFGSLAFL	45.1	14.4	8.57
F56 (39)	YISAWPDSL	34.8	>50	DNB
C84 (39)	ELVSEFSRV	37.5	>50	0.30
L9V	IISAVVGI**V**	38.8	>50	0.69
I2L	I**L**SAVVGIL	42.2	22.9	1.76
I2L/L9V	I**L**SAVVGI**V**	42.5	10.0	2.48
ML (30)	MLLSVPLLL	52.5	1.8	19.53
RT (31)	ILKEPVHGV	50.0	7.7	9.69
MelA (36)	EAAGIGILTV	40.9	47.2	0.44
MelA-A2L	E**L**AGIGILTV	50.0	1.6	9.98

Crystallization, Data Collection and Processing—Crystals were grown by hanging drop vapor diffusion as described previously (19). Crystallographic data of A2-GP2 were collected on a single crystal at the National Synchrotron Light Source, Brookhaven National Labs, beamline X-12B at −170 °C (Oxford Cryosystems). Evaluation of the diffraction pattern with DENZO autoindexing function showed the space group to be triclinic P1. 180 degrees of data were collected at a distance of 90 mm from the Quantum 4 CCD detector (ADSC Poway, CA) with one-degree oscillations and 3 min of exposure time/frame. Data were processed with DENZO, and intensities were scaled with SCALEPACK (20). Data statistics are shown in Table II.

Structure Determination and Refinement—The A2-GP2 structure was determined by molecular replacement using AMoRe (21) within the CCP4 program suite (22). The A2-hepatitis peptide complex (PDB accession code 1HHH) was used as the search model (23). Because the domains tend to vary in their relative orientations with respect to one another in different crystal forms, the search model was divided into three pieces, the peptide-binding superdomain ($\alpha_1\alpha_2$), the α_3 domain, and β_2-microglobulin. Initial rounds of positional refinement used X-PLOR from 8–2.4 Å resolution data. Later rounds were performed with Refmac using all data from 30.0 to 2.4 Å. Final rounds of refinement used torsional dynamics with CNS (24–26) with all data. Electron density maps were generated using DM and functions for 2-fold non-crystallographic averaging, histogram matching, and solvent flattening. Manual intervention was performed using O (27). 103 water molecules were added to the structure using the program ARP (28) combined with Refmac and confirmed by visual inspection of the electron density maps. The refinement statistics are listed in Table II.

RESULTS

HER-2/neu-derived Peptides Bind Poorly to A2—We began these studies to assess the correlation of immunological activity with peptide binding affinity to HLA-A2.1 (A2). Thermal stability of class I MHC-peptide complexes, as measured by

TABLE II
Summary of crystallographic data

The crystallographic structure of A2-GP2 was determined by molecular replacement using the A2-hepatitis B 10-mer (Protein Data Bank code 1HHH) as the search model. The structure was refined by a combination of X-PLOR and Refmac. Individual Bs were refined in the penultimate cycle followed by the addition of waters.

Data statistics	
Space group	P1
Cell Dimensions	a = 50.34 Å b = 63.61 Å c = 75.14 Å α = 81.98 ° β = 76.25 ° γ = 77.83 °
Molecules/Asymmetric Unit	2
Resolution	30–2.4 Å
R_{merge} (%)[a]	9.3 (23.3)[b]
$<I/\sigma>$	7.80 (3.46)
Unique reflections	34,962
Total reflections	66,839
Completeness (%)	98.2 (97.6)
Refinement	
Resolution	30–2.4 Å
R_{free} (%) (number of reflections)[c]	28.4 (1,714)
R_{work} (%) (number of reflections)[c]	24.2 (31,969)
Rs fit[d]	83.8%
No. of non-hydrogen atoms	6,292
No. of waters	103
Error[e]	0.26 Å
Average B factor	16.8 Å^2
R.M.S. deviations from ideality	
Bonds	0.009 Å
Angles	1.468 °
Residues in Ramachandran plot	
Most favored	91.6%
Additional allowed	8.1%
Generously allowed	0.3%
Disallowed	0.0%

[a] $R_{merge} = \Sigma_{hkl} \Sigma_i |I_i - <I>| / \Sigma_{hkl} \Sigma_i I_i$, where I_i is the observed intensity and <I> is the average intensity of multiple observations of symmetry related reflections.

[b] Number in parenthesis refers to the highest resolution shell (2.44–2.40) for A2-GP2 unless otherwise stated.

[c] $R = \Sigma_{hkl} ||F_{obs}| - k|F_{cal}|| / \Sigma_{hkl} |F_{obs}|$, where R_{free} is calculated for a randomly chosen 5% of reflections and R_{work} is calculated for the remaining 95% of reflections used for structure refinement.

[d] *Rs* fit is the average real space fit of all atoms on an electron density map from DM with 2-fold noncrystallographic averaging, histogram matching, and solvent flattening.

[e] Error is the mean estimate of the coordinate error based on maximum likelihood methods (Refmac).

circular dichroism, have been shown to correlate with the free energy of peptide binding to class I MHC (29). Therefore, the thermal stabilities of recombinant A2 complexes folded *in vitro* with seven HER-2/neu peptides identified as important epitopes for breast cancer immunotherapy in the literature (GP2, S1, L10, E74, E75, F56, and C84; see Table I for sequences) were determined. As can be seen from Fig. 1*A*, complexes formed with GP2, F56, and C84 have extremely low melting temperatures. Complexes formed with S1, L10, and E75 (summarized in Table I) have higher melting temperatures. E74 bound so poorly as to be undetectable in any of our assays (data not shown). A cell surface binding assay (Fig. 1*B*) using T2 cells with exogenously added peptide confirms the results found by the circular dichroism experiments. Two peptides, one hydrophobic and one hydrophilic, were chosen as representative "high affinity" binders. ML is derived from the signal sequence of calreticulin (30), and RT is derived from HIV-1 reverse transcriptase (31). The thermal stability (T_m) and the relative binding constant (K_r) determined by the T2 assay correlate well (91.3% correlation coefficient). This suggests that K_r is proportional to K_D, because, as stated above, the T_m has previously been shown to be proportional to the K_D (29).

Adding BFA to the cell surface stability assay allows us to measure the amount of time a peptide-MHC complex stays on the surface of cells. As can be seen in Fig. 1*C*, the GP2 peptide has an extremely short half-life of ~21 min at 37 °C (Table I). Some of the other HER-2/neu-derived peptides have longer half-lives, but none are as long as peptides such as ML or RT (Fig. 1*C* and Table I). We could not detect binding of the E74 peptide in any of our assays. The fact that CTL activity toward E74 can be seen and we cannot measure binding is probably a function of the extreme sensitivity of CTL. Only ~100 class I-peptide complexes/cell are required to trigger an activated T cell (32).

Anchor Substitutions Do Not Significantly Improve Binding of GP2—Substitutions at peptide anchor positions have been shown to greatly increase the thermal stability of an influenza matrix peptide (12). In the present work, we chose one of the three poor binding peptides, GP2, to study the anchor substitutions of HER-2/neu-derived peptides. The GP2 anchors (Ile at position 2 and Leu at position 9 of the peptide) are found in peptides that bind with high affinity to A2, but these anchors are not optimal (8). Therefore, optimized APL based on GP2 were synthesized that replaced the Ile at position 2 with Leu (I2L) or the Leu at position 9 with Val (L9V). As can be seen in Fig. 1*D*, these substitutions did increase the thermal stability (~2–6 °C) but not to the degree that was seen for similar substitutions in the influenza matrix peptide (~7–9 °C) (12) or for a variant of a melanoma peptide (MelA and MelA-A2L, ~9 °C). The cell surface stability assay using T2 cells supports the CD data that we have measured (Fig. 1*E*). The half-lives of the APL complexes on the cell surface are increased with respect to GP2 (Fig. 1*F*). However, they are not close to the time constants seen for the positive control, high affinity binders ML or RT.

Crystallographic Structure of A2-GP2—To understand why GP2 binds poorly to A2 and why the anchor substitutions do not significantly increase the stability, we determined the crystallographic structure of A2-GP2. The molecular replacement solution was unambiguous with a correlation coefficient of ~73% after rigid body fitting. The model was refined in X-PLOR (33). During refinement, the peptide was omitted to reduce the potential for model bias. Density modification was performed with DM (22) using the X-PLOR output coordinates to generate unbiased averaged electron density maps of the peptide and to fit the structure of A2. Unlike all of the pMHC structures that we have determined to date, the entire length of the main chain of the peptide was not visible in the density modified electron density maps at this stage. After 10 cycles of model building with O (27) and computational refinement with X-PLOR and Refmac and finally with CNS, the refinement converged to the statistics shown in Table II. In general, the maps are clear and unambiguous. The entire A2 molecule is well resolved and fits the density well as evidenced by an average real space correlation coefficient of 83.8%. The positions of the termini of the GP2 peptide are also unambiguous and never altered through the course of refinement. However, unlike all reported pMHC structures, the center of the peptide never became clear in the density (Fig. 2). In addition, standard $2F_o - F_c$ maps, simulated annealing omit maps, unaveraged omit maps, and composite omit maps failed to show density for the center of the peptide. In particular, the orientation of residue 6 (Val) is completely uninterpretable, and the positions of residues 5 and 7 (Val and Gly, respectively) are not well defined.

DISCUSSION

One hypothesis used to explain why tumors are not recognized and eliminated by the immune system is that potentially

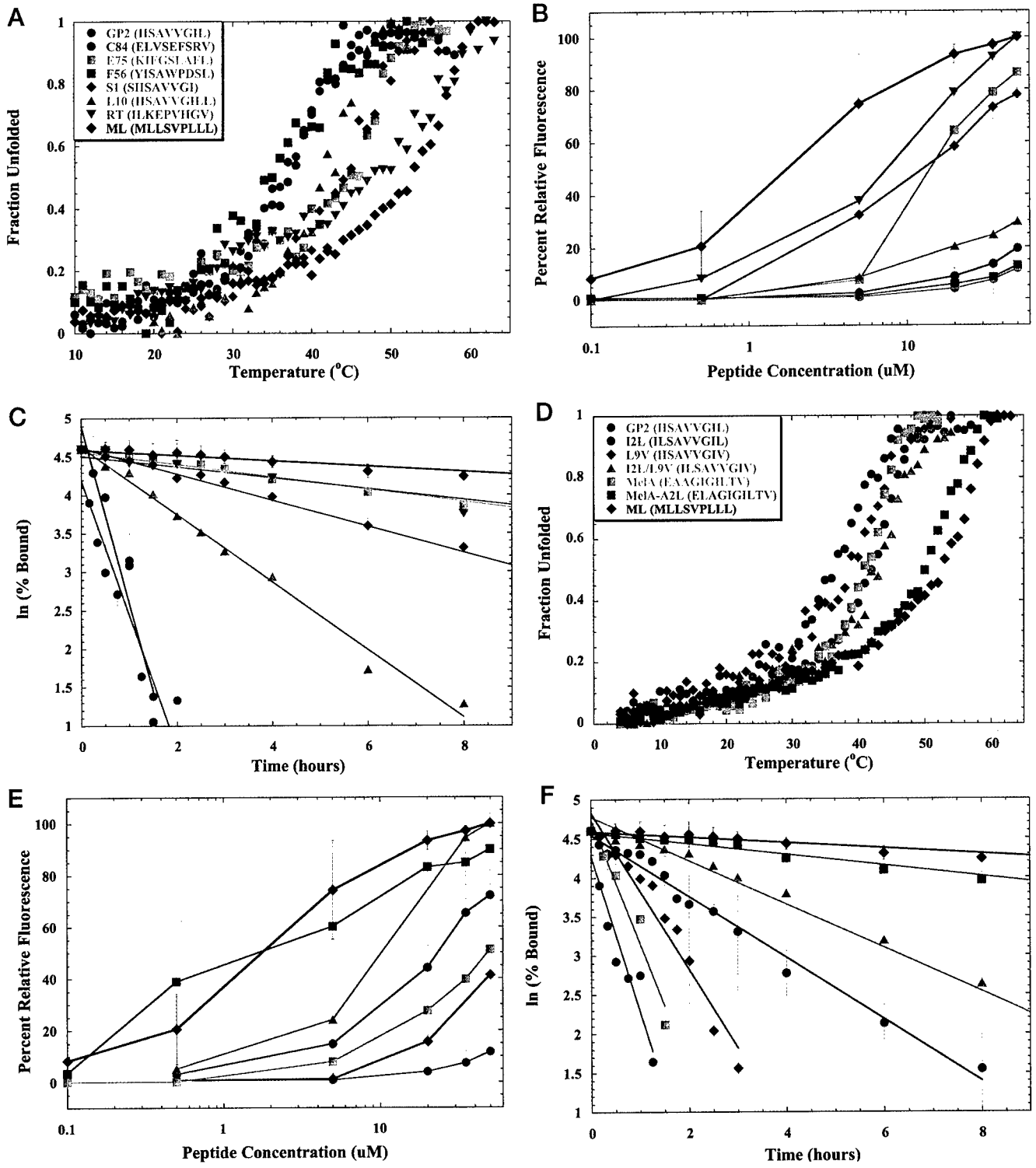

FIG. 1. **HER-2/neu-derived peptides bind poorly to A2, and anchor substitutions do not increase the stability of GP2-derived APL.** The symbols and colors shown in *A* are also those used in *B* and *C*. Likewise, the symbols and colors shown in *D* are also those used in *E* and *F*. *A*, thermal stability of A2-peptide complexes as measured by CD. 4–12 μM protein was denatured by heat in a circular dichroism spectropolarimeter. The change in CD signal at 218 nm is an indication of the loss of secondary structure within the protein. Each curve is the average of three independent experiments. The error in the T_m is the sum of the curve fit error and the Peltier temperature controller error and is ~1 °C. *B*, cell surface measurements confirm relative affinities measured by circular dichroism. T2 cells were incubated with the indicated concentrations of peptide and the amount of cell surface A2 measured by flow cytometry using an A2-specific monoclonal antibody BB7.2. *C*, cell surface half-lives of A2-peptide complexes were determined by treating the peptide-pulsed cells (as in *B*) with BFA to halt vesicular transport. Aliquots of cells were removed at the indicated times and the remaining A2 on the cells determined by incubating with BB7.2. *D*, CD experiments show that anchor substitutions of GP2 do not greatly increase the stability. The best peptide is the double substitution I2L/L9V, but even it is deficient compared with ML. *E*, T2 cell surface stabilization confirms the CD data. *F*, the cell surface half-lives are moderately increased compared with GP2.

immunologically reactive peptides do not bind well to class I MHC molecules. If the peptides dissociate from class I MHC molecules too quickly, the cells presenting the peptides do not have a sufficient concentration of the specific pMHC at the surface of the cell to be recognized by circulating T cells. We examined binding of a selection of known immunologically recognized

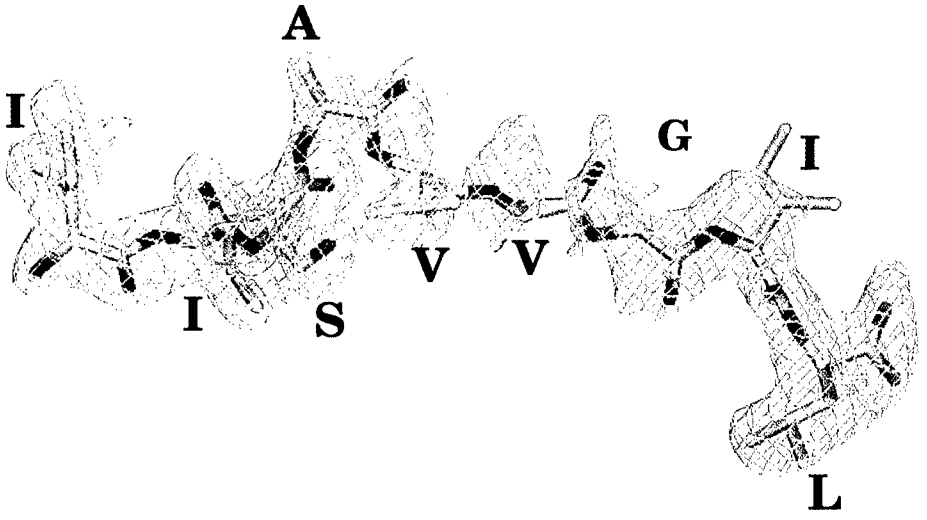

FIG. 2. **The center of the GP2 peptide is disordered.** The averaged omit electron density map of the GP2 peptide with a cover radius of 1.5 Å. The map was calculated using modified phases from DM.

peptide ligands from the tyrosine kinase family member HER-2/neu. Despite the presence of CTL that recognize these peptides bound to A2, the tumors are not eliminated. These HER-2/neu peptides displayed a spectrum of binding affinities, but all were lower than the level observed for high affinity binders, such as ML or RT. Of particular interest to the immunology of tumor recognition was the clustering of many of these peptides in the "low affinity" category. Remarkably, all of these peptides, (GP2, C84, and F56) have good anchor residues for A2.

There are two primary reasons to examine this phenomena in detail. The first is to understand how class I MHC binds peptides. There is a great deal known about how class I MHC binds many peptides with great sequence diversity, but there is very little information about how the protein binds any particular peptide well or poorly. There are now many examples of crystal structures of high affinity peptides bound to class I MHC. GP2 is a perfect example of a poor binding peptide and as such offers the first opportunity to understand poor binding. The second reason to examine GP2 is that poor affinity peptides are potentially better targets for immunotherapy. The rationale for this has to do with T cell education. T cells are selected for survival by two mechanisms (positive and negative selection) in the thymus (35). If a self-peptide binds to class I MHC with high affinity, there is a larger concentration of pMHC in the thymus and thus a greater chance that T cells would be able to recognize the complex well. Presumably, this set of T cells would be deleted from the T cell receptor repertoire, and they would not be in the periphery. If the self-peptide binds with poor affinity, the concentration of that peptide-MHC molecule in the thymus may be too low for recognition during the selection process. Therefore, there is a greater probability of finding these T cells in the periphery.

A complex of A2 with GP2 bound has poor thermal stability (T_m, 36.4 °C) and a very short cell surface half-life (~21 min). Many laboratories including ours have improved the binding affinity of peptides by changing the anchor residues to those most preferred by A2 (13, 36). As an example, we show that a small change in the anchor position of the melanoma peptide MelA results in a peptide with much greater binding affinity. However, trials with substitutions of GP2 at the anchor positions showed that the affinity was not significantly improved (Table I). Our goal is to be able to design APL for cancer immunotherapy. To be able to do this in a reasonable fashion, we needed to determine the crystallographic structure of A2-GP2 and determine why this peptide binds poorly.

The crystallographic structure shows uninterpretable electron density within the center of the peptide. Our interpretation of these data is that the peptide does not assume one unique conformation in the center as has been seen for all other single peptide-MHC structures to date (reviewed in Ref. 4). Interestingly, this is analogous to the situation found in the crystal structure of a class I MHC complex that contained a mixture of many different peptides (37). These data suggest that anchor substitutions do not significantly increase the affinity of GP2 because they do not address the fundamental problem that the peptide has in binding. The center does not make stabilizing contacts with the binding cleft of the class I MHC molecule.

This result begs another important immunological question. Does the flexibility in the center of the peptide increase or decrease immunogenicity? On the one hand, the flexibility decreases the already small concentration of a specific molecular surface that can interact with the T cell receptor on a circulating T cell. On the other hand, multiple peptide conformations generate more molecular surfaces that can be potentially recognized by circulating T cells. Perhaps in the context of a peptide that binds well, increased flexibility is more immunogenic, but in the context of a poor binding peptide increased flexibility does not increase immunogenicity because of the reduced concentration effect.

There is increasing interest in using peptides that bind to class I MHC for immunotherapy. As is the case of vaccination used to prevent viral infection, the potential therapeutic value is significant. As more antigens are discovered that are recognized by CTL and yet bind poorly to class I MHC molecules, the rules that predict binding affinity will be more critical. The phenomena observed here for GP2 certainly applies to other poor binding peptides whose binding affinity is not increased by altering the anchor residues. Increased affinity can be obtained for many of these peptides, but a full understanding of how peptides bind to class I MHC is still needed. By examining the binding of GP2 at the atomic level, we have made another step toward understanding peptide binding well enough to make predictions that will increase peptide affinity and minimize immunological consequences.

Acknowledgments—We thank Drs. Jeffrey Frelinger and Jonathan Serody for extensive immunological conversations, Drs. Charlie Carter and John Sondek for critical reading of the manuscript, the staff at the National Synchrotron Light Source for assistance in crystallographic data collection, Brian Cox for technical assistance, and members of the Collins and Frelinger labs for stimulating discussions.

REFERENCES

1. Lehner, P. J., and Trowsdale, J. (1998) *Curr. Biol.* **8,** R605—R608
2. Ploegh, H. L. (1998) *Science* **280,** 248–253

3. Peoples, G. E., Goedegebuure, P. S., Smith, R., Linehan, D. C., Yoshino, I., and Eberlein, T. J. (1995) *Proc. Natl. Acad. Sci. U. S. A.* **92,** 432–436
4. Batalia, M. A., and Collins, E. J. (1997) *Biopoly* **43,** 281–302
5. Madden, D. R., Gorga, J. C., Strominger, J. L., and Wiley, D. C. (1992) *Cell* **70,** 1035–1048
6. Falk, K., Rotzchke, O., Stevanovic, S., Jung, G., and Rammensee, H.-G. (1991) *Nature* **351,** 290–296
7. Garrett, T. P. J., Saper, M. A., Bjorkman, P. J., Strominger, J. L., and Wiley, D. C. (1989) *Nature* **341,** 692–696
8. Rammensee, H. G., Friede, T., and Stevanovic, S. (1995) *Immunogenetics* **41,** 178–228
9. Colbert, R. A., Rowland-Jones, S. L., McMichael, A. J., and Frelinger, J. A. (1994) *Immunity* **1,** 121–130
10. Ruppert, J., Sidney, J., Celis, E., Kubo, R. T., Grey, H. M., and Sette, A. (1993) *Cell* **74,** 929–937
11. Pogue, R. R., Eron, J., Frelinger, J., and Matsui, M. (1995) *Proc. Natl. Acad. Sci. U. S. A.* **92,** 8166–8170
12. Bouvier, M., and Wiley, D. C. (1994) *Science* **265,** 398–402
13. Overwijk, W. W., Tsung, A., Irvine, K. R., Parkhurst, M. R., Goletz, T. J., Tsung, K., Carroll, M. W., Liu, C., Moss, B., Rosenberg, S. A., and Restifo, N. P. (1998) *J. Exp. Med.* **188,** 277–286
14. Ross, J. S., and Fletcher, J. A. (1998) *Stem Cells* **16,** 413–428
15. Fisk, B., Blevins, T. L., Wharton, J. T., and Ioannides, C. G. (1995) *J. Exp. Med.* **181,** 2109–2117
16. Yoshino, I., Goedegebuure, P. S., Peoples, G. E., Parikh, A. S., DiMaio, J. M., Lyerly, H. K., Gazdar, A. F., and Eberlein, T. J. (1994) *Cancer Res.* **54,** 3387–3390
17. Garboczi, D. N., Hung, D. T., and Wiley, D. C. (1992) *Proc. Natl. Acad. Sci. U. S. A.* **89,** 3429–3433
18. Parham, P., and Brodsky, F. M. (1981) *Human Immunol.* **3,** 277–299
19. Zhao, R., Loftus, D., Appella, E., and Collins, E. J. (1999) *J. Exp. Med.* **189,** 359–370
20. Otwinowski, Z., and Minor, W. (1996) in *Methods Enzymol.* **276,** 307–326
21. Navaza, J., and Saludjian, P. (1998) *Methods Enzymol.* **276,** 581–594
22. Dodson, E. J., Winn, M., and Ralph, A. (1998) *Methods Enzymol.* **277,** 620–633
23. Madden, D. R., Garboczi, D. N., and Wiley, D. C. (1993) *Cell* **75,** 693–708
24. Brunger, A. T. (1992) *Nature* **355,** 472–474
25. Pannu, N. S., and Reed, R. J. (1996) *Acta Crystallogr. Sect. A* **52,** 659–668
26. Adams, P. D., Pannu, N. S., Read, R. J., and Brunger, A. T. (1997) *Proc. Natl. Acad. Sci. U. S. A.* **94,** 5018–5023
27. Jones, T. A., Zou, J.-Y., Cowan, S. W., and Kjeldgaard, M. (1991) *Acta Crystallogr. Sect. A* **47,** 110–119
28. Lamzin, V. S., and Wilson, K. S. (1998) *Methods Enzymol.* **277,** 269–305
29. Morgan, C. S., Holton, J. M., Olafson, B. D., Bjorkman, P. J., and Mayo, S. L. (1997) *Protein Sci.* **6,** 1771–1773
30. Chen, Y., Sidney, J., Southwood, S., Cox, A. L., Sakaguchi, K., Henderson, R. A., Appella, E., Hunt, D. F., Sette, A., and Engelhard, V. H. (1994) *J. Immunol.* **152,** 2874–2881
31. Tsomides, T. J., Walker, B. D., and Eisen, H. N. (1991) *Proc. Natl. Acad. Sci. U. S. A.* **88,** 11276–11280
32. Lanzavecchia, A., Lezzi, G., and Viola, A. (1999) *Cell* **96,** 1–4
33. Brunger, A. (1992) *X-PLOR*, version 3.1, Yale University Press, New Haven, CT
34. Deleted in proof
35. Chan, S., Correia-Neves, M., Benoist, C., and Mathis, D. (1998) *Immunol. Rev.* **165,** 195–207
36. Romero, P., Gervois, N., Schneider, J., Escobar, P., Valmori, D., Pannetier, C., Steinle, A., Wolfel, T., Lienard, D., Brichard, V., van Pel, A., Jotereau, F., and Cerottini, J. C. (1997) *J. Immunol.* **159,** 2366–2374
37. Guo, H. C., Jardetzky, T. S., Garrett, T. P., Lane, W. S., Strominger, J. L., and Wiley, D. C. (1992) *Nature* **360,** 364–366
38. Kono, K., Rongcun, Y., Charo, J., Ichihara, F., Celis, E., Sette, A., Appella, E., Sekikawa, T., Matsumoto, Y., and Kiessling, R. (1998) *Int. J. Cancer* **78,** 202–208
39. Fisk, B., Savary, C., Hudson, J. M., O'Brian, C. A., Murray, J. L., Wharton, J. T., and Ioannides, C. G. (1995) *J. Immunother. Emphasis Tumor Immunol.* **18,** 197–209